



U.S. DRIVE Highlights of Technical Accomplishments 2011



February 2012

Preface

The U.S. DRIVE Partnership is a voluntary government-industry partnership focused on precompetitive, advanced automotive and related infrastructure technology research and development (R&D). Partners are the United States Department of Energy (DOE); the United States Council for Automotive Research LLC (USCAR), a consortium composed of Chrysler Group LLC, Ford Motor Company, and General Motors Company; Tesla Motors; five energy companies (BP America, Chevron Corporation, ConocoPhillips, ExxonMobil Corporation, and Shell Oil Products US); two electric utilities, DTE Energy and Southern California Edison; and the Electric Power Research Institute.

By providing a framework for frequent and regular interaction among technical experts in a common area of expertise, the Partnership accelerates technical progress, helps to avoid duplication of efforts, ensures that publicly funded research delivers high-value results, and overcomes high-risk barriers to technology commercialization.

The Partnership selected the following technical highlights from many hundreds of DOE-funded projects. Each one-page highlight represents what DOE, automotive, energy, and utility industry partners collectively consider to be significant progress in the development of advanced automotive and infrastructure technologies. The report is organized by technical area, with highlights categorized into three groups:

Vehicles

Advanced Combustion and Emission Control

Electrical and Electronics

Electrochemical Energy Storage

Fuel Cells

Materials

Vehicle Systems Analysis

Crosscutting

Codes and Standards

Grid Interaction

Hydrogen Storage

Fuels

Fuel Pathway Integration

Hydrogen Delivery

Hydrogen Production

Prior year accomplishments reports are available on the DOE website, www.vehicles.energy.gov/about/partnerships/roadmaps-other_docs.html, and the USCAR website, www.uscar.org.

Through cooperation and partnership between industry and government, advanced automotive technology research continues to make tremendous progress. Advanced technologies, such as electrified vehicles, for example, are entering the market in increasing numbers, and technologies that were only concepts less than a decade ago are now approaching initial commercial readiness. These advancements are the result of partners working together to achieve a common goal. With continued progress resulting from the joint efforts of government, industry, and academic experts, the U.S. DRIVE Partnership is helping to increase the competitiveness of American industry, safeguard American R&D and manufacturing jobs, and secure U.S. leadership in the development of advanced automotive technologies to enable a clean and sustainable transportation energy future.

Note—Common abbreviations used throughout this report are as follows:

ANL – Argonne National Laboratory
BNL – Brookhaven National Laboratory
EPA – Environmental Protection Agency
EDV – Electric Drive Vehicle
EUCAR – European Council for Automotive R&D
EV – Electric Vehicle
EVSE – Electric Vehicle Supply Equipment
DOE – Department of Energy
FCV – Fuel Cell Electric Vehicle
HEV – Hybrid Electric Vehicle
INL – Idaho National Laboratory
LANL – Los Alamos National Laboratory
NIST – National Institute of Standards and Technology
NREL – National Renewable Energy Laboratory
ORNL – Oak Ridge National Laboratory
PHEV – Plug-In Hybrid Electric Vehicle
PNNL – Pacific Northwest National Laboratory
SNL – Sandia National Laboratories
SRNL – Savannah River National Laboratory
USABC – United States Advanced Battery Consortium
USAMP – United States Automotive Materials Partnership

Table of Contents

VEHICLE TECHNOLOGIES.....	1
Advanced Combustion and Emission Control.....	1
<i>High Efficiency and Full Load Range Low-Temperature Combustion – Using Gasoline in a Diesel Engine</i>	2
<i>Dual-Fuel Combustion Enables Efficiency Improvement as High as 5% over Diesel Combustion</i>	3
<i>Hydrogen Engine Exceeds DOE Efficiency Targets</i>	4
<i>New Spray Model Accounts for Nozzle-Flow Effects</i>	5
<i>The Engine Combustion Network – A Collaboration on Engine Fuel Spray Research</i>	6
<i>Order of Magnitude Speedup of High-Fidelity Combustion Chemistry Simulation</i>	7
<i>HCCI Achieves 48% Indicated Thermal Efficiency</i>	8
<i>Optical Engine Research Rapidly Reveals How High-Efficiency RCCI Combustion Controls Burning Rates</i>	9
<i>New Understanding of EGR Cooler Fouling Mechanisms Provides Information for Improving Cooler Designs</i>	10
<i>Diagnostic Technology for Real-Time Measurement of Fuel in Oil Transferred to Industry</i>	11
<i>Spark-Assisted, High-Dilution, Stoichiometric HCCI with Ethanol-85 – Potential Path to Higher Efficiency</i>	12
<i>2011 Super Duty Diesel Truck with NO_x Aftertreatment</i>	13
<i>Turbocharger Design Improves Engine Efficiency</i>	14
Electrical and Electronics	15
<i>Advanced Integrated Electric Traction System Meets 2010 Technical Targets</i>	16
<i>Computational Prediction and Discovery of New Magnet Materials</i>	17
<i>Smaller, Highly Efficient Planar Bonded Power Electronics Module</i>	18
<i>Advances in Current Source Technology for Component Minimization and Integration</i>	19
<i>Design of Lightweight, Low-Cost, High Thermal Performance Inverter-Scale Heat Exchanger</i>	20
Electrochemical Energy Storage.....	21
<i>New Electrode Designs for Ultrahigh Energy Density</i>	22
<i>High-Voltage, Single-Ion Conducting Electrolytes</i>	23
<i>LiF-Anion Binding Agent Electrolytes for Enhanced Abuse</i>	24
<i>Fabrication of High-Energy Si Anodes Suitable for Large Format Lithium-Ion Batteries</i>	25
<i>High-Energy Composite Cathode Materials</i>	26
<i>Development of LiCoPO₄ Cathode and High-Voltage Electrolyte</i>	27
<i>Improved Performance of Doped High-Voltage Spinel Cathodes</i>	28

<i>Materials Search Engine with Lithium Electrode Explorer</i>	29
<i>Improving the Power of High-Energy, Lithium-Rich Cathodes</i>	30
<i>In Situ X-Ray Diffraction Development and Diagnostics of Cathode Materials</i>	31
<i>Determination of Aging Path Dependence in Batteries</i>	32
<i>A New Multi-Scale Model Framework to Help Industry Design Better Lithium-Ion Batteries</i>	33
<i>3M Silicon-Based Anode Exceeds Targets</i>	34
<i>Low-Energy Energy Storage System from Maxwell Technologies</i>	35
<i>High Energy Density Electrode Demonstrated for Electric Vehicle Batteries</i>	36
<i>PHEV Cell Projected to Meet USABC Calendar Life Goal</i>	37
<i>JCI Develops New Prismatic Cell and System Technology</i>	38
<i>Multifunctional Inorganic-Filled Separator for Large Format Lithium-Ion Batteries</i>	39
Fuel Cells	40
<i>Novel Characterization and Models Advance Understanding of Fuel Cell Performance Limitations</i>	41
<i>Fuel Cell System Cost Projected at \$49/kW</i>	42
<i>“Best in Class” Membrane Electrode Assembly Meets DOE Component Durability Requirements</i>	43
<i>3M High-Temperature Membrane Meets Durability Targets</i>	44
<i>Multi-Metallic Nanoparticles with Tailored Composition Reduce Cost, Improve Durability of Fuel Cell Catalyst</i>	45
<i>Novel Techniques for Measurement of Key Fuel Cell Transport Parameters</i>	46
<i>Two-Dimensional Dynamic Model Developed for Fuel Cell Freeze Start Operation</i>	47
<i>Novel Techniques Provide Insight into Fuel Cell Component Degradation</i>	48
<i>High Spatial Resolution of Neutron Imaging for Water Management Analysis in Fuel Cells</i>	49
Materials	50
<i>Development of the Ablation Casting Process for High-Volume Production</i>	51
<i>Friction Stir Spot Welding of Advanced High-Strength Steels II</i>	52
<i>Lower-Cost Carbon Fiber from Textile-Based Precursors</i>	53
<i>Enhanced Formability of Aluminum at Room Temperature Through Pulse-Pressure Forming</i>	54
<i>Ultrafine Grain Magnesium Foil and Sheet by Large Strain Extrusion Machining</i>	55
<i>Direct Compounding of Structural Engineering Composite</i>	56
<i>Lightweight Sealed Steel Fuel Tanks for Advanced Hybrid Electric Vehicles</i>	57
<i>Reliability Tools for Resonance Inspection</i>	58
Vehicle Systems Analysis	59
<i>Thermal Research to Improve Electric Vehicles</i>	60
<i>Idle Stop Vehicle Fuel Consumption Benefits Based on a Comprehensive Dynamometer Study</i>	61
<i>Electric Drive Vehicle Advanced Battery and Component Testbed</i>	62

CROSSCUTTING TECHNOLOGIES.....	63
Grid Interaction	63
<i>National Permit Template Can Help Make Homes Electric Vehicle-Ready</i>	<i>64</i>
<i>Auto-REM Module Developed for Effective Vehicle-Grid Communication</i>	<i>65</i>
<i>Electric Vehicle Measurement Device Developed for End Use Metering.....</i>	<i>66</i>
<i>Vehicle-Grid Interoperability (SAE J2931) Demo.....</i>	<i>67</i>
Codes and Standards.....	68
<i>Science-Based, Data-Driven International Standard for Fuel Quality Published.....</i>	<i>69</i>
Hydrogen Storage.....	70
<i>Selection of Ammonia Borane Hydrogen Storage System Concept.....</i>	<i>71</i>
<i>Reduced Size Improves Performance of Hydrogen Storage Materials.....</i>	<i>72</i>
<i>Alane: Improved Hydrogen Release and Regeneration</i>	<i>73</i>
<i>Development of Integrated System Model for the Evaluation of Hydrogen Storage Technologies</i>	<i>74</i>
FUEL TECHNOLOGIES	75
Fuel Pathway Integration	75
<i>Hydrogen Threshold Cost Apportionment.....</i>	<i>76</i>
<i>Infrastructure Costs for Biomass-Based Hydrogen Production</i>	<i>77</i>
<i>Hydrogen Fuel Station Cost Analysis for Early Transition</i>	<i>78</i>
Hydrogen Delivery	79
<i>Electrochemical Hydrogen Compressor Development</i>	<i>80</i>
Hydrogen Production	81
<i>Reforming of Bio-Oil for Production of Hydrogen.....</i>	<i>82</i>
<i>Significant Cost Reductions in Capital Costs of Electrolyzer Stacks</i>	<i>83</i>

Advanced Combustion and Emission Control



High Efficiency and Full Load Range Low-Temperature Combustion – Using Gasoline in a Diesel Engine

This project utilizes low cetane fuels like gasoline to create long ignition delays (more mixing time) to retain the efficiency and power density of a modern diesel engine while drastically reducing its NO_x emissions level.

Argonne National Laboratory

Researchers at Argonne National Laboratory (ANL) have demonstrated diesel-like efficiencies with significantly reduced oxides of nitrogen (NO_x) emissions by operating an automotive diesel engine on 87 RON gasoline. The significance of this project lies in its potential to reduce the cost and complexity of exhaust aftertreatment systems while drastically improving the fuel efficiency of the engine compared to conventional spark-ignited gasoline. In addition, only one fuel is required, which simplifies the entire operational strategy for the engine.

The GM 1.9 L Turbodiesel at ANL, shown in Figure 1, has been operated at a variety of speeds and loads in an effort to study the engine operating conditions that lead to maximum efficiency with the lowest possible emissions level. Parameters such as fuel injection timing, number of injections, Exhaust Gas Recirculation level, and turbo boost are being studied. In Figure 2, the Brake Specific Fuel Consumption (BSFC) and Brake Specific NO_x (BSNO_x) levels are shown for five separate engine operating conditions. The points shown in Figure 2 are 10% load (2 bar BMEP), 25% load (5 bar BMEP), 40% load (8 bar BMEP), 60% load (12 bar BMEP), and 90% load (18 bar BMEP). As shown, the efficiencies compare very favorably to diesel (especially in the mid-load ranges of 5–12 bar BMEP), while the NO_x emissions are significantly reduced for all cases. For the 18 bar BMEP condition, more work can be done to improve the existing 50% reduction over stock diesel. Mid-load conditions, where the engine operates most of the time in a vehicle, showed an almost 80% reduction in NO_x levels.

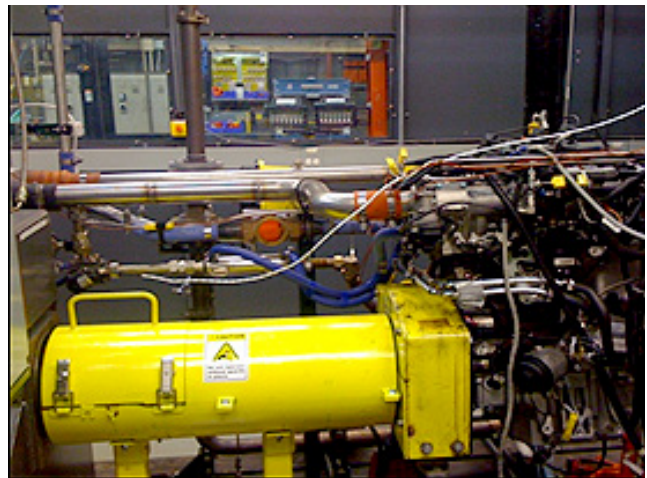


Figure 1. GM 1.9 L Turbodiesel Engine Test Cell

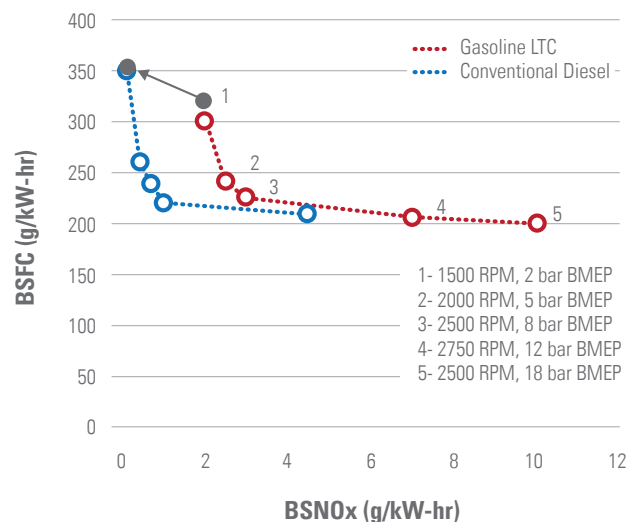


Figure 2. Stock Diesel and Gasoline LTC BSFC vs. BSNO_x (NO_x reduction is 50% or greater for all shown conditions)

Dual-Fuel Combustion Enables Efficiency Improvement as High as 5% over Diesel Combustion

Multi-cylinder engine research bridges simulation and single-cylinder research engine progress with production viable hardware to evaluate real-world challenges and opportunities of RCCI combustion.

Oak Ridge National Laboratory and University of Wisconsin

Reactivity controlled compression ignition (RCCI) combustion involves the in-cylinder blending of two fuels with differing reactivity to tailor the reactivity of the fuel charge for improved control of the combustion process. Simulations and single-cylinder engine experiments at the University of Wisconsin have shown the approach's potential for high indicated efficiencies with very low oxides of nitrogen (NO_x) and particulate matter (PM) emissions. The objective of this study was to understand the potential of RCCI under more real-world conditions in a light-duty, multi-cylinder engine (MCE) with production viable hardware. MCE experiments explored fuel injection strategy, dilution levels, piston geometry (including compression ratio), and fuel properties.

The MCE experiments demonstrated RCCI's potential to produce very low NO_x and PM emissions while achieving diesel-like or higher brake thermal efficiency (BTE), as much as 5% higher at higher loads, across a wide range of steady-state operating points consistent with the light-duty drive cycles (Figure 1). NO_x emissions were approximately an order magnitude lower than conventional diesel combustion (CDC). Carbon monoxide (CO) and hydrocarbon (HC) emissions were observed to be much higher than CDC, as well as more comparable to levels seen in gasoline engines. The combination of high CO and HC emissions with low exhaust gas temperatures is a significant challenge due to the limited effectiveness of current oxidation catalysts at low temperatures.

Other challenges for MCE implementation include matching turbo-machinery with high exhaust gas recirculation (EGR) and providing sufficient EGR cooling with production viable hardware. EGR is important for additional control of in-cylinder pressure rise rates and

combustion noise along with reactivity (octane) stratification at higher engine loads, but can be challenging to implement.

Ethanol-gasoline blends were investigated to better understand the potential of biofuels. The high octane and charge cooling effects of ethanol were found to have the benefit of expanding RCCI operation with reduced or no EGR (Figure 1). This effectively allows for higher load operation with better matching of turbo-machinery and reduced heat rejection requirements, which are more consistent with production viable hardware.

This data is being used in combination with a vehicle model to estimate the drive-cycle fuel economy/emissions potential of RCCI operation.

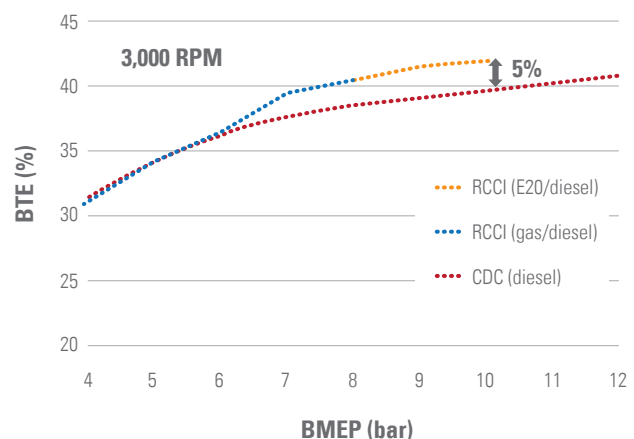


Figure 1. Increased brake thermal efficiency (BTE) of RCCI (blue) using gasoline and diesel compared with CDC (red) of up to 5% as engine load is increased at 3,000 RPM. Load expansion of RCCI with E20 shown in green and labeled.

Hydrogen Engine Exceeds DOE Efficiency Targets

A hydrogen internal combustion engine concept utilizing advanced direct injection achieves 45.5% peak brake thermal efficiency and is expected to meet stringent emissions goals without the need for any aftertreatment system based on vehicle simulations.

Argonne National Laboratory, Sandia National Laboratories, and Ford Motor Company

In a collaborative effort, researchers at Argonne National Laboratory (ANL) developed and demonstrated an internal combustion engine (ICE) fueled with hydrogen (H_2) that meets the U.S. Department of Energy's (DOE's) 2010 light-duty efficiency and emissions targets. These targets—including a peak brake thermal efficiency (BTE) of 45% and a part load efficiency of 31% while meeting Tier 2 Bin 5 emissions—are extremely challenging for automotive-size combustion engines.

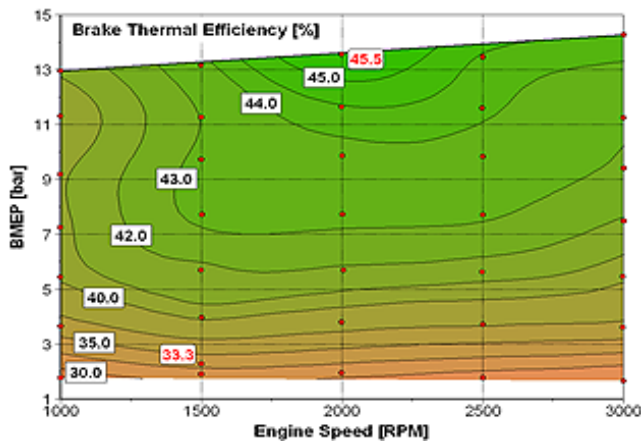


Figure 1. BTE map of the direct injection hydrogen combustion engine

Recent results covering the typical operating range of an ICE estimate the peak BTE at 45.5% with a part load efficiency of 33.3%. The H_2 ICE concept utilizes advanced direct injection technology with injector designs that were specially developed to meet the challenging goals of this project. Due to the absence of carbon in the fuel, oxides of nitrogen (NO_x) are the only critical pollutant from H_2 combustion engines. However, a trade-off between efficiency and NO_x emissions

was discovered. Vehicle simulations were performed based on steady-state maps using ANL's Autonomie software. These simulations suggest that this H_2 engine concept could achieve NO_x emissions levels below 0.02 grams per mile (Tier 2 Bin 2) in a mid-size sedan without any aftertreatment system. Even with 3 L displacement and without hybridization, the vehicle would achieve an estimated equivalent fuel economy (FE) of 39 mpg, thus exceeding 2016 Corporate Average Fuel Economy targets. If the engine was further downsized, FE is estimated to reach more than 45 mpg.

The success of this DOE-funded activity is based on joint research with ANL focused on experimental work, multi-dimensional engine modeling, and vehicle simulations; Sandia National Laboratories performing experiments on an optical engine; and Ford Motor Company providing hardware and technical guidance.

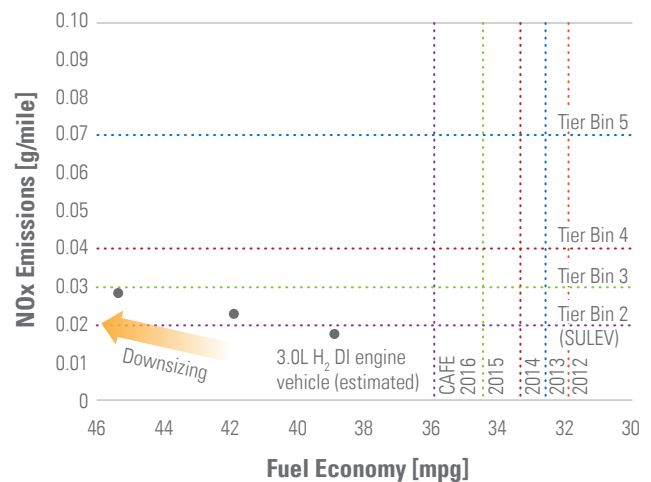


Figure 2. Estimated FE and NO_x emissions of a hydrogen combustion engine powered mid-size vehicle with no NO_x emissions aftertreatment system

New Spray Model Accounts for Nozzle-Flow Effects

A new primary breakup spray model accounts for nozzle-flow effects such as cavitation and turbulence, in addition to aerodynamic breakup. This model is applied to capture the influence of orifice geometry changes on spray and combustion development.

Argonne National Laboratory, University of Illinois at Chicago, and Caterpillar

Nozzle orifice geometry is known to influence the flow inside a nozzle, which in turn affects spray development, thus impacting combustion and emission processes. In the past, modeling studies focused on the influence of nozzle orifice geometry and fuel property effects on the flow inside the orifice only, mainly due to the lack of a suitable primary breakup model that accounted for differences in nozzle flow.

mass in the core (peak of the Gaussian curve) and dispersion (tail of the plot) are accurately captured by only the KH-ACT model. The KH breakup model (which only accounts for aerodynamic breakup) underpredicts spray dispersion and overpredicts spray mass in the core. The KH-ACT model enables investigation of the influence of nozzle orifice geometry and fuel properties on spray (liquid length), combustion (flame lift-off length), and emission characteristics (Figure 2). This enhanced primary breakup model provides engine manufacturers with a more predictive tool for effective injection system design.

The success of this activity was based on joint research with ANL focused on experimental work and multi-dimensional spray-combustion modeling; the University of Illinois at Chicago performing spray modeling; and Caterpillar providing hardware and support.

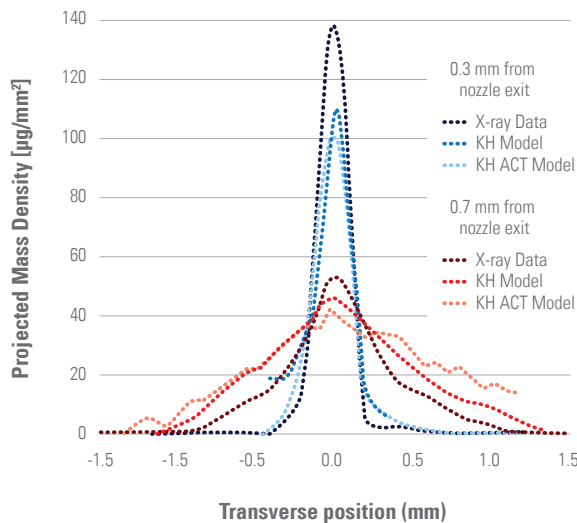


Figure 1. Comparing the KH-ACT breakup model and a standard primary breakup model (KH) against X-ray radiography data from ANL

In a collaborative effort, researchers at Argonne National Laboratory (ANL) developed the Kelvin-Helmholtz Aerodynamic Cavitation Turbulence (KH-ACT) model—a physics-based primary breakup spray model that accounts for in-nozzle flow effects such as cavitation and turbulence, as well as aerodynamic breakup. Development of the KH-ACT model was based on X-ray radiography data from ANL, which provides quantitative near-nozzle fuel distribution (Figure 1). Spray

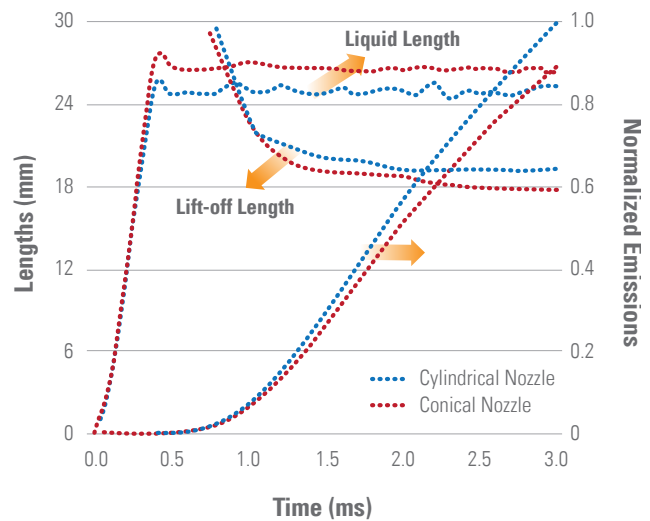


Figure 2. The KH-ACT model capturing the influence of nozzle orifice geometry on spray, combustion, and emission characteristics

The Engine Combustion Network – A Collaboration on Engine Fuel Spray Research

An international collaboration and Web database on engine fuel spray combustion research is established to provide highly leveraged research to accelerate the development of predictive engine spray models.

Sandia National Laboratories

All future high-efficiency engines are likely to have fuel directly sprayed into the engine cylinder. Engine developers agree that a major barrier to the rapid development and design of these high-efficiency, clean engines is the lack of accurate fuel spray computational fluid dynamic (CFD) models. The spray injection process largely determines the fuel-air mixture processes in the engine, which subsequently drives combustion and emissions. More predictive spray combustion models will enable rapid design and optimization of future high-efficiency engines, providing more affordable vehicles and also saving fuel.

To address this barrier, Sandia National Laboratories established a multi-institution, international collaboration called the Engine Combustion Network (ECN), which aims to improve spray understanding and develop predictive spray models. ECN provides highly leveraged, vetted datasets for spray model development by utilizing contributions from many experimental and modeling participants.

As shown below, advanced diagnostic capabilities are applied using a set of identical fuel injectors at specialized facilities throughout the world. Measurements needed to rigorously evaluate spray models include internal injector conditions, droplet formation, mixing and vaporization, ignition, combustion, and pollutant formation. The massive dataset assembled from the unique contributions of all participants is made available online (www.sandia.gov/ECN) to facilitate CFD model evaluation. To date, multiple groups have provided data, performed simulations at well-defined conditions, and compared results side-by-side at the first ECN workshop on May 13–14, 2011.

ECN is now targeting other spray types and conditions and formulating plans for full-engine combustion system datasets for model validation.

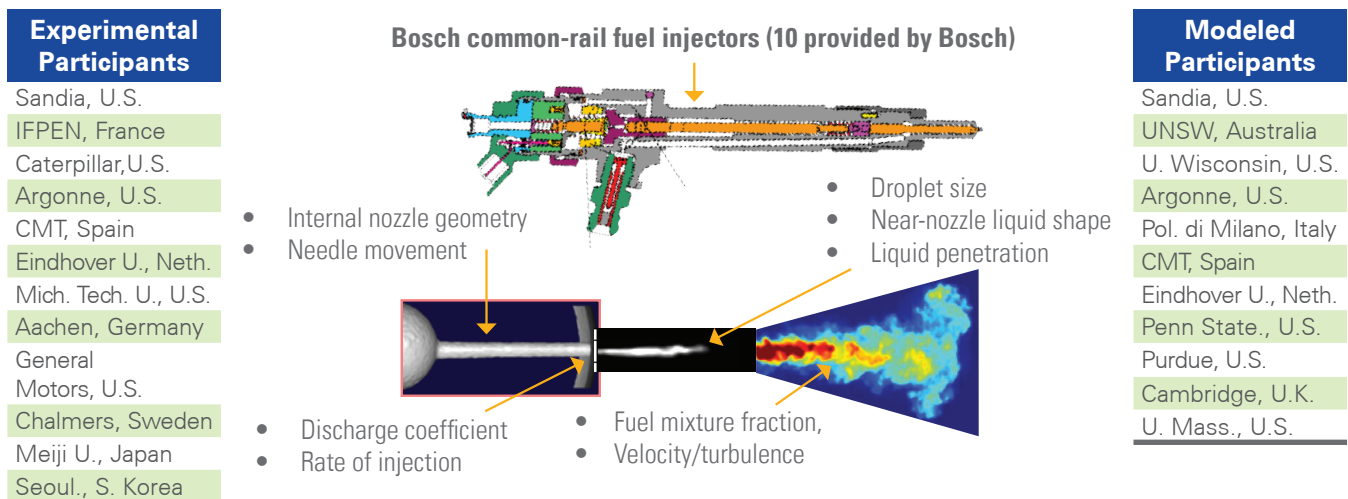


Figure 1. List of international ECN experimental and modeling participants and example diagnostics (see bullets) to quantify engine spray combustion

Order of Magnitude Speedup of High-Fidelity Combustion Chemistry Simulation

New approaches to computing complex fuel chemistry enable faster, more accurate simulations for combustion system design of new high-efficiency, low-emission engines.

Lawrence Livermore National Laboratory

The Lawrence Livermore National Laboratory (LLNL) Combustion Chemical Kinetics and Simulation group has pioneered the development of combustion models that include very detailed chemistry for combustion of real fuels. These models include all of the possible reactions that can occur for a hydrocarbon fuel—from the fuel molecules, through the intermediate reaction products, to the final products that evolve from the combustion process.

For long-chain hydrocarbons representative of diesel fuel (e.g., cetane), there can be thousands of different molecules and tens of thousands of chemical reactions affecting the rate of combustion.

While these detailed chemical kinetic models can give accurate prediction of ignition, combustion calculations with large realistic fuel models require significant computing resources. LLNL has put significant effort into speeding up simulations of combustion chemistry by developing more efficient computational solvers. One approach the laboratory applies to speedup combustion chemistry simulation is developing better algorithms for conventional computer architectures.

LLNL also developed software applications for combustion simulation on low-cost, high-performance, desktop-scale workstations that contained graphical processing units (GPUs). The GPUs used by desktop computers for video rendering and gaming are essentially very specialized, compact, inexpensive supercomputers that can be adapted for scientific

simulations. Demonstrated in Figure 1 is an 11-fold speedup for ignition delay calculation of a large hydrocarbon molecule (methyl-decanoate). The speedup is achieved with the LLNL kinetics solver running on a desktop computer equipped with a GPU. Opportunities exist for much more speedup through continued solver algorithm development and coupling these solvers to 3D engine combustion software. This speedup can therefore be directly applied to 3D simulations, giving designers access to supercomputer performance at the price of a desktop.

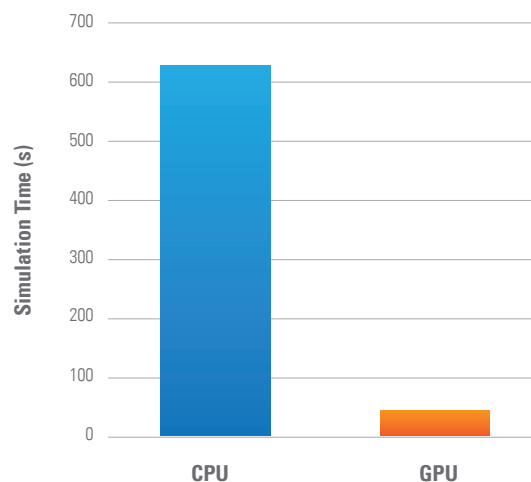


Figure 1. GPU-based chemistry solvers have demonstrated 11x speedup over CPU-based solvers for ignition delay calculations

HCCI Achieves 48% Indicated Thermal Efficiency

Indicated thermal efficiencies of 48% with ultra-low NO_x and soot emissions have been demonstrated in the lab over a range of loads in an engine using HCCI combustion, with fuels typical of U.S. pump gasolines.

Sandia National Laboratories

Improving the efficiency of internal combustion engines is critical for meeting global needs to reduce petroleum consumption and carbon dioxide emissions. Homogeneous Charge Compression Ignition (HCCI) engines have a strong potential for contributing to these goals, as they have high efficiencies and very low engine-out oxides of nitrogen (NO_x) and particulate emissions.

Thermal efficiencies of HCCI engines are well above those of spark-ignition engines, typically comparable to diesel engines with similar displacement. Moreover, recent research has shown that HCCI efficiencies are higher for intake-boosted operation, and by applying partial fuel stratification in combination with intake boost, efficiencies can be increased even further.

Motivated by these findings, the potential for improving HCCI's already high efficiencies has been systematically examined for a range of intake boost pressures and loads using fuels that are representative of U.S. pump gasolines. Figure 1 presents the key results of this study. The points connected by the black curve in the lower part of the figure show the thermal efficiencies achieved in earlier work, which showed the potential of intake boosting to substantially expand the high-load limit of gasoline-fueled HCCI. As shown, thermal efficiencies typically were about 44%, reaching 46.8% at 16.3 bar IMEP (indicated mean effective pressure). Although efficiencies of about 44% are quite respectable for an engine of this displacement (0.98 liters/cylinder), the increased efficiency at 16.3 bar IMEP suggests that higher efficiencies may be possible at other loads.

The current study systematically examined the effects of engine operating parameters, including intake temperature, Exhaust Gas Recirculation, fueling rate,

engine speed, intake pressure, and fueling strategy (premixed versus partial fuel stratification). As shown in Figure 1, with appropriate selection of operating parameters, thermal efficiencies of 47%–48% can be achieved for loads ranging from 8–16 bar IMEP. Adjustments in several of these operating parameters improved efficiency, with the two most significant being: (1) reducing the load 10%–20% below the maximum possible for a given boost pressure, and (2) using partial fuel stratification to slow the combustion. These improved efficiencies could equate to an increase in fuel economy of about 9% compared to the previous efficiency of 44%. All high-efficiency points shown have no engine knock, NO_x emissions a factor of 10 or more below Tier 2, Bin 5 levels, and near-zero soot emissions.

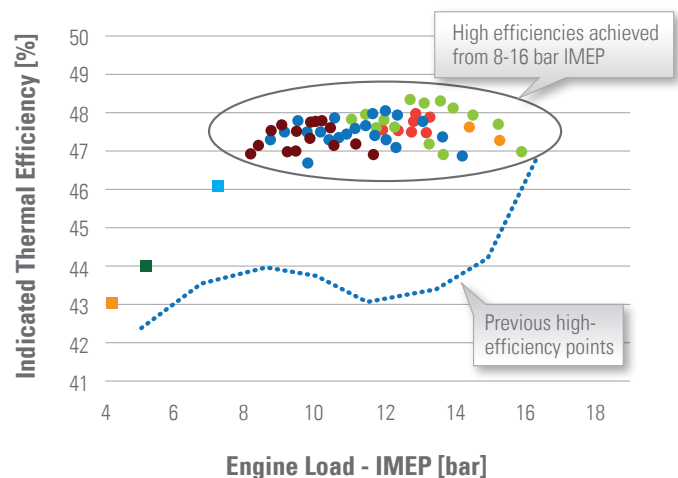


Figure 1. Indicated thermal efficiencies of about 48% have been achieved for loads from 8–16 bar IMEP, for a potential fuel economy improvement of about 9% compared to previous high efficiencies of approximately 44%, for gasoline-fueled HCCI. Fuels representative of pump gasolines used for all points.

Optical Engine Research Rapidly Reveals How High-Efficiency RCCI Combustion Controls Burning Rates

Images of fuel mixing and combustion from inside an engine show how dual-fuel injection (both high-octane gasoline and low-octane diesel) controls the fuel burning rate to enable new high-efficiency RCCI operation.

Sandia National Laboratories and University of Wisconsin

Engine designers have long known that burning fuel more quickly increases efficiency. However, with quick burns, engines become more prone to uncontrolled pressure spikes. The spikes (see red and blue curves in Figure 1) create loud noise (knock) and can even damage the engine. A lower burning rate is desirable, so most engines avoid rapid burning, even at the cost of lower efficiency.

A new type of dual-fuel (gasoline and diesel) engine is being developed to control the burning rate and avoid pressure spikes while maintaining high efficiency. The strategy depends on the different chemical reactivities of high-octane gasoline and low-octane diesel fuels, hence the name “Reactivity-Controlled Compression-Ignition (RCCI).” Practical engine tests show that tailored injections of the two fuels are crucial to being able to control the burning rate. Although, the tests don’t reveal how dual-fueling controls burning rates, nor do they reveal how to design the best RCCI engine.

To understand how dual-fueling works, fuel mixing and RCCI combustion were imaged from inside a special “optical” engine. The engine and optical diagnostics were developed over the course of two decades to understand and improve diesel combustion. Using these tools, a high degree of RCCI understanding was developed within one year.

In Figure 1, a time sequence of combustion luminosity (the bright areas in the three images) shows where combustion is occurring inside the engine. Laser-induced fuel-fluorescence measurements also provide the pre-combustion octane number distribution—an indicator of fuel reactivity. Octane number color-contour maps are overlaid on each black-and-white luminosity image. Changes in bright regions from the first

image (top) to the last show that low octane number (higher reactivity) regions ignite first, followed by higher octane number (lower reactivity) regions. The net result is a controlled burning rate (green curve) that is much slower than burning spikes obtained with either gasoline or diesel alone (blue and red curves).

The full set of optical measurements acquired shows how fuel injection can be adjusted to tailor the octane map and optimize performance for a range of operating conditions. Furthermore, the measurements support development of computer models that are essential for engine design.

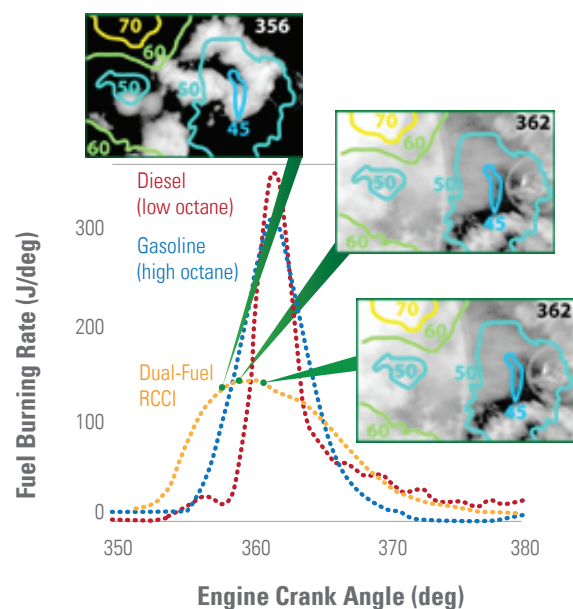


Figure 1. Graph: Fuel burning rates with unwanted spikes for either gasoline or diesel fuels alone, and lower burning rate for dual-fuel RCCI. Images: Contours of measured octane number overlaid on luminosity images that show the progression of combustion.

New Understanding of EGR Cooler Fouling Mechanisms Provides Information for Improving Cooler Designs

Fundamental studies of EGR cooler fouling mechanisms suggest that use of multiple EGR coolers in parallel, or inclusion of, an oxidation catalyst may help avoid plugging failures in some applications.

Oak Ridge National Laboratory

Using high levels of cooled exhaust gas recirculation (EGR) is a key aspect of many advanced combustion technologies, as well as a mainstay for controlling oxides of nitrogen (NO_x) emissions from diesel engines. In most advanced combustion processes, reductions in NO_x and particulate matter (PM) emissions come at the expense of increased levels of hydrocarbon (HC) and carbon monoxide emissions.

Fouling of the EGR cooler by HC and PM from the exhaust gas stream (shown in Figure 1) can reduce the performance of the cooler in a matter of hours, causing the temperature of the EGR stream to rise, potentially producing higher NO_x emissions and changing the dynamics of the combustion process.

Research has shown that extended operation at low-deposit temperature conditions (i.e., low loads and speeds) can result in a deposit layer that is less insulative than those formed at higher temperatures because the void volume is lower and substantially filled with condensed HCs. The increased thermal conductivity of low-temperature deposits enables continued fouling at relatively high rates compared to more insulative deposit layers. High HC concentrations relative to the PM concentration in the gas stream, which is typical of advanced combustion processes, can increase the likelihood of this situation. Experience has shown that incidences of plugging in the field are most often associated with deposit layers high in HCs, which results in a less-frangible deposit that can become cohesive enough to produce thick deposits that can inhibit the EGR flow through the cooler.

A key aspect of high rates of deposition of HCs relative to PM is the gas flow velocity through the cooler during low-temperature conditions. If the velocity is relatively low compared to the maximum designed velocity for the cooler, deposition tends toward HC-dominated layers and results in an increased risk of plugging. Thus, applications that operate frequently at cold start, low-load, or idle conditions are highly likely to experience EGR cooler plugging, particularly if the EGR cooler design process focuses primarily on high-temperature conditions. Potential design directions that can reduce the risk of plugging in these circumstances include the use of an oxidation catalyst upstream of the cooler or multiple EGR coolers with one cooler sized and used for low-load conditions to avoid plugging and another sized for moderate and high EGR-demand conditions.

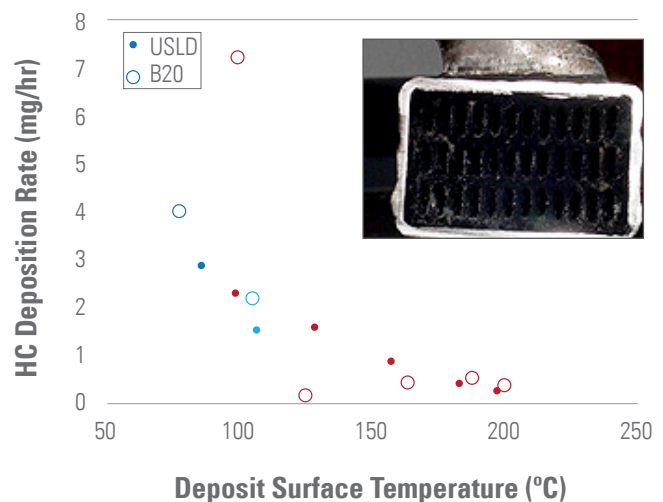


Figure 1. HC deposition rate versus temperature for 0.05 kg/min/tube EGR stream containing 100 PPM HCs. Inset shows a fouled EGR cooler.

Diagnostic Technology for Real-Time Measurement of Fuel in Oil Transferred to Industry

A research tool developed at Oak Ridge National Laboratory to measure fuel dilution of oil in advanced combustion technology engines via a fiber-optic probe and laser-induced fluorescence has been licensed to Da Vinci Emissions Services.

Oak Ridge National Laboratory

In a Cooperative Research and Development Agreement project with Cummins, Inc., Oak Ridge National Laboratory developed a unique tool to assist engineers who develop calibrations for fuel injection in engines. The tool is 30 times more sensitive than the conventional method used to measure fuel dilution of oil. This advanced tool assists engineers in the automotive and trucking industries with complex technical challenges that must be met to develop future engines and vehicles that improve fuel economy while meeting stringent emission regulations.

The tool monitors the amount of fuel entering the engine oil via a fiber-optic probe inserted into the oil system. Fuel dilution of oil can occur as fuel injection techniques push the boundaries in search of more fuel-efficient combustion; additional challenges also exist in creating custom combustion processes to enable management of emission control devices. Avoiding fuel dilution for these advanced combustion techniques is critical to ensuring durable engine products, and the fuel in oil tool provides a real-time method for measuring fuel dilution.

The fuel in oil measurement technology operates on the principle of laser-induced fluorescence spectroscopy. Light from a laser is launched into a fiber optic, which carries the light to the oil sample. Fluorescent light from the oil and a dye added to the fuel are collected and analyzed to determine the amount of fuel in the oil.

Previous techniques to measure fuel dilution of oil required hours of engine testing and additional days of analysis via a gas chromatography technique. The new fuel in oil tool gives measurement of fuel dilution in the course of minutes, providing rapid feedback to engine developers. The diagnostic is enabling engineers to reduce development time of fuel-efficient engine technologies.

The technology was transferred to Da Vinci Emission Services, Ltd. of San Antonio, Texas. The company is marketing a product based on the technology to a variety of engine development companies.

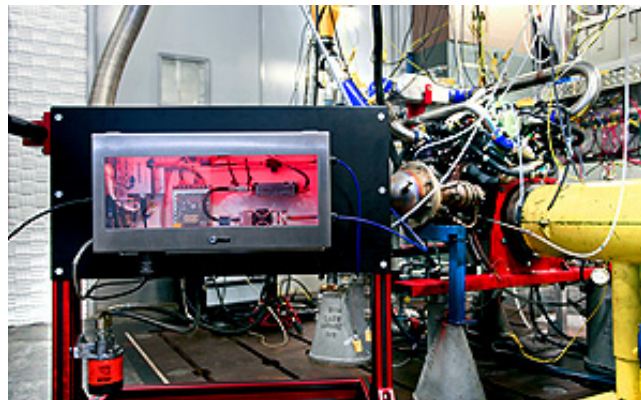


Figure 1. Photo of Da Vinci Emission Services' DAFIO product for fuel in oil measurement

Spark-Assisted, High-Dilution, Stoichiometric HCCI with Ethanol-85 – Potential Path to Higher Efficiency

The fuel properties of ethanol combined with advanced combustion increase efficiency up to 17% and expand operable load range.

Oak Ridge National Laboratory

By using E85 under advanced combustion conditions (30.5%–38.5% indicated thermal efficiency [ITE]), a 17% ITE was achieved relative to conventional spark-ignited (SI) operation with gasoline. Additionally, efficiency improvements were achieved over a wide range in load, from 2.5–7.0 bar NMEP (net indicated mean effective pressure), making the efficiency improvements applicable over a large portion of the engine map.

Experiments were conducted on a 2.0 L GM Ecotec engine with direct fuel injection. The engine has been highly modified to enhance versatility for research purposes. Modifications include conversion to single-cylinder operation, a fully flexible hydraulically actuated valve train, and increased compression ratio.

The advanced combustion strategy uses mixed-mode combustion to take advantage of the desirable characteristics of conventional SI combustion and homogeneous charge compression ignition (HCCI). Combustion of a dilute mixture of fuel and air is initiated with a spark, consuming up to 40% of the fuel. The remaining fuel is consumed rapidly in a manner similar to HCCI. As a result, the combustion strategy has been named spark assisted-HCCI (SA-HCCI).

Efficiency advantages of SA-HCCI relative to SI combustion are due to unthrottled operation and rapid combustion. Advantages relative to HCCI include enhanced control of combustion, compatibility with emissions control devices due to stoichiometric operation, and an expanded operational load range. HCCI studies typically report a maximum load of approximately 4.0 bar NMEP, whereas SA-HCCI can be operated up to

7.0 bar NMEP with E85. As a result, efficiency benefits of SA-HCCI can be realized over a larger portion of the engine map than pure HCCI operation.

While this operating strategy is also applicable to gasoline, SA-HCCI operation with E85 produces higher ITE and higher maximum NMEP, as can be seen in Figure 1. The higher ITE with E85 can be attributed to inherent thermochemical property differences between gasoline and ethanol, including the higher latent heat of vaporization. The increase in NMEP for E85 can be attributed to higher octane, which allows for more optimized combustion phasing with acceptable pressure rise rates.

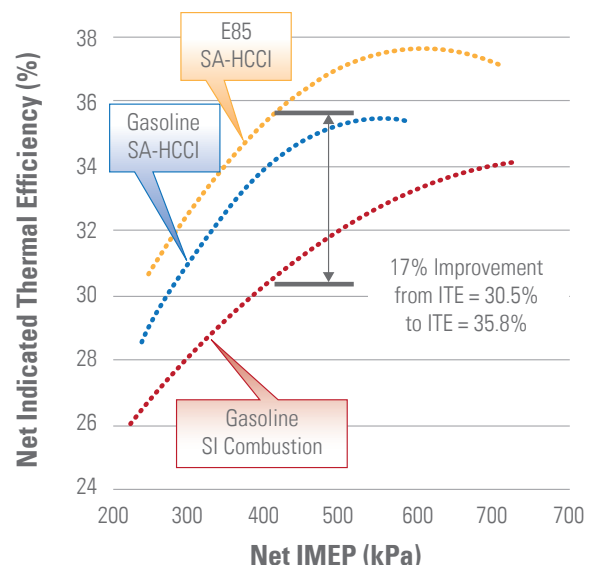


Figure 1. Net ITE at 2,000 rpm as a function of NMEP for SI combustion with gasoline and SA-HCCI combustion with gasoline and E85

2011 Super Duty Diesel Truck with NO_x Aftertreatment

Diesel engine aftertreatment: Minimizing NO_x emissions with SCR.

Ford Motor Company

Ford's 2011 Super Duty diesel truck—which utilizes aftertreatment technology jointly developed by Ford and the U.S. Department of Energy (DOE)—delivered a multitude of firsts for the company. It was the first Ford diesel engine developed entirely in-house, the first to operate on B20 (a blend of 20% biofuel, 80% petroleum diesel), and the first to comply with stringent 2010 emissions standards that require a reduction in oxides of nitrogen (NO_x) by more than 80% compared to 2007 emissions levels.

To meet these new standards, Ford had to dramatically reduce the NO_x emissions of its diesel vehicles. Through cost-sharing, DOE supported Ford's development of an aftertreatment technology, which was not popularly favored. Lean NO_x control for diesels was seen as a large risk; in turn, the cost-share was set at 65% DOE and 35% Ford. Ford led the engineering effort with partners ExxonMobil and FEV. Under the code name "Ultra Clean Fuels," the project lasted from 2001 to 2005 and was considered a success.

The system—urea-based selective catalytic reduction (SCR)—is the most cost-effective technology available to remove enough NO_x from diesel exhaust to comply with the new emissions guidelines, and Ford was ready to take on the after-combustion investment. Although relatively new to the United States, SCR has gained popularity in Europe over the last five years. Within three years of its introduction to Europe, the SCR-equipped vehicles reduced fuel costs by the equivalent of nearly one half billion dollars, saved more than 74 million gallons of diesel, and spared the environment from more than 880,000 tons of carbon dioxide.

The Ford-patented diesel aftertreatment system is a three-stage process. The first step occurs when the exhaust stream enters the diesel oxidation catalyst. Hydrocarbons and carbon monoxide are converted to water and carbon dioxide. Second, the NO_x is minimized through SCR by dosing diesel exhaust fluid (DEF), an aqueous solution of urea that is transformed to ammonia within the exhaust. The ammonia enters the SCR module, which contains a non-precious metal catalyst, and NO_x is converted to harmless nitrogen and water. Finally, the diesel particulate filter traps any soot. Several system aspects, including catalyst types, urea injection concepts, and filter regeneration strategies, had origins in the Ford/DOE program.

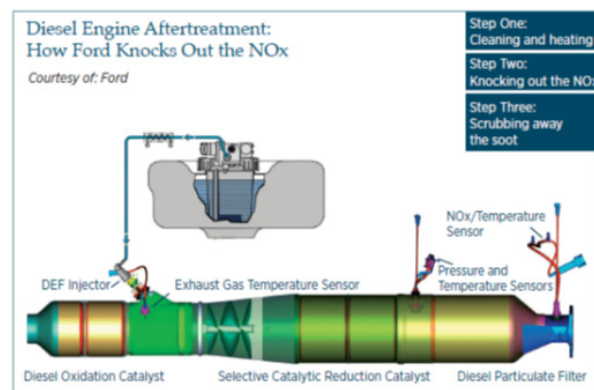


Figure 1. Three-stage diesel engine aftertreatment system

Turbocharger Design Improves Engine Efficiency

An advanced turbocharger design with active casing treatment is a truly technical breakthrough. When tested, together with a mixed flow turbine, it demonstrates a 3% efficiency improvement at part load and full load, along with a 30% increase in rated power. U.S. Patent #0173975 awarded July 21, 2011.

Ford Motor Company, Wayne State University, and ConceptsNREC

A conventional turbocharger compressor may have one casing treatment on the compressor cover to extend surge margin (a failure mode at low flow) and choking capacity (a performance limiting factor at high flow). However, to optimize the efficiency of the turbocharger impeller (shown in yellow in Figure 1), a single-slot casing treatment cannot serve both mass flow regions of operation. Computational fluid dynamics studies revealed that to have optimal performance under each mass flow condition, the injection slot in the compressor cover needs to be in a different location. Having separate slots for surge and choke control, and actively switching between them (Figure 1), enables an efficient design of the compressor impeller without sacrificing surge margin or extended flow capacity near the choke condition.

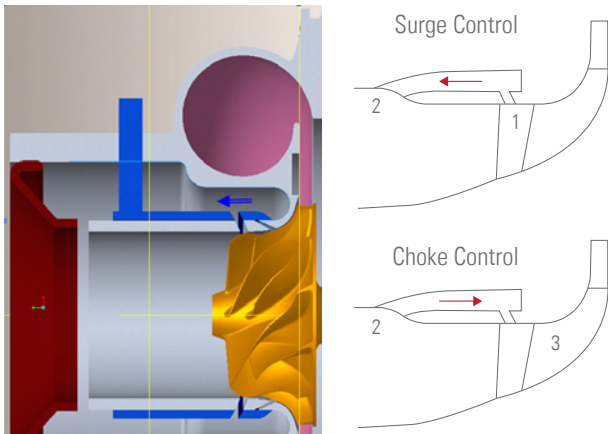


Figure 1. Active casing treatment shown in blue. Opening LH slot controls surge, opening RH slot controls choke.

Together with an advanced mixed flow turbine design, engine dynamometer testing confirmed the predicted improvement in performance and efficiency over the base turbocharger:

- 3%–5% reduction in Brake Specific Fuel Consumption, a measure of engine efficiency, at the same level of feed gas oxides of nitrogen (Figure 2)
- 30% increase in rated power and peak torque, while reducing turbine inlet temperature (Figure 3).

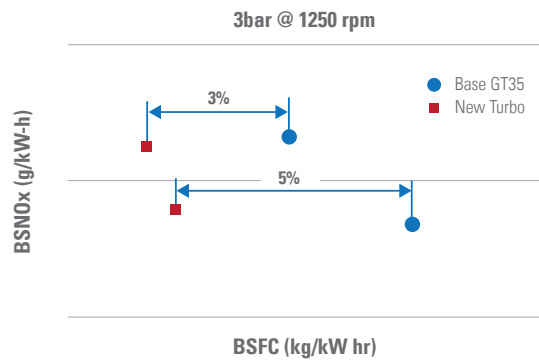


Figure 2. Engine dynamometer tests show improved Brake Specific Fuel Consumption, a measure of efficiency, at part load conditions.

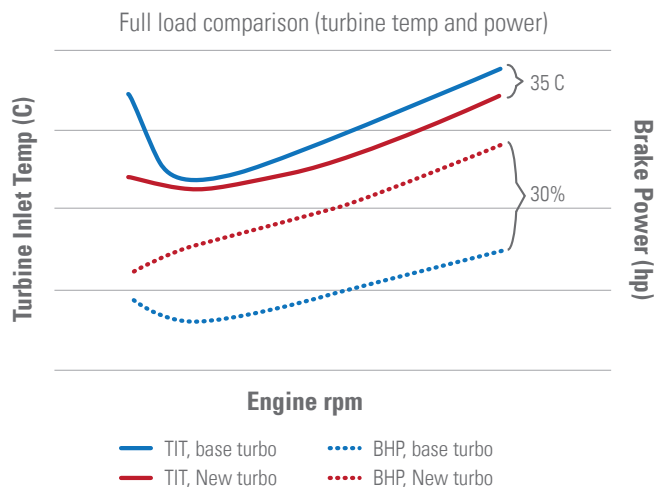


Figure 3. Engine full load performance improves substantially over base turbocharger design.

Electrical and Electronics



Advanced Integrated Electric Traction System Meets 2010 Technical Targets

New integrated electric traction system successfully meets all 2010 cost, weight, volume, and efficiency targets while also meeting automotive application requirements.

General Motors

The U.S. Department of Energy (DOE) elaborates the compelling need for a commercialized, competitively priced electric traction drive system to proliferate the acceptance of hybrid electric vehicles (HEVs), extended range electric vehicles, electric vehicles, and fuel cell vehicles in the market. The objective of this particular program is to develop advanced technologies for an integrated Electric Traction System (ETS) that is capable of 55 kW peak power and 30 kW of continuous power. The technology should also be scalable to 120 kW peak power and 65 kW of continuous power. These performance metrics must be achieved while meeting the aggressive technical targets for cost, weight, volume, and efficiency. General Motors not only achieved all 2010 targets, but also achieved 2015 targets for weight and volume (shown in Figure 1).

	2010	GM
Cost, \$/kW	<19	<16
Specific power, kW/kg	>1.06	>1.2
Power density, kW/L	>2.6	>3.5
Efficiency	>90%	>90%

Figure 1. Technical Target vs. Project Results

This project investigated a wide range of technologies, including ETS topologies, components, and interconnects. Each technology and its validity for automotive use were verified. The technologies were then integrated into a high-temperature ETS design. This ETS met all of DOE’s 2010 cost, weight, volume, and efficiency objectives, as well as the 2015 specific power and power density objectives. Under this work, GM assessed 29 technologies; investigated 36 configurations/types power electronics and electric machines; filed 41 patents; and ensured technology compatibility with vehicle production.

Additionally, the ETS developed was rated for 105C coolant, allowing the elimination of the secondary coolant loop currently on HEVs. Verification of ETS performance was done by Oak Ridge National Laboratory through witness testing at GM (shown in Figure 1).

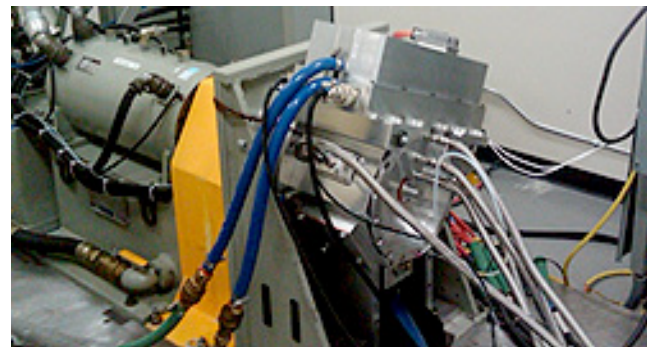


Figure 2. Dyno Evaluation of Electric Traction System

In addition to the development of a high-temperature ETS, the development of industrial suppliers took place because of this project. GM has worked closely with suppliers to develop components for ETS technology. Components that have been the focus of this project are power modules, capacitors, heavy copper boards, current sensors, and gate drive and controller chip sets. Working with suppliers, detailed component specifications were developed. Current, voltage, and operation environment during the vehicle drive cycle was evaluated to develop higher resolution/accurate component specifications. This improvement in specifications allowed for lower-cost components to be developed and the number of viable suppliers to be increased.

Computational Prediction and Discovery of New Magnet Materials

Computational algorithm development represents a new paradigm to accelerate the materials discovery process for non-rare earth magnets.

Ames Laboratory

Taking a page from the drug industry's playbook, computational materials discovery now is being applied to the pursuit of superior permanent magnetic (PM) materials that do not contain rare earth (RE) elements, which are quickly rising in global strategic importance. Ames Laboratory has developed computational algorithms and codes to perform supercomputer assisted phase diagram exploration and materials structure prediction and discovery, especially for iron-based alloys. This breakthrough speeds up the search process by at least 1,000 times, making it possible to perform accelerated computational studies to identify candidate chemical compositions and structures that have desirable properties.

PMs are essential in hybrid and electric vehicles for drive motors, accessory motors, sensors, and actuators. Magnets also are vital in the most compact and powerful electrical generators driven by wind, water, and conventional fossil fuels. Because of the role such devices play in new energy economies, there is a skyrocketing demand for strong PM materials. With the dominant market position of China in the supply of RE ore, pure RE oxides and metals, and—increasingly—finished RE products, there is a strategic national need to find replacement materials.

Ames' algorithm development represents a new paradigm to accelerate the discovery process. This computational approach is effectively coupled with a strong experimental synthesis effort in the Beyond Rare Earth Magnets partnership, supplying mutual feedback to greatly speed up the materials discovery process far beyond old-fashioned, trial-and-error methods. The algorithms, code, and experience gained in this effort will be directly applicable to other accelerated materials discovery efforts as well.

Using the cluster computers available at Ames Laboratory, an initial structure search for Fe-Co binary alloys has successfully predicted structures at a range of compositions that have energies lower than those structures proposed in the literature (see Figure 1). With the help of new peta-scale computing power from Oak Ridge National Laboratory, Ames hopes to be able to explore much larger structural space, including Fe-Co-X alloys. Ames is confident that many new promising structures of Fe-based compounds can be discovered from these calculations to guide experimental design and synthesis of new non-RE PMs.

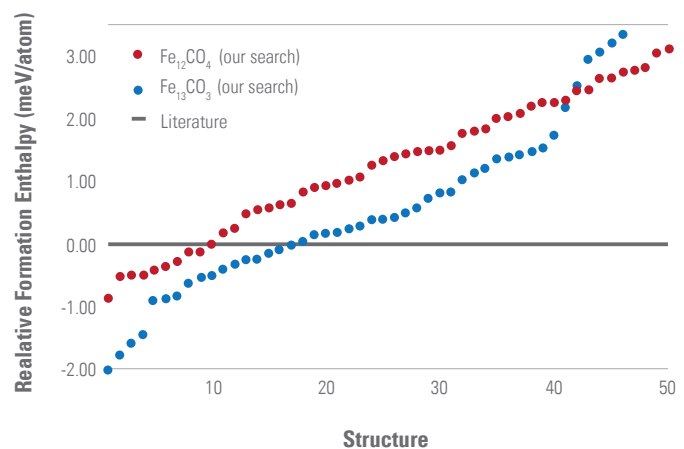


Figure 1. Structures of $\text{Fe}_{12}\text{Co}_4$ and $\text{Fe}_{13}\text{Co}_3$ obtained from a genetic algorithm search have energies lower than the best structures proposed in literature

Smaller, Highly Efficient Planar Bonded Power Electronics Module

An advanced automotive power module with double-sided planar interconnection and integrated heat exchangers has been developed at ORNL. The packaging technology features comprehensive improvements in efficiency, density, and cost.

Oak Ridge National Laboratory

Oak Ridge National Laboratory (ORNL) is developing advanced automotive power electronics packaging technologies to help achieve U.S. DRIVE targets. This involves multidisciplinary capabilities, which include material development and characterization; thermal, electrical, and thermo-mechanical expertise; as well as reliability, process, and manufacturing considerations.

Figure 1 shows a prototype of a 200 A/1,200 V phase-leg power module, fabricated in-house at the ORNL Packaging Laboratory. The module features double-sided planar electrical interconnections and integrated mini-coolers. The versatility of the module allows it to be placed on pin fins for air cooling, or it can be cooled with liquid mini-coolers on one or both sides for increased heat rejection.

The module's planar interconnections allow large bonding contact areas. The package is constructed so that the switch die are oriented in face-up/face-down insulated gate bipolar transistor/diode die pairs. This packaging arrangement leads to significantly reduced parasitic parameters; an 80% reduction from the 2010 Prius power module. The double-sided cooling capability reduces the thermal resistivity of the entire module assembly to $0.33^{\circ}\text{C}\cdot\text{cm}^2/\text{W}$, which is 30% less than the 2010 Prius module (see Figure 2).

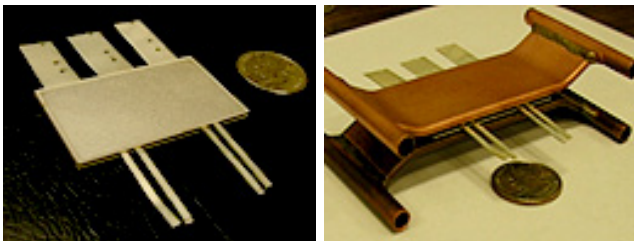


Figure 1. Prototype of a 200 A/1,200 V phase-leg power module with double-sided planar interconnection (left) and with integrated mini-coolers (right)

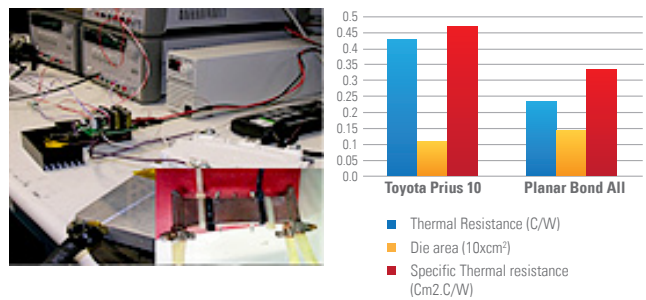


Figure 2. Thermal performance test (left) and comparison to the 2010 Toyota Prius

The ORNL concept is a paradigm shift of power module packaging technologies. It reduces the conventional multiple hybrid packaging processes to two steps, as shown in Figure 3. In the first step, all of the components are assembled into a fixture for processing. The second step involves heating the assembly to form the bonds and create the final package. The simplicity of the process helps reduce costs and improve the manufacturability of the module.

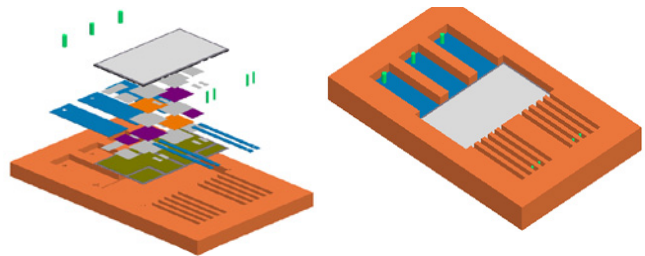


Figure 3. Planar_Bond_All process flow: all components assembling into a fixture (left); heating of assemblies (multiple) in oven (right)

The improved performance and anticipated cost reductions of the package should result in considerable strides in achieving U.S. DRIVE power density and cost targets.

**U.S. patent pending, serial number 61/509312.*

Advances in Current Source Technology for Component Minimization and Integration

By utilizing a new current source technology, a boost converter, inverter, and charger are incorporated into a single module, making significant advancement toward achieving U.S. DRIVE size, weight, and cost-reduction targets.

Oak Ridge National Laboratory

Voltage source inverters (VSIs) using film capacitors are universally employed in hybrid electric vehicles, plug-in hybrid electric vehicles (PHEVs), and electric vehicles. This technology, although mature and well-established, has many drawbacks. It requires an expensive and bulky direct current (DC) bus capacitor and produces high electromagnetic interference, detrimental voltage stresses on the motor insulation, high-frequency losses, and harmful bearing leakage currents. Long-term reliability issues also exist due to possible DC bus shoot through conditions. Additionally, to increase the output voltage of a VSI, a larger battery pack must be used or a DC-DC converter must be incorporated into the system. Both of these options result in unwanted cost, weight, and volume.

To overcome the limitations of VSIs, Oak Ridge National Laboratory (ORNL) researchers have utilized new reverse blocking semiconductor devices in a new topology called current-fed Z source inverter (ZCSI), which integrates the boost converter, inverter, and battery charger functionalities; improves fault tolerance; and substantially reduces capacitor requirements. The new design is capable of functioning as a universal charger for PHEVs, which allows charging of low-voltage and high-voltage batteries from single (120 V/240 V) or three-phase supplies (Figure 1). By incorporating all three power electronics functions into a single module, significant advancements will be made toward achieving U.S. DRIVE size, weight, and cost-reduction targets.

ORNL designed, fabricated, and tested a 10 kW ZCSI prototype (Figure 1). Test results demonstrate:

- Capacitance reduction to 200 μF (2,000 μF for VSI)
- Output voltage capability range from 0–3 times (0–.99X for VSI)

- Output voltage total harmonic distortion of 6%–12% (70%–200% for VSI)
- 4.9 kW/kg, 16.6 kW/L (4.3 kW/kg, 7.1 kW/L for Camry VSI)
- High efficiency (more than 97%, even with a relatively low source voltage of 250 V).

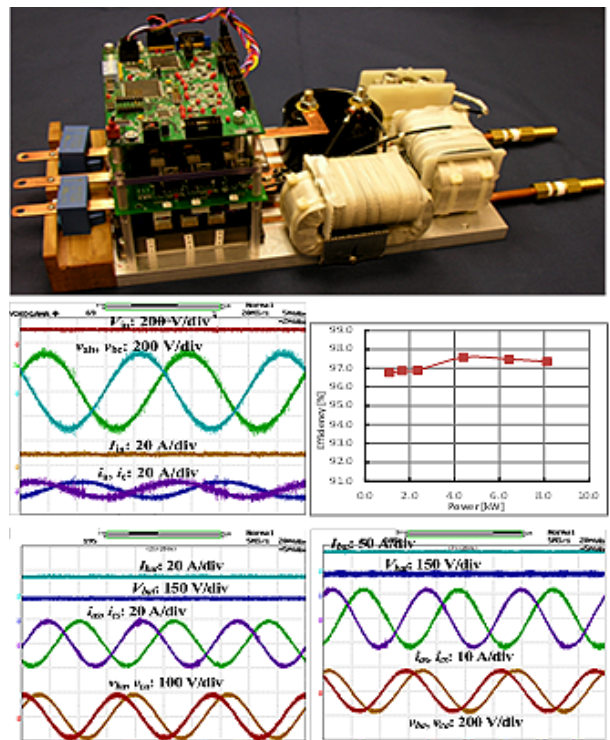


Figure 1. ORNL 10 kW ZCSI prototype (top). Test waveforms showing voltage boost by 3x (middle left). Efficiency chart at $V_{in} = 250$ V (middle right). Test waveforms for charging in boost mode (bottom left) and in buck mode (bottom right).

Design of Lightweight, Low-Cost, High Thermal Performance Inverter-Scale Heat Exchanger

A lightweight, water-ethylene glycol-based jet-impingement heat exchanger has been designed and is expected to yield up to 34% lower thermal resistance than the baseline channel-flow-based heat exchanger.

National Renewable Energy Laboratory

The National Renewable Energy Laboratory, in collaboration with UQM Technologies Inc., has designed a jet-impingement-based heat exchanger (see Figure 1) for a commercial inverter. This work is intended to contribute toward meeting 2015 U.S. Department of Energy Advanced Power Electronics and Electrical Motors Program power density and cost targets for power electronics components.

The new heat exchanger has been shown by computation fluid dynamics (CFD) modeling to reduce the silicon device junction-to-coolant thermal resistance by at least 34%, and consequently increase power density by at least 52%, over a heat exchanger based on a conventional channel-flow configuration. This improvement comes while keeping the parasitic power the same and at an industry-standard 10 liters/minute ($1.67 \times 10^{-4} \text{ m}^3/\text{s}$) flow rate for a water-ethylene glycol coolant (50%–50% by volume). The salient features of the design include using impinging jets (see Figure 2) in conjunction with micro-finned surfaces (from Wolverine Tube Inc.) on the copper base plates, as well as a lightweight, low-cost plastic material (as opposed to aluminum) as the manifold structure for the liquid.

Finite element analyses, as well as CFD modeling have helped guide the design and validate the levels of improvement. The next phase involves experimental validation of the performance of the heat exchanger.

Experiments completed in parallel have shown no degradation of the thermal performance of the micro-finned enhanced surfaces after three months of continuous jet impingement. The continuous impingement tests will continue for a duration of up to one year.

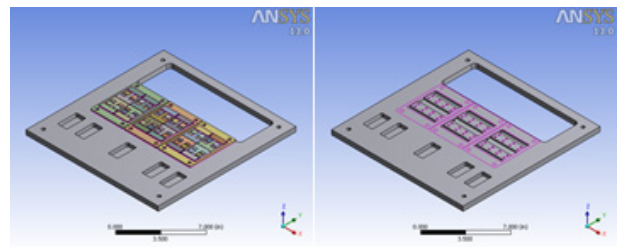


Figure 1. The figure on the left shows the three power modules in the inverter with the heat exchanger in place, while the figure on the right shows the jet-impingement manifold design.

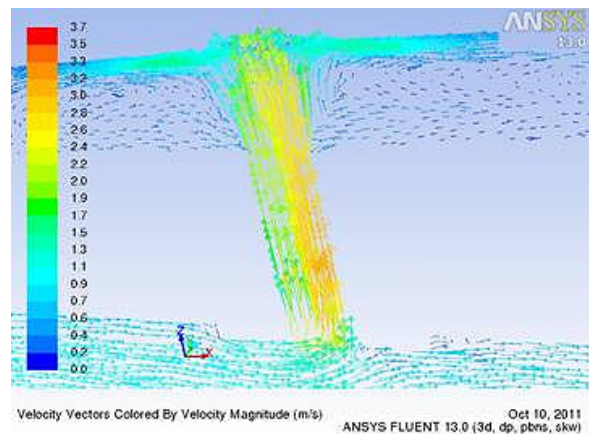


Figure 2. This figure shows velocity vectors in the heat exchanger design based on the impinging jet configuration. The manifold for the fluid is designed to be low-cost, lightweight plastic because in this design, the impinging liquid carries away all the heat and the rest of the heat sink/manifold does not have to contribute to the heat transfer.

Electrochemical Energy Storage

The image features a solid green background. In the center, the text "Electrochemical Energy Storage" is written in a blue, sans-serif font, split across two lines. Below the text, there are two decorative, wavy, light green lines that sweep across the lower half of the page, creating a sense of motion or energy.

New Electrode Designs for Ultrahigh Energy Density

A new electrode construction technique enables much thicker (10 times) electrodes, resulting in potentially much higher lithium-ion cell energies.

Massachusetts Institute of Technology and Lawrence Berkeley National Laboratory

State-of-art lithium-ion cells have, by volume, only 50% active material; the remainder of the cell volume is taken up by non-energy storing materials, like separator, packaging, etc. If this percentage of energy storing to non-energy storing material could be increased, the energy density of cells and entire batteries would be increased. The objective of this project is to develop a scalable electrode fabrication approach to enable rechargeable lithium batteries of increased active materials utilization and thus energy.

The approach is based on a sintered electrode architecture into which an additional level of microstructural control is introduced: aligned, low-tortuosity porosity. In collaboration with Lawrence Berkeley National Laboratory (LBNL), a freeze-casting process was developed that results in directional solidification. The ice-created microstructure that is formed creates desired pore morphologies and rejects solid particles from the growth front.

This approach was applied to LiCoO_2 . A series of experiments were focused toward increasing the degree of pore alignment and controlling/reducing lateral pore spacing while increasing overall sintered density. Previous work at LBNL on other materials has shown that freezing rate can influence the scale of the microstructures produced. In addition, hygroscopic additives—such as sugar, glycerol, ethanol, methanol, and sodium chloride—alter microstructure by changing the morphology of the freezing ice crystals.

An example of results from electrochemical testing of the freeze-cast LiCoO_2 samples is shown in Figure 1. Capacity versus rate is compared for sintered electrodes with and without the aligned low-tortuosity pore features. At low rates ($C/10$), the capacity of all samples is similar. At higher rates, the results diverge significantly. Comparing at 1C rate, the Gen 1 sample that has aligned porosity shows a large increase in capacity over both of the sintered samples. The Gen 2 sample, which has more highly aligned pores, shows further improved capacity retention, with the same capacity retention being achieved at 2C rate. Thus, high capacity at plug-in hybrid electric vehicle/battery electric vehicle rate capabilities is demonstrated.

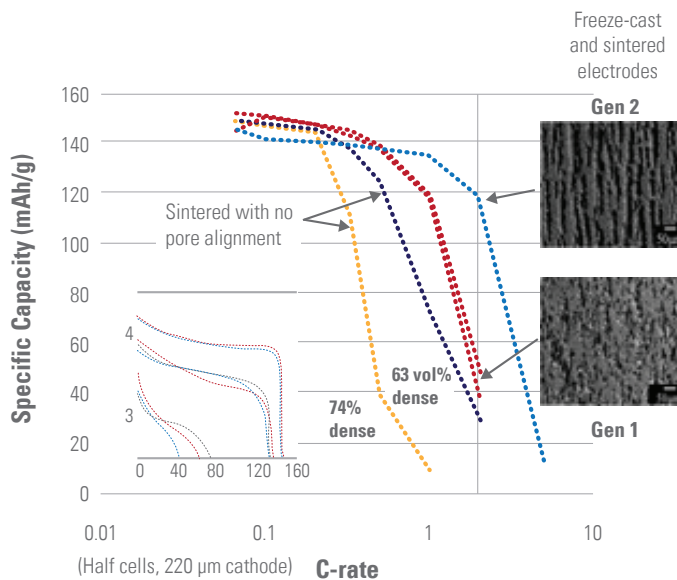


Figure 1. Specific capacity vs. C-rate for sintered LiCoO_2 electrodes prepared with and without aligned low-tortuosity porosity

High-Voltage, Single-Ion Conducting Electrolytes

High-voltage, single-ion conductor electrolytes promise to enable two of the necessary advances to high-energy lithium-ion cells: high-voltage cathodes and much thicker electrodes.

Lawrence Berkeley National Laboratory

Single-ion conductor gels (SIC) possess the solution for many of the problems with present electrolytes. They can be used with no liquid electrolyte, improving safety issues. Because they possess a unity transference number, there is no concentration polarization through the composite electrodes. Thus, SICs can facilitate the use of thicker composite electrodes, thereby leading to higher energy density cells. In addition, it is hoped that the use of electrolytes without LiPF_6 could display both improved calendar and cycle life and safety.

In past years, this group has demonstrated that SIC materials possess the bulk transport properties required. However, the interfacial impedance has been much too high. In the past year, this group has developed a new polysulfone/carbonate blend that shows promise in addressing these issues. The impedance of the polysulfone-turbo fuel stratified injection (TFSI) gel against lithium metal is an order of magnitude less than the base material, and the impedance (approximately four times that of a commercial cell) is now very close to enabling its use in a practical cell.

As a first step in that direction, the performance of these materials when used as binders in composite electrodes was investigated (to enable much thicker electrodes). Figure 1 shows the discharge capacities of two cells as a function of rate, which demonstrates that these materials are approaching practical performance. This figure shows the much better capacity at high rates of the single-ion conductor binder, which is expected due to the lack of concentration polarization.

Additional work, not shown, demonstrated the stability of the PS-TFSI SIC gel at high voltages up to at least 4.5 V. This indicates the material will be stable with several high-energy cathodes, including the spinel-type and composite cathodes. Tests on this stability are under way.

The interfacial impedance of these SIC materials is still high, but may be reduced by modification of the surfaces of composite electrodes, which will be pursued in the near future.

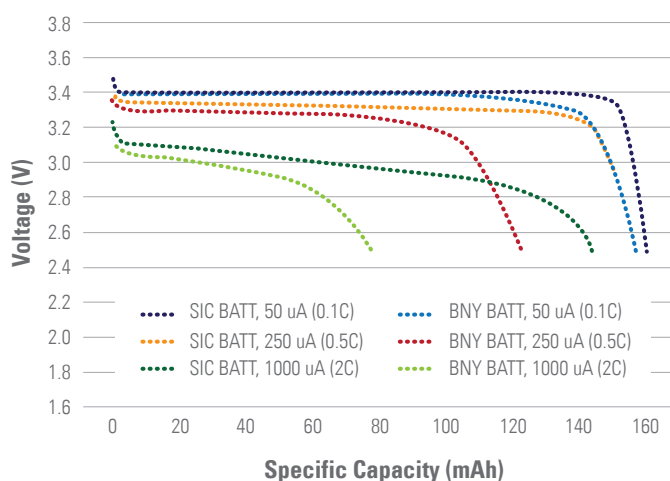


Figure 1. Discharge capacity as a function of rate comparison for single-ion conductors versus binary salt electrolytes

LiF-Anion Binding Agent Electrolytes for Enhanced Abuse

Dramatic improvements have been obtained in the thermal stability of cathodes in Li-anion binding agent electrolytes and improvements in cell runaway response with the same electrolytes.

Sandia National Laboratories

Abuse tolerance continues to be a major concern of lithium-ion (Li-ion) battery developers and users, especially with the large cells being used in the automotive sector. The use of lithium fluoride (LiF) salt has been considered as an alternative to lithium hexafluorophosphate (LiPF₆) because of its chemical and thermal stability, but early generation anion binding agents (ABA), used to improve LiF solubility, were large molecules that were incompatible with Li-ion cells. Sandia National Laboratories, in collaboration with Binrad Industries, has developed LiF/ABA salts to be used in Li-ion cells to show improved thermal stability.

The use of the ABA electrolytes in Li-ion cells gives rise to some interesting behavior and interactions with cathode materials compared to conventional electrolytes. Figure 1 (top) shows heat flow as a function of temperature for a nickel manganese cobalt (NMC)-based cathode in ABA and LiPF₆ electrolytes by differential scanning calorimetry (DSC). (NMC433 = LiNi_{0.3}Mn_{0.3}Co_{0.3}O₂). The specific heat generated by the NMC433 cathode is considerably less than in LiPF₆ (611 versus 1132 J/g). At this time, the mechanism for this cathode stabilization, which will result in a more abuse tolerant cell, is unclear; however, work will continue in Fiscal Year 2012 to better understand this phenomenon.

In cells, this same cathode runaway passivation is also observed. Figure 1 (bottom) shows cell accelerated rate calorimetry (ARC) data for an NMC433 cell with LiPF₆ and ABA electrolytes. The ARC profile NMC433 cell with 1.2 M LiPF₆ in EC:EMC (3:7) (black trace) is characteristic of NMC chemistry in the EC:EMC electrolyte. The onset for the low rate exotherm is at approximately 70°C, and the high rate runaway onset is at approximately 240°C and has a maximum peak heating rate of 300°C per minute. However, the ARC

profile for that same electrode couple in the 1.0 M LiF/ABA in EC:EMC (3:7) electrolyte shows no high rate runaway. While this is consistent with the cathode passivation observed in the DSC measurements, the magnitude of cathode passivation in the full cell experiment is greater than expected. With the promise observed in these results, work is continuing with the ABA electrolytes to better understand their thermal stability and optimize their performance in Li-ion cells.

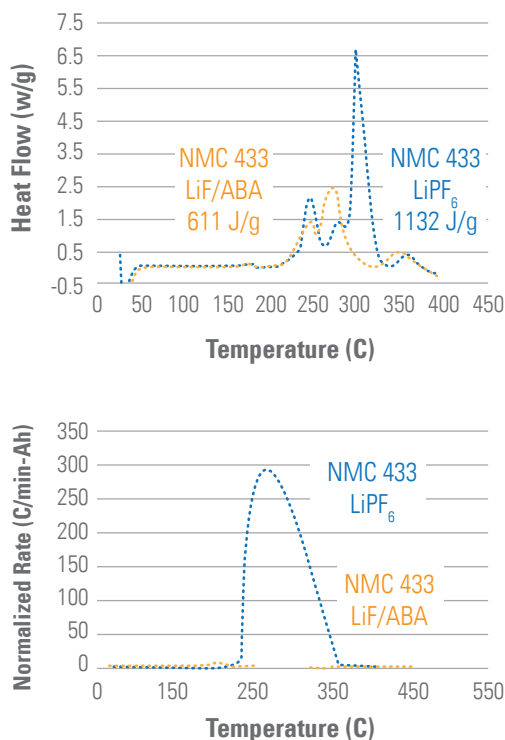


Figure 1. (Top) DSC profiles of NMC433 at 4.3 V in 1.2 M LiPF₆ in EC:EMC (3:7) and 1.0 M LiF/ABA in EC:EMC (3:7), (Bottom) ARC profiles for NMC433 18650 cells in 1.2 M LiPF₆ in EC:EMC (3:7) and 1.0 M LiF/ABA in EC:EMC (3:7) at 4.3 V

Fabrication of High-Energy Si Anodes Suitable for Large Format Lithium-Ion Batteries

Previous efforts to make amorphous Si electrodes resulted in extremely thin electrodes. Current work has succeeded in fabricating industrially relevant, high-energy electrodes.

National Renewable Energy Laboratory

Silicon (Si) offers almost 10 times the energy of current anode materials, but suffers from a number of issues associated with its large volume changes during cycling. Amorphous Si (**a**-Si) exhibits improved cycling but has not yet achieved the necessary durability or rate capability. In addition, a-Si has only been demonstrated for thin films, significantly $<1\mu\text{m}$ (commercial electrodes are $10\mu\text{m}$ or thicker), and in nanostructured electrodes that are not suitable for vehicular applications.

In hot wire chemical vapor deposition (HWCVD) of **a**-Si powders, the substrate temperature was kept at room temperature to avoid growing crystalline Si (**c**-Si). However, local hot spots formed that resulted in the nucleation of **c**-Si. Figure 1a displays an *in situ* image of the Si, at 100 times magnification, and the green spots represent the μ -Raman spot size. The large particles in Figure 1a are approximately $30\mu\text{m}$ in diameter and have a Raman line consistent with **c**-Si, (blue curve, Figure 1b). Other portions of the samples appeared amorphous, (broad red curve Figure 1b), and a mixed phase was also observed (narrow orange curve in Figure 1b).

By optimizing the synthesis conditions, **a**-Si was produced, as shown in Figure 1c, and the Raman spectrum, as shown in Figure 1d. X-ray diffraction of the **a**-Si powders showed no crystalline peaks, and $15\mu\text{m}$ electrodes displayed a voltage profile consistent with that of **a**-Si. An initial capacity of approximately 2,500 mAh/g (almost 10 times that of graphite) was obtained. The electrodes were subsequently coated with Al_2O_3 using atomic layer deposition (≤ 1 nm thick), and the first cycle coulombic efficiency was improved from 60% to 80%. The Coulombic efficiency was improved to 99% after the first cycle, but the capacity was limited to approximately 1,000 mAh/g. Electrode and

coating optimization are still required to improve the cycle life, especially at high rate, and to further reduce the first cycle capacity loss.

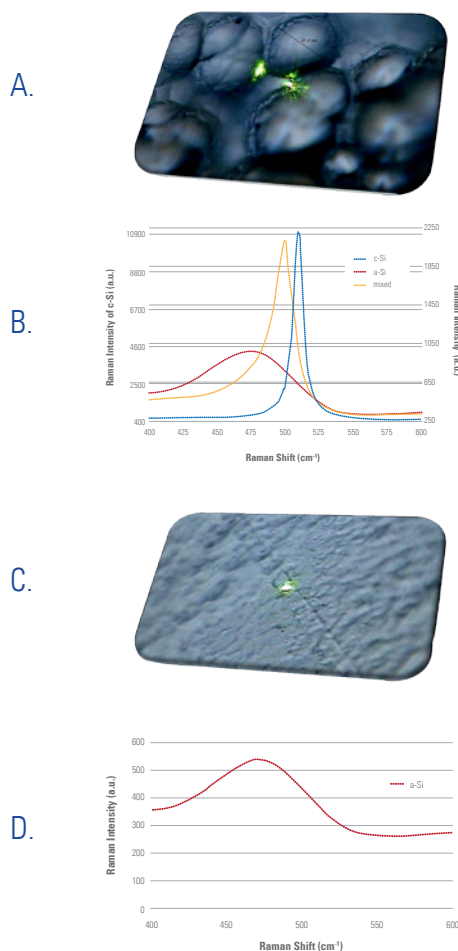


Figure 1. Topographical image of mixed phase HWCVD Si a) and b) corresponding Raman spectra compared with c) image of optimized a-Si and d) corresponding Raman spectrum

High-Energy Composite Cathode Materials

A sodium (Na) lithium (Li)-ion exchange process is found to cost-effectively produce high-energy and high-rate cathode materials that promise to enable 40-mile PHEV battery development.

Argonne National Laboratory

Higher-energy, high-power, long-lived, and cost-effective cathode materials are needed to enable lower cost batteries for long-range plug-in hybrid electric vehicles (PHEVs) and electric vehicles. Cathode materials with composition LiMO_2 (M=a combination of Mn, Ni, and Co) are layered oxides having two-dimensional layers that support reversible lithium (Li) cycling and typically provide good energy and power. However, site disorder occurs between Li and the transition metal "M," which impedes cycling due to M partially blocking Li diffusion.

In this work, Li ion-exchange of the layered Na phases (Na[M]O_2) is used to minimize site disorder in LiMO_2 . The large radii of Na^+ (1.02 Å) causes an increase in the interlayer slab space, enhancing Li diffusion, and the separation of layers and cation sites are conserved in the LiMO_2 product. The M in Na_xMO_2 contains a combination of Li with Ni and Mn. Not only is this combination expected to minimize site disorder in the layered structure, but the additional Li results in the formation of LiM_6 (M=Mn and/or Mn/Ni) domains in the layer that add a stabilizing component to the material.

The stoichiometry of the product synthesized from Li ion-exchanged from the layered precursor $\text{Na}_{0.9}\text{Li}_{0.3}\text{Ni}_{0.25}\text{Mn}_{0.75}\text{O}$ was (IE-LNMO) $\text{Li}_{1.32}\text{Na}_{0.02}\text{Ni}_{0.25}\text{Mn}_{0.75}\text{O}_y$. X-ray diffraction spectra, not shown, contain evidence of a Li_2MnO_3 component. The first charge voltage profile is characterized by an initial sloping region up to 4.5 V, followed by a voltage plateau, which slowly progresses to the 4.8 V cut-off, much like the layered/layered cathodes. The first charge capacity is 252 mAh/g, and the first discharge capacity is 234 mAh/g, an irreversible capacity loss of only 7%. Figure 1 provides the capacity versus cycle number to 40 cycles. The discharge capacity values range between 220 mAh/g and 225 mAh/g and are steady with excellent coulombic efficiency. Note that

current cathode materials provide approximately 150 mAh/g at approximately 3.7 V. The inset to Figure 1 shows the rate capability of this material, which delivers superior capacity to present day cathodes beyond a 6C rate. Thus, this new material shows excellent energy density and good rate capability.

Future work will examine the effect that the ion-exchange media has on the structure and electrochemical performance of the resulting active materials.

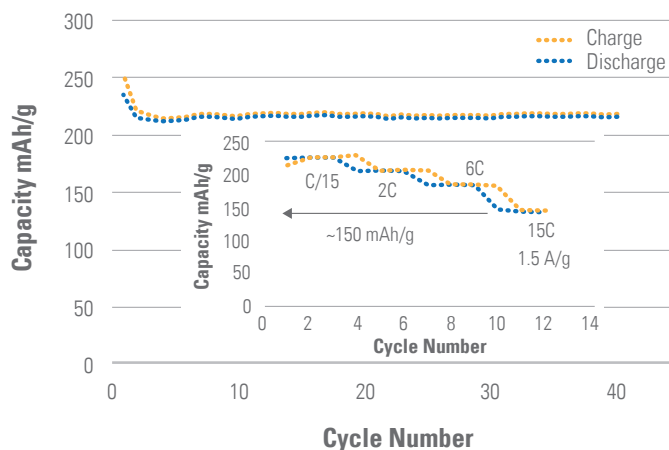


Figure 1. Capacity versus cycle number (at c/15 rate or 15 mA/g), and inset is the capacity versus current rate, of Li/IE-LNMO cell between 4.8 V and 2.0 V

Development of LiCoPO_4 Cathode and High-Voltage Electrolyte

LiCoPO_4 is a 4.8 V cathode material with potentially 40% higher energy density than that of LiFePO_4 , and a new electrolyte additive has been found to significantly improve high-voltage stability of standard electrolytes.

Army Research Laboratory

Many high-energy cathodes under development operate at high voltages. At those voltages, standard electrolytes are not stable and new, high-voltage electrolytes are needed. The phosphate ester-based additives at Army Research Laboratory (ARL) benefit from greater amounts of fluorination and enhance the high-voltage stability of carbonate electrolytes. The additive, tris(hexafluoroisopropyl)phosphate (HFIP), is a highly fluorinated phosphate ester with a fluorine/hydrogen (F/H) ratio of 6. Several other phosphate esters, with varying F/H ratios, were tested as additives. The performance of those cells seemed to relate directly to the F/H ratio of the additive (see Figure 1, top).

LiCoPO_4 is a 4.8 V cathode material with 40% higher energy density than that of LiFePO_4 . The material is an ideal test vehicle for high-voltage electrolyte development. However, its relatively poor cycle life, resulting from lack of structural stability, plus the lack of high-voltage electrolytes, became a challenge to using this material. ARL developed a Fe- LiCoPO_4 in which a portion of the Co is substituted by Fe^{2+} and Fe^{3+} . Long-term cycling of cells in electrolyte containing HFIP is shown in Figure 1.

Planned work includes the synthesis of new phosphate ester variants that contain no protons for the evaluation of the effectiveness of forming protective layers on electrodes; evaluation of HFIP containing electrolytes at elevated and low temperatures for stability and rate performance of $\text{LiNi}_{0.5}\text{Mn}_{1.5}\text{O}_2$ /graphite full cells; evaluation of Fe-modified LiCoPO_4 in a full cell configuration in electrolytes containing additives, including fluorinated phosphate esters; and understanding how HFIP works for developing more effective additives.

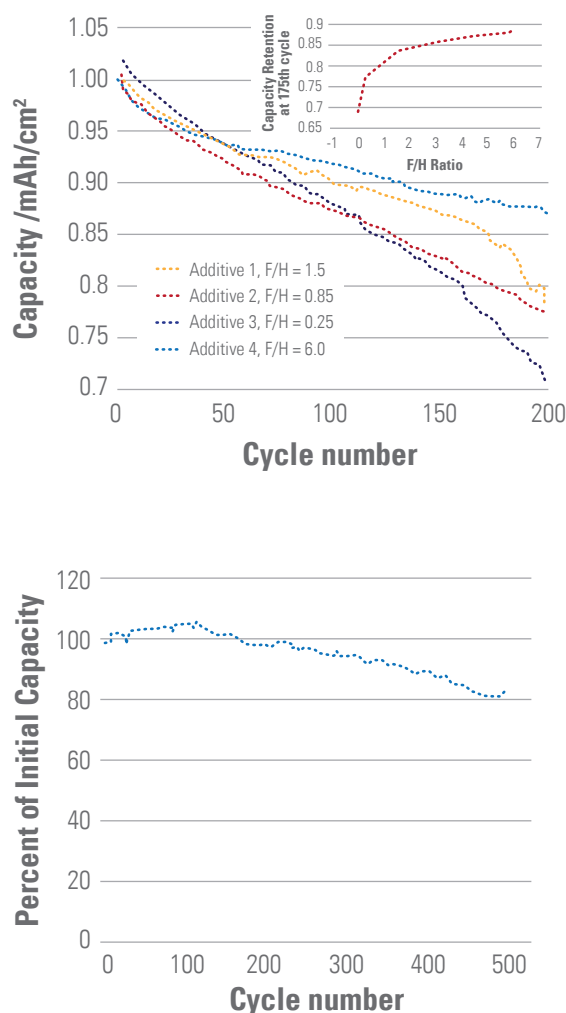


Figure 1. (Top) Capacity as a function of cycle number at room temperature for $\text{LiNi}_{0.5}\text{Mn}_{1.5}\text{O}_2$ /Li half cells in 1 M LiPF₆/EC:EMC (3:7 w/o) with various fluorinated phosphate esters of different F/H ratios; (Bottom) cycling of Fe-substituted LiCoPO_4 against Li in 1 M

Improved Performance of Doped High-Voltage Spinel Cathodes

A doped high-voltage cathode has shown improved cycle and overall stability after the addition of an appropriate electrolyte additive.

Pacific Northwest National Laboratory

Lithium-ion batteries with high-energy densities are required to reach national goals for electric vehicles, including plug-in hybrid electric vehicles. To increase the energy of a cathode, the voltage and/or capacity of the material must be increased.

High-voltage spinels of general composition $\text{LiNi}_{0.5}\text{Mn}_{1.5}\text{O}_4$ show promise as a high-voltage, high-energy cathode material. They are also being used as a high-voltage electrolyte test material given their relatively stable structure at high voltage (4.8 V). By adding appropriate doping and electrolyte additives, Pacific Northwest National Laboratory (PNNL) has successfully developed a chromium (Cr)-doped, high-voltage spinel, $\text{LiNi}_{0.45}\text{Cr}_{0.05}\text{Mn}_{1.5}\text{O}_4$. This material exhibited stable cycling and greatly improved efficiency.

Figure 1 reveals that, after Cr-doping, the cycling stability was significantly improved. This improvement is assigned to the increased content of disordered phase and/or Mn^{3+} ions that facilitate Li^+ ion diffusion. Meanwhile, the surface modification caused by Cr-doping may alleviate Mn dissolution in the electrolyte. However, the main influencing parameter on performance is the content of Mn^{3+} instead of doping. Thus, if the Mn^{3+} concentration in pure $\text{LiNi}_{0.5}\text{Mn}_{1.5}\text{O}_4$ can be modified to the same amount as in $\text{LiNi}_{0.45}\text{Cr}_{0.05}\text{Mn}_{1.5}\text{O}_4$, the cycling stability also may be improved, which is now under investigation.

PNNL also found that low concentrations of Li bis(oxalato)borate (LiBOB) not only improves the first cycle efficiency of $\text{LiNi}_{0.45}\text{Cr}_{0.05}\text{Mn}_{1.5}\text{O}_4$ from 76% to 85%, but the rate capability also increases with 0.25% LiBOB (not shown). LiBOB is believed to form a protection film on the cathode surface, which is resistive to the damaging HF and POF_3 generated

by reactions of the LiPF_6 salt in the electrolyte. Therefore, further decomposition of the solvents and the dissolution of Mn in the high-voltage spinel will be alleviated, thus improving the Coulombic efficiency and cycling stability.

The influence of Mn^{3+} concentration on performance will be investigated further next year. A novel synthesis approach, which can control Mn^{3+} content without Cr-doping, will be investigated. The effect of non-active materials—including electrolyte solvent, additive, cathode pans, and separator membranes—will also be evaluated with high-voltage cathode materials.

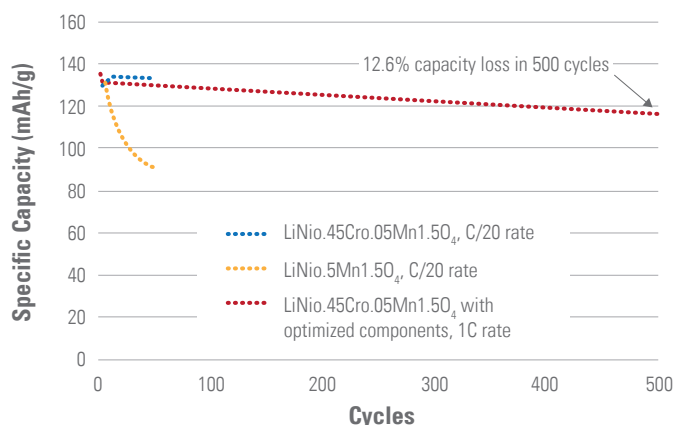


Figure 1. Comparison of cycling stability for $\text{LiNi}_{0.5}\text{Mn}_{1.5}\text{O}_4$ (dashed line) and $\text{LiNi}_{0.45}\text{Cr}_{0.05}\text{Mn}_{1.5}\text{O}_4$ (dotted line). $\text{LiNi}_{0.45}\text{Cr}_{0.05}\text{Mn}_{1.5}\text{O}_4$ tested with optimized electrolyte and other components exhibits excellent stability (solid line).

Materials Search Engine with Lithium Electrode Explorer

LBL and Massachusetts Institute of Technology have successfully launched the first Google-like materials search engine. The website contains more than 15,000 computed compounds for general searches and a Li-battery electrode explorer.

Lawrence Berkeley National Laboratory and Massachusetts Institute of Technology

There is increasing evidence that many of the performance-limiting processes present in lithium-ion electrode materials are highly complex reactions occurring at the atomic level. This group is using first-principles density-functional theory modeling to study those processes. By understanding the underlying reasons for the electrode materials performance, one can suggest improvements or design schemes directed at the root cause of the process. In addition, a major goal of current battery research is the discovery and development of new materials with better energy, better stability, and lower cost, among other properties. A tool to facilitate these continuing searches promises to accelerate the process of materials discovery.

This group has successfully launched the first Materials Project website and database. The purpose of the site is "Accelerating materials discovery through

advanced scientific computing and innovative design tools." The website provides free, searchable access to general materials properties covering more than 15,000 inorganic compounds, with the number of compounds increasing continuously. The site contains tools ('apps') designed to aid in materials design for specific application areas, such as lithium-ion battery technology. Figure 1 shows the announcement flyer, which features many of the website's possible search capabilities—among them, an example electrode material with its computed voltage profile and oxygen evolution as a function of charge. A sample result is shown in Figure 2. The Materials Project continues to compute more properties and materials—both known and unknown.



Figure 1. Announcement of the Materials Project database (www.materialsproject.org)

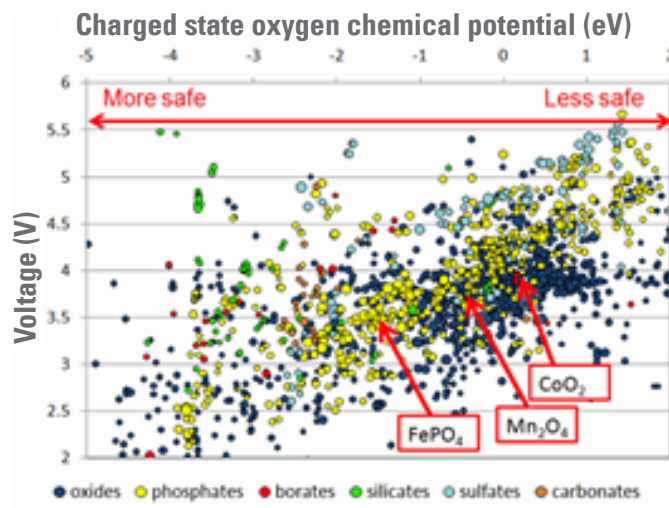


Figure 2. Sample graph of a portion of the 15,000 compounds contained in the Materials Project database

Improving the Power of High-Energy, Lithium-Rich Cathodes

A nanometer-thick coating on the high-energy, lithium-rich or layered/layered cathodes dramatically improves rate capability, one of the critical needs for commercialization.

Oak Ridge National Laboratory

Layered/layered lithium-excess cathode materials, $x\text{Li}_2\text{MnO}_3 \cdot (1-x)\text{LiMO}_2$ or $\text{Li}_{1+x}\text{M}_{1-x}\text{O}_2$, where M= Mn, Ni, and Co offer capacities greater than 260 mAh/g when operated at high voltage (>4.6 V), offer higher energy densities than almost any other cathodes. However, these materials have significant rate (power) limitations. Further, cycling at higher voltage results in formation of thick surface films due to electrolyte decomposition. Surface coating of the high-voltage lithium-excess material $0.6\text{Li}_2\text{MnO}_3 \cdot 0.4\text{Li} [\text{Mn}_{0.3}\text{Ni}_{0.45}\text{Co}_{0.25}]\text{O}_2$ with a few nanometer thick layer of lithium phosphorus oxynitride (Lipon) shows dramatic improvement in the rate performance, resulting in higher capacity utilization compared to the uncoated pristine cathode composition. Lipon was deposited on the lithium-excess cathode material using magnetic sputtering with a total deposition time ranging between 1 to 3 hours.

As shown in Figure 1, the pristine materials' capacity is reduced by 50% when the discharge rate is increased from C/5 to 2C (a 5-hour discharge rate versus a 30-minute discharge rate), while the Lipon coated lithium-excess MNC cells retain more than 80% capacity. Further, the Lipon coated sample demonstrates respectable capacity at even 15C (120 mAh/g).

Other experiments determined that thicker Lipon coating (>tens of nanometers) reduced the overall electronic conductivity of the electrode, leading to poor capacity retention and eventual cell failure. Detailed interfacial and microscopy studies are underway to understand the effect of the coating on the overall cell performance.

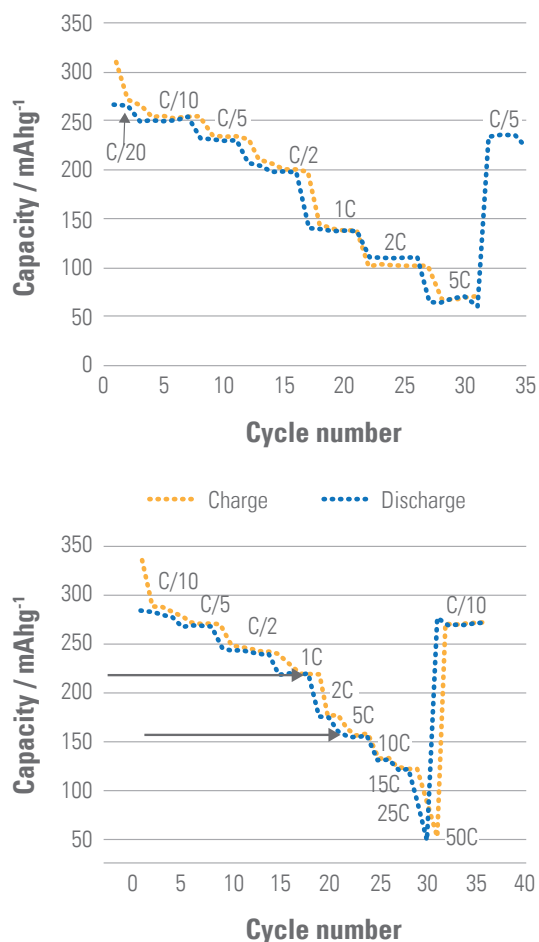


Figure 1. Rate performance comparison between Pristine (uncoated) lithium-excess MNC (top) and Lipon coated lithium-excess MNC (bottom). The measurements were performed at 25°C with similar electrode composition (85% active materials, 7.5 % PVDF, and 7.5 % carbon [Timcal Super C65]).

In Situ X-Ray Diffraction Development and Diagnostics of Cathode Materials

This technique will enable evaluations of critical nanometer-scaled microstructural and micro-chemical changes as a function of battery test conditions, electrode materials, electrolyte, and electrolyte additives.

Brookhaven National Laboratory

Understanding lithiation and delithiation reactions in lithium-ion (Li-ion) batteries is extremely challenging. Contributing to this challenge is the lack of *in situ* techniques that permit research to observe structural and chemical changes during charging and discharging reactions.

In this work, a new synchrotron-based *in situ* X-ray diffraction (XRD) technique was developed to study the structural changes of cathode materials of Li-ion batteries during chemical lithium extraction in a $\text{NO}_2\text{BF}_4/\text{CH}_3\text{CN}$. This new technique was used to investigate the phase transitions of LiFePO_4 .

As shown in Figure 1, taking advantage of the high-resolution linear-position sensitive silicon detector, the reflections from LiFePO_4 and FePO_4 can be clearly distinguished and identified. The changes of peak intensity as a function of reaction time (about 48 minutes total) or XRD scan number (about 50 scans total) are plotted in Figure 1b. The intensity of pattern corresponds to the color scale (left). With increasing reaction time, the peak intensities for FePO_4 increase while those for LiFePO_4 decrease. The formation of second phase FePO_4 can be observed at scan 4, indicating a short time (about 4 minutes) was needed for the newly formed FePO_4 phase to grow enough crystal size to be detected by XRD. This is quite different than the *in situ* XRD results of using electrochemical delithiation where the appearance of FePO_4 takes a much longer time. The final pattern for fully delithiated lithium iron phosphate is shown in Figure 1c.

Future work will include comparative *in situ* XRD and absorption spectroscopic studies of $\text{LiFe}_{1-x}\text{MnxPO}_4$ ($x=0$ to 1) cathode materials with different particle size and morphology during chemical and electrochemical delithiations, and the use of time resolved XRD to study the thermal stability of atomic layer deposition surface coated $\text{Li}_2\text{MnO}_3\text{-LiMO}_2$ ($\text{M}=\text{Ni}, \text{Co}, \text{Mn}, \text{Fe}$) cathode materials during heating.

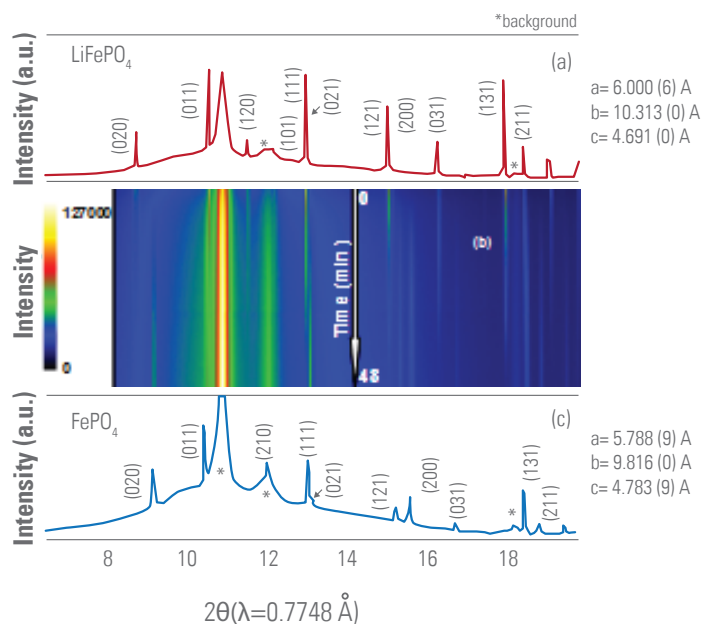


Figure 1. XRD during *in situ* chemical delithiation of LiFePO_4 : (a) XRD pattern for LiFePO_4 ; (b) contour plot of peak intensities vs. reaction time; (c) XRD pattern of FePO_4 (end of reaction)

Determination of Aging Path Dependence in Batteries

Tools are developed to understand mechanisms of cell aging using application-relevant testing protocol, accurate and effective diagnostic techniques, and advanced physics-based life models.

Idaho National Laboratory and University of Hawaii

Existing lithium-ion battery systems lack proven long-term reliability and abuse-tolerance in real-world vehicle scenarios, which impedes large-scale battery implementation in renewable energy storage and electric drive applications. Batteries age in very complex ways, involving numerous mechanisms, which is often observed as path-dependent behavior. Researchers at the University of Hawaii and Idaho National Laboratory have made advances toward overcoming the challenges behind aging path dependence based on sophisticated technology that can correctly determine a battery's condition and provide accurate diagnosis on the state of the battery in the aging process. Robust battery diagnostic tools and complementary thermodynamic and physics-based models enable explanation of aging phenomena. This approach can revolutionize battery management and enables a realistic solution to operate battery system reliably and safely under highly diverse usage scenarios.

One thrust area is to determine how daily thermal cycles (DTC) will impact aging rates in batteries that are employed in electric drive applications, since such batteries will undergo thousands of cycles during their service life. Figure 1 shows interim test results for capacity loss in representative plug-in hybrid electric vehicle cells that undergo DTC conditions that vary in severity, indicating that more severe DTC can more than double capacity loss, presumably due to accelerated mechanical degradation of cell materials. To help understand mechanisms behind aging trends, as seen in Figure 1, tools are employed that look squarely at realistic aging metrics. In Figure 2, (a) and (b) are examples of diagnostic techniques covering incremental capacity analysis and contributions to capacity loss over time.

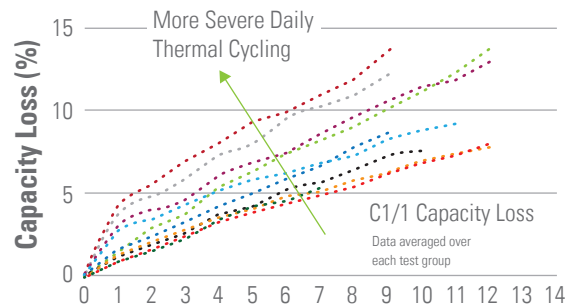


Figure 1. Capacity loss as a function of DTC. The long-term consequence of such trends is to shorten battery warranties.

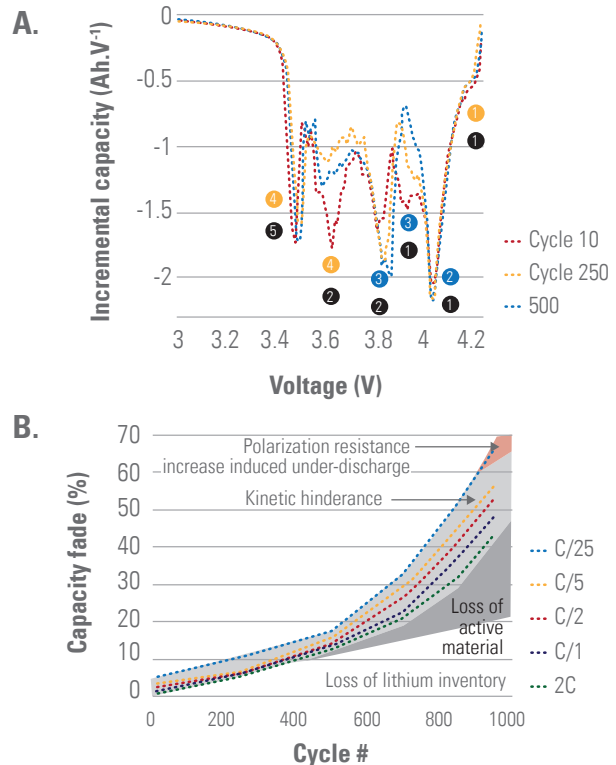


Figure 2. (a) diagnostic tool that uses incremental capacity analysis to infer degradation process in a battery, (b) battery degradation is analyzed with contributions in a chronicle fashion.

A New Multi-Scale Model Framework to Help Industry Design Better Lithium-Ion Batteries

NREL formulated and published a ground-breaking methodology for multi-domain modeling of lithium-ion batteries encompassing multi-physics in varied length scales.

National Renewable Energy Laboratory

Battery performance, aging, and safety response occurs in complex relations among various physics, at intricate geometries, and in varied length and time scales. The lack of a proper, comprehensive battery model to investigate the coupled interactions that determine the electrical, thermal, electrochemical, mechanical, and chemical response of battery systems under various use scenarios hinders expediting battery development and thus the widespread market penetration of electric drive vehicles. Through a multi-year effort, the National Renewable Energy Laboratory (NREL) developed a multi-domain modeling approach known as the Multi-Scale Multi-Dimensional (MSMD) framework for predictive computer simulation and design of lithium-ion (Li-ion) batteries with different chemistries or geometries.

This year, NREL's ground-breaking, multi-domain, multi-scale modeling framework was further developed and then published in the *Journal of the Electrochemical Society* article, "Multi-Domain Modeling of Lithium-Ion Batteries Encompassing Multi-Physics in Varied Length Scales." This publication is the stepping stone for transfer of NREL's technology.

NREL's MSMD framework introduces multiple computational domains for corresponding length scale physics and decouples geometries between sub-model domains while coupling physics bi-directionally. The MSMD framework serves as an expandable development platform, providing a pre-defined but expandable communication protocol and a generic and modularized flexible architecture. Multiple constituent sub-models and solution methods for the MSMD framework have been developed, or are in development, to address various needs for computer simulations to enhance knowledge on multi-physics behaviors of Li-ion batteries considering the impact of their designs. The model application to computational studies has been demonstrated to reveal the complex multi-physics interaction in various Li-ion battery systems.

Through the U.S. Department of Energy's Computer-Aided Engineering for Electric Drive Vehicle Batteries program, NREL is sharing know-how with the three award contractor teams. The team of General Motors and ANSYS has started to implement the approach of NREL's MSMD framework into the team's battery software development.

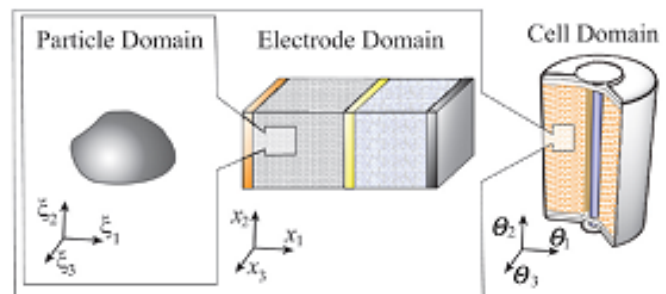


Figure 1. The MSMD framework resolves intricate Li-ion battery geometries into multiple computational domains for corresponding length scale physics

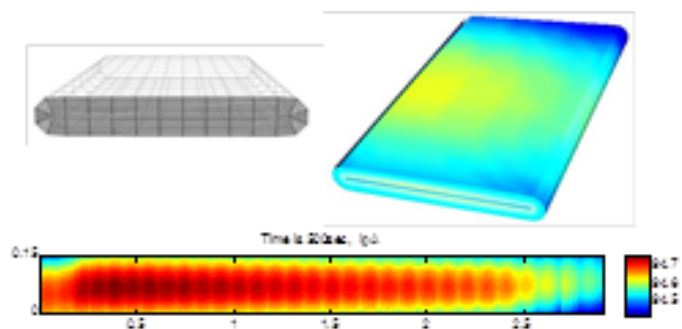


Figure 2. The MSMD application to a computational study on large format prismatic wound cell behaviors; transfer reaction current density distribution after 500 second at 4C discharge of a 20Ah cell with continuous tab

3M Silicon-Based Anode Exceeds Targets

3M developed new classes of high-energy anode materials, demonstrated manufacturability, and optimized electrode/cell design to achieve high cycle life. These materials are now being commercialized.

3M

It is widely recognized that Silicon (Si) or Tin(Sn)-based alloys are the only alloy materials that can deliver significant gains in energy density over graphite. With the above guidelines in mind, this project's research focused on Si-based alloys, as the raw-materials cost of Sn-based alloys was deemed too high for plug-in hybrid electric vehicle (PHEV) applications. The design of the alloy was based on the active/inactive alloy concept, with a target reversible volumetric capacity of 1,500 mAh/cc after full lithiation and expansion. At this capacity, the alloy is expected to have a volumetric expansion of 100% during lithiation and increase the energy density of a lithium-ion cell by 15%–20%, depending on the cathode formulation.

The purpose of this research program is to develop practical, high-energy anode materials for PHEV power sources. Therefore, the following performance and practical goals were set:

- 15%–20% improvement in energy density
- 300 cycles with 20% fade
- Demonstrate manufacturability
- Demonstrate acceptable thermal stability
- Demonstrate good rate capability
- Low-cost raw materials
- Inexpensive existing manufacturing processes
- Aqueous slurries using existing slurry coating procedures
- Industry standard cell assembly.

To be commercially adopted, a new metal anode material must meet all of the above requirements. In this program, 3M met all performance and practical goals, and the materials are now being commercialized.

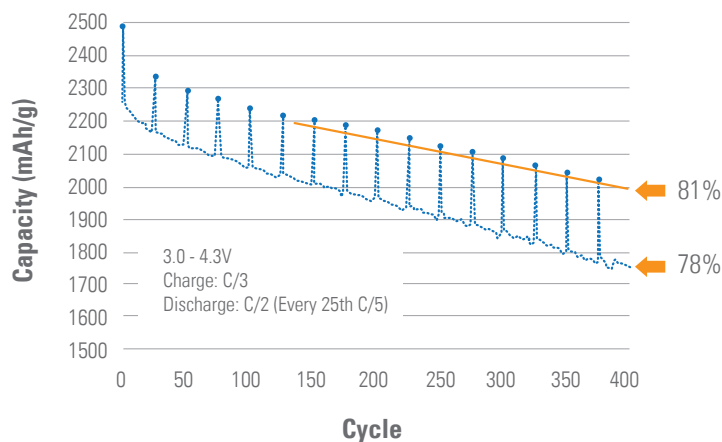


Figure 1. Capacity retention for 18650 cell using 3M alloy, L-20772, in 2:1 blend with graphite

Low-Energy Energy Storage System from Maxwell Technologies

New ultracapacitor device for power assist hybrid electric vehicles demonstrates more than a doubling in energy density over the best commercial ultracapacitors.

Maxwell Technologies and U.S. Advanced Battery Consortium

In December 2009, the U.S. Advanced Battery Consortium (USABC) for the first time issued a request for proposals for a low-energy energy storage system (LEESS) for power assist hybrid electric vehicles. One of the two LEESS development programs selected by USABC was Maxwell Technologies (contract awarded in January 2011). During the first year of the two-year program, Maxwell has been successful in demonstrating a new low-cost manufacturing process and improved electrolyte in this higher voltage asymmetric capacitor, which also exhibits higher energy density and lower projected costs than current ultracapacitors.

The asymmetric capacitor offers several potential advantages for power assist hybrid applications, combining the high power of a capacitor with greatly increased energy. Maxwell has successfully produced laboratory cells that can be cycled at higher voltages than current ultracapacitors. These cells have demonstrated a more than doubling in energy density over the best commercial ultracapacitors.

Cells were manufactured using Maxwell's proprietary dry electrode processing. This method significantly reduces the number of necessary manufacturing steps, and because it eliminates the use of solvents, it is more environmentally friendly. The result is a greater than 30% cost reduction in electrode production compared to wet methods.

Further, improvements in cycling performance were brought about by the elimination of solvent impurities and their related negative impacts. To date, the Maxwell cell demonstrates a greater than 15% increase in energy density relative to a comparable asymmetric capacitor made from a commercial wet process.

With respect to low operating temperature, a proprietary electrolyte formulation has been created for the second generation cells. This electrolyte meets USABC goals at -30 degrees Celsius. Stability trials and life evaluation with this electrolyte is the next body of work to be executed.

Maxwell is also developing a new system for manufacturing the cells and the pack. Cells will be placed in trays that are efficiently stacked and coupled with electronics and cooling into a complete compact system (see Figure 1). This system will meet or exceed USABC power and energy requirements and is projected to approach USABC volume and weight targets. The main focus of this program is cost; Maxwell continues to refine the cell and pack design to minimize cost and approach the USABC target for selling price for this new USABC LEESS HEV application.

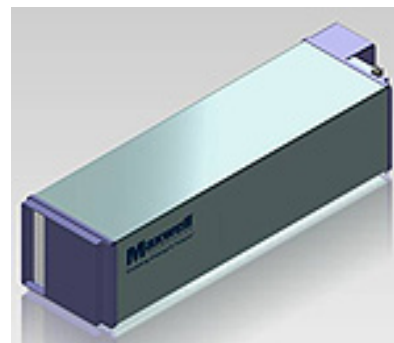


Figure 1. Proposed pack design including all cells, electronics, and thermal management

High Energy Density Electrode Demonstrated for Electric Vehicle Batteries

Cobasys has developed and demonstrated cell-specific energy density increases to 165 Wh/kg without compromising life, performance, and abuse tolerance.

Cobasys and U.S. Advanced Battery Consortium

The most important attributes for future electric vehicles (EVs) are high range and low cost. To satisfy these goals, development of new battery pack technology that demonstrates the U.S. Advanced Battery Consortium's goals for improved specific energy and energy densities, while maintaining good safety and life, is required. In addition, further improvements in battery system design and component integration will be required to achieve acceptable cost levels.

Enhancement of the energy density at the cell level, using two different chemistry designs, is one focus of study. The first approach is through development of moderate NCM (mod-NCM, $\text{LiNi}_x\text{Co}_y\text{Mn}_{1-x-y}\text{O}_2$) chemistry design, which uses incrementally improved conventional cathode materials with high current density.

The second uses newly developed cathode materials called extreme NCM (ext-NCM, $\text{Li}_2\text{MnO}_3 \bullet \text{LiNi}_x\text{Co}_y\text{Mn}_{1-x-y}\text{O}_2$) with very high specific capacity.

EV cells with 165 watt hours (Wh)/kilogram (kg) energy density, using mod-NCM cathode materials, were successfully demonstrated, improving the cell-level specific energy density by 50% over current state-of-the-art technologies, representing an intermediate step to achieving the project target. The main materials' compositions were chosen to satisfy power, life, and safety performance based on screening test results with small cylindrical surrogate cells and large prismatic cells.

As a new cathode material, practical consideration of ext-NCM required that several challenges be identified and overcome. Through an extensive baseline study, this was accomplished in 2011. Rate capability and

life performance must be improved to be applicable for EVs. Cobasys has made significant progress in improving cell-life performance through development of new electrolyte systems, as seen in Figure 1.

To enhance the energy density of the overall battery pack system, development of new pack materials that maintain strength and durability but reduce mass and cost is required. Additionally, feature integration is critical to overall reduction in components and cost. Using the most current cell performance demonstrated in the large form factor, it can be estimated that the overall system-specific energy density has been improved to 130 Wh/kg.

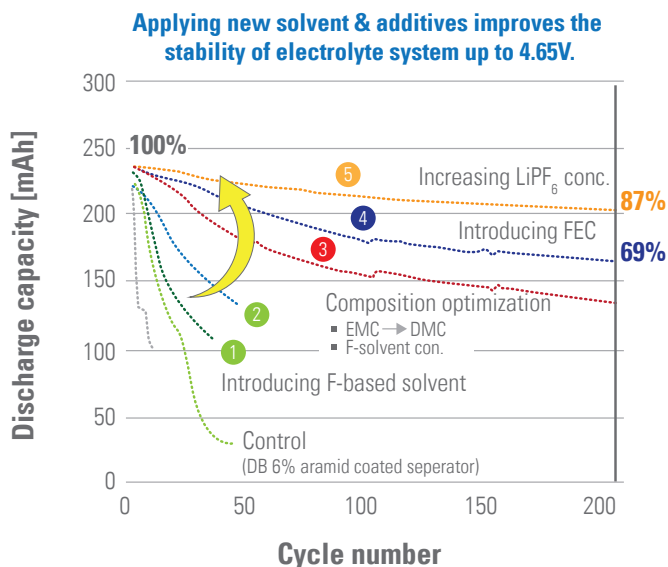


Figure 1. Improvement of cycle performance of ext-NCM cell with high-voltage electrolyte (87% capacity retention after 200 cycles with #5 electrolyte, Fluorinated solvents+DMC+LiPF₆)

PHEV Cell Projected to Meet USABC Calendar Life Goal

Based on analysis of results from a multi-temperature matrix of long-term calendar life test data, A123's 19.6 Ah prismatic PHEV cells are projected to exceed the USABC 15-year calendar life goal.

A123 Systems and U.S. Advanced Battery Consortium

In support of the U.S. Department of Energy (DOE) objective to improve fuel economy and enable petroleum displacement, A123 has developed plug-in hybrid electric vehicle (PHEV) cells for U.S. Advanced Battery Consortium (USABC) 10- and 40-mile applications. The focus of the USABC PHEV program is to: (1) leverage the benefits of A123's proprietary Nanophosphate® cathode powder, such as high specific power and long cycle life, in a prismatic cell, and (2) reduce system cost and weight. Program activities were focused on the development of materials and electrodes, which enabled a pouch cell design, optimization of thermal management at the cell and module level, and improved energy density to enable cell count reduction through efficient module/pack design.

During the course of this program, two generations of prismatic pouch cells were developed and evaluated versus program targets. The first prototypes evolved from preliminary laboratory samples into fully featured pre-production products. Prior to production, a next-generation cell was developed, which included improvements in active materials and processes and provided superior performance. During late 2010 and early 2011, these next-generation cells were produced for delivery to the national laboratories and for internal testing to benchmark against USABC performance targets. These final delivery cells were tested at various states of charge and temperatures to provide data that could be used to project calendar life under automotive usage conditions consistent with USABC test protocols. The cells have completed more than seven months of accelerated life testing at 23, 30, 35, 45, and 55 degrees Celsius (°C) for 100%, 80%, and 60% states of charge. Figure 1 below shows relative capacity fade over time, with a superimposed solid line

projecting the curve of capacity fade over 15 years. Development of a model using final delivery cell data at all states of charge and temperatures provides a projection of 15.5 years to 30% capacity fade at 30°C, indicating that USABC performance estimates for power, energy, cycle, and calendar life requirements can be achieved.

The cell developed under this USABC-funded program is manufactured in A123's Romulus, Michigan, and Livonia, Michigan, facilities, which produce cells, modules, and pack assemblies. These cells have been shipped to customers and are currently in vehicles on the road today.

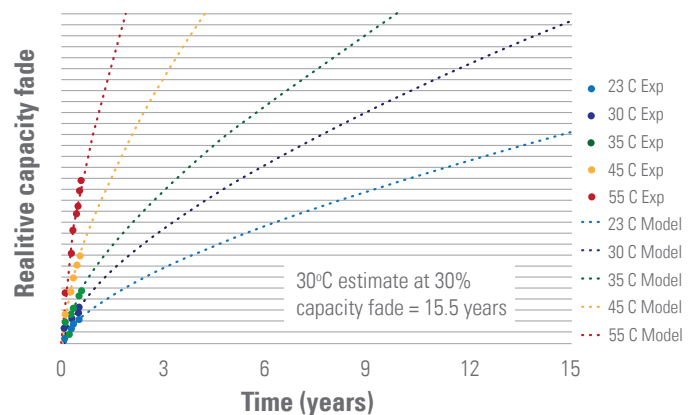


Figure 1. A123 Systems Gen PHEV cell calendar life results and projections at various temperatures, and 80% SOC

JCI Develops New Prismatic Cell and System Technology

JCI developed a new PHEV prismatic cell/system technology that offers twice the all-electric range and a 15% reduction in system volume over the baseline technology.

Johnson Controls Inc. and U.S. Advanced Battery Consortium

In June 2011, Johnson Controls Inc. (JCI) completed a three-year development program to develop a new prismatic cell and system battery technology using the $\text{Li}[\text{Ni}_{1/3}\text{Mn}_{1/3}\text{Co}_{1/3}]\text{O}_2$ (NMC)/graphite chemistry. This technology is planned for commercialization in 2013 and will be built in the United States, offering a compelling product for the plug-in hybrid electric vehicle (PHEV) market. The improvement in system-level energy density afforded by the prismatic form factor offers increased packaging efficiency and lower cost metrics critical to U.S. DRIVE goals.

The program allowed the Milwaukee Technical Center to develop the equipment and skill-base resources required to execute full in-house builds of prismatic cells, modules, and systems. 2011 saw the completion of two final builds. The March 2011 build provided 270 cells for the final system deliverables and incorporated automated winding control, improved electrode coil dimensions, foil treatment, and optimized electrolyte formulation. The April 2011 build produced 80 cells for the final system deliverables submitted to the national laboratories at the end of April and reflected final refinements to cell design and size. It also featured application of an HRL (Heat Resistant Layer) to the anode, which testing has shown to provide measurable improvement to abuse tolerance. Specifically, both nail penetration and overcharge tests performed in 2011 on cells with the HRL yielded consistently superior results (EUCAR 4 or less) than previous tests on corresponding cells without the HRL.

The final 2011 builds also demonstrated process capability through statistically significant improvements in key cell attributes (capacity, power, stand-loss reduction) and part-to-part consistency. More than 500 cells and three full systems were built over the course of the program. These were used to validate both life and thermal models and to support a vast and complex matrix of abuse tests.

The new 20-mile all-electric range prismatic system delivered meaningful improvements over the 10-mile (cylindrical cell technology) baseline system. In 2011, earlier program projections were confirmed with final hardware, demonstrating a 15% reduction in system volume for twice the range, a 40% improvement in volumetric energy density (Wh/L), and a 13% reduction in dollars per kilowatt hour. Both cycle and calendar life of the new technology are projected to match or surpass that of the original. Abuse tests of the new prismatic cells have thus far achieved EUCAR4 ratings or better on all standard U.S. Advanced Battery Consortium (USABC) tests. These successes have earned support for a follow-on USABC program that will focus on further improvements in cell-level energy density.

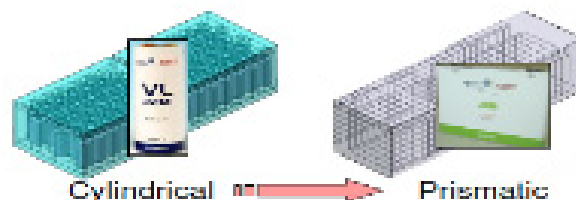


Figure 1. Prismatic form factor offers packaging efficiency improvement opportunity

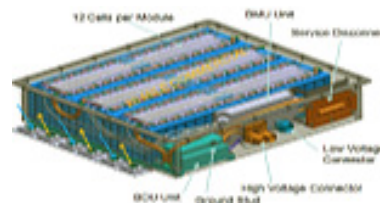


Figure 2. Prismatic system design concept (2 full prismatic systems delivered to national laboratories)

Multifunctional Inorganic-Filled Separator for Large Format Lithium-Ion Batteries

Inorganic-filled separators demonstrate improved thermal stability, lower resistance, and longer cell cycle life compared to conventional separators for lithium-ion batteries for vehicle applications.

ENTEK Membranes LLC and U.S. Advanced Battery Consortium

ENTEK has developed 16–25 μm thick inorganic-filled ultrahigh molecular weight polyethylene separators that offer greatly improved dimensional stability (>90% reduction in shrinkage) compared to conventional polyolefin lithium-ion (Li-ion) battery separators at temperatures exceeding 150 degrees Celsius. Composite separators were manufactured with inorganic fillers that included precipitated silica, fumed silica, fumed alumina, and surface-treated versions thereof. All of these separators had high porosity ($\geq 67\%$), improved wettability, and a very low resistance factor (2–3).

A series of 18650-size cells containing graphite anodes and nickel cobalt manganese cathodes were built with separators containing the above fillers. In all cases, the cycle life for the cells containing inorganic-filled separators was better (45%–100%) than that of cells made with a commercial polyolefin separator. Cells containing precipitated silica-filled separators had lower self-discharge, 75% greater storage life, and 80% improved cycle life compared to cells containing the purely polymeric controls (Figure 2). ENTEK has therefore selected precipitated silica (Figure 1) as the filler of choice for further development work, in order to meet the U.S. Advanced Battery Consortium cost target of \$1/m².

In summary, ENTEK has demonstrated improved thermal stability, cycle life, and low-temperature power capability in 18650 cells built with inorganic-filled separators. Rolls of precipitated silica-filled separators have been supplied to Li-ion battery manufacturers for the construction of larger cells (>7 Ah). The improved cycle life and power capability demonstrated in cells with inorganic-filled separators offers the potential for tangible cost reductions in Li-ion batteries for hybrid

and electric vehicle applications. The performance improvements demonstrated by ENTEK should allow battery manufacturers to decrease the typical oversizing of battery systems needed for compensating the performance loss at low temperatures and degradation over lifetime.

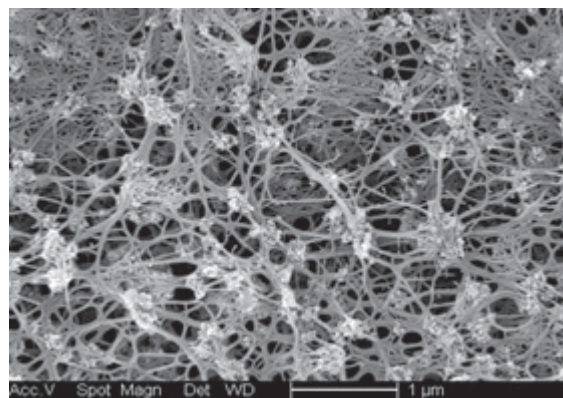


Figure 1. Surface of silica-filled separator showing open structure and high porosity

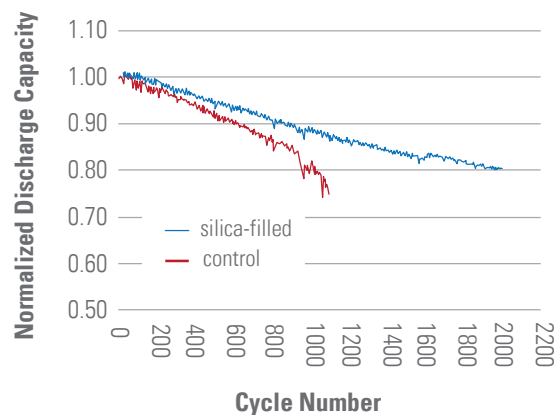


Figure 1. 18650 cells with silica-filled separator, graphite anode, and Ni-Co-Mn oxide cathode have 80% greater cycle

Fuel Cells



Novel Characterization and Models Advance Understanding of Fuel Cell Performance Limitations

General Motors has combined novel micro- and macro-scale diagnostics and models for state-of-the-art fuel cell materials. Both models and data have been disseminated via a publicly accessible website.

General Motors

Transport processes play a fundamental role in governing the ultimate capability of fuel cells. The maximum power density, and thus the size of the stack, is dependent on oxygen transport to the electrode surface. The product water transport away from the electrode can physically block gas pathways for the reactants, which impacts limiting current density and plays a primary role in freeze/cold start capability arising from water build-up in the electrode and adjoining gas diffusion layer (GDL). The foregoing issues are exacerbated by lower precious metal loading. Detailed phenomenological understanding of these processes is required to develop optimal materials and designs to enable wide-scale automotive fuel cell commercialization.

This collaboration has advanced this understanding through a multi-pronged approach that characterizes the relevant material properties utilizing existing and novel diagnostics; develops a multi-dimensional cell model for both single phase (gas) and two-phase (gas + liquid water); and generates a complete set of validation data from down-the-channel ("macro-scale") experiments. As a key part of the program, the complete data set has been made publically accessible (www.pemfcd.org), an unprecedented level of open disclosure.

Key accomplishments are the development of characterization methods to measure transport properties in thin films of ionomer and transport relationships as a function of saturation (liquid water content). Two key components of the down-the-channel model are the relationships between channel water saturation and both GDL to channel interfacial

transport resistances and the channel pressure drop. Therefore, it is critical to establish a well-defined channel water saturation metric. A technique has been developed to quantify the in situ channel water saturation through the combined utilization of high-speed videos of the flow field channels during operation and digital image processing [4]. The image processing algorithm automatically detects static and dynamic liquid water and also characterizes the flow structure of each water object. The water coverage ratio parameter, along with channel pressure drop, as function of saturation provide crucial information pertaining to transport resistance associated with liquid water accumulation in the flow field channels.

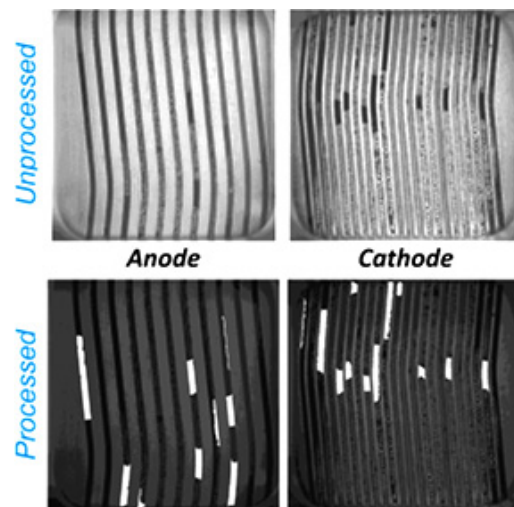


Figure 1. Representative unprocessed/processed high-speed images of liquid water distribution in anode and cathode channels. The processed images can provide quantified information about the local and overall water coverage ratio.

Fuel Cell System Cost Projected at \$49/kW

Strategic Analysis, Inc. incorporated the latest fuel cell performance models and advancements in low-cost materials and components, which led to a 55% cost reduction since 2006.

Strategic Analysis, Inc.

Fuel cell cost analysis is critical for demonstrating the significant progress that has been made through research and development (R&D) activities and in identifying potential research focus areas to further reduce costs. The recent study by Strategic Analysis, Inc. (SA), formerly Directed Technologies, Inc. (results shown in Figure 1), has independently estimated the cost of automotive fuel cell systems for high-volume production (500,000 units per year) at \$49/kilowatt (kW), a reduction of more than 50% since 2006. The 2015 target is \$30/kW.

In the past year, SA based its automotive fuel cell power plant system model on a fuel cell stack polarization curve derived from the fuel cell model at Argonne National Laboratory (ANL). SA updated the balance-of-plant with recent data and feedback from component developers and ANL. SA derived its own manufacturing process assumptions based on patent review and interactions with component and subsystem developers; obtained price quotations for raw materials; and validated assumptions with extensive industry interaction, peer review, and U.S. DRIVE Fuel Cell Tech Team reviews. Since the

beginning of the study, analyses have been refined by replacing less rigorous quotation-based material and component analyses with more detailed bottom-up cost analyses. The analyses have also been used to help determine areas of focus for future cost reduction. Balance-of-plant, in particular compressor/expanders, and bipolar plate surface treatment technologies, have been identified as areas for potential cost reductions in the future.

In addition to the annual cost status update, in Fiscal Year 2011 SA ranked manufacturing processes for the components of the fuel cell system used in its analysis to help determine where further manufacturing R&D is required. SA optimized operating temperature, pressure, stoichiometric ratio, and catalyst loading of the system to minimize system cost; performed an extensive analysis of quality control processes; and performed a life-cycle cost analysis to determine the effect of lower efficiency on both fuel and system cost. SA has provided a cost function for others to use in their models, such as ANL's automotive fuel cell system model.

		Base Case (2010 status)	Base Case w/ Updates	Base Case w/ Updates & ANL Curve	Optimized Case
Annual Production Rate	systems/year	500,000	500,000	500,000	500,000
Stack Efficiency @ Rated Power	%	55%	55%	55%	55%
Cell Voltage @ Rated Power	V/cell	0.676	0.676	0.676	0.676
Oxygen Stoichiometric Ratio		2.5	2.5	2.5	1.5
Peak Stack Operating Pressure	atm	1.69	1.69	1.69	3
Peak Stack Operating Temperature	°C	90	90	90	95
Total Platinum-Group Catalyst Loading	mgPt/cm ²	0.15	0.15	0.15	0.186
MEA Areal Power Density @ Rated Power	mW/cm ²	833	833	732	1,110
Power Density Equation Selected		Standard	Standard	ANL Curve fit	ANL Curve fit
System Cost	\$/kW_{net}	\$51.38	\$51.92	54.72	\$47.81

Figure 1. 2011 Automotive Fuel Cell System Cost Status Update with Optimized Case

“Best in Class” Membrane Electrode Assembly Meets DOE Component Durability Requirements

Performance of nanostructured thin film MEA with low Pt loading from 3M reduces projected fuel cell system cost.

3M

3M’s membrane electrode assembly (MEA)—which uses 3M-developed nanostructured, thin-film (NSTF) electrocatalyst technology—meets or exceeds most U.S. Department of Energy (DOE) 2017 catalyst performance and durability targets. The MEAs contain PtCoMn catalysts with Pt loadings of 0.05 mgPt/cm² on the anode and 0.15 mgPt/cm² on the cathode, deposited using an enhanced process that offers greater simplicity and more cost-effective coating. The MEAs use a 3M-made, 3M-supported membrane with a chemical additive and standard 3M gas diffusion layers (GDLs). Results of this project are the basis for U.S. DRIVE cost projections that have enabled significant cost reduction in the fuel cell stack over the past several years.

The top graph in Figure 1 shows the series of polarization curves measured periodically over a total of 435 hours at 1.2 volts. As shown, fuel cell operation only had a minimal effect on performance. Surface area loss was 10%; specific activity was unchanged, and the performance at 1.5 A/cm² dropped only 10 mV. The bottom graph in Figure 1 shows the polarization curves before and after 30,000 voltage cycles.

In addition, 3M has demonstrated 9,000 hours of membrane durability during load cycling tests in 50 cm² cells using a non-supported 3M polymer electrolyte membrane (PEM) with chemical stabilizers, showing great progress toward achieving PEM fuel cell durability, one of the technology’s greatest challenges. 3M also has made advancements in understanding and improving low-temperature operation of NSTF electrodes by identifying the importance of anode GDL backing properties.

Ongoing work includes short stack testing to compare performance and durability of six different MEA configurations. There are three types of membranes and three types of cathode catalysts in the stack that 3M will use to down-select the preferred technology.

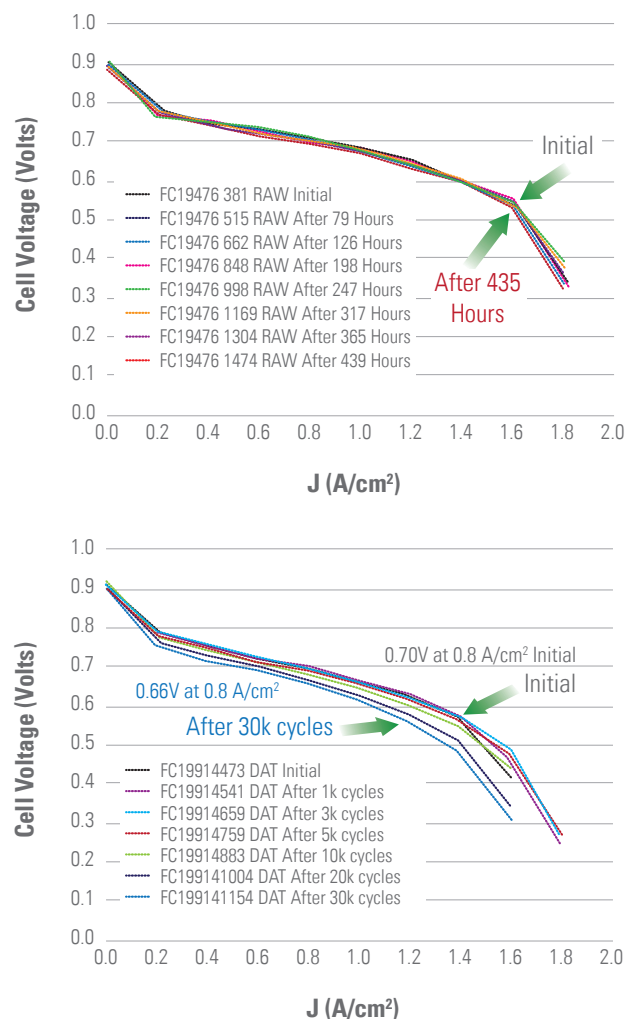


Figure 1. Polarization curves vs. time using U.S. DRIVE durability testing protocols (1.2 V hold and CV cycling tests)

3M High-Temperature Membrane Meets Durability Targets

3M demonstrated that its new membranes, capable of operating under hot and dry conditions, meet 2015 targets for both chemical and mechanical durability.

3M

3M demonstrated that its Per Fluoro Imide Acid (PFIA) membranes meet 2015 targets for both chemical and mechanical durability. Previously, 3M demonstrated that the PFIA membranes are capable of operating under hot and dry conditions. By operating under hot-dry conditions, balance of plant can be simplified by reducing radiator demands and by reducing or eliminating the need for a humidifier. Although hot-dry operation is desirable, the membranes must also operate under cold and wet conditions and cycle between these conditions due to vehicle starts/stops and operation in varying climates. These conditions cause mechanical stresses on the membranes, and previous attempts to obtain membranes with good conductivity at high temperature-low relative humidity (RH) have resulted in membranes with poor mechanical durability under these cyclic conditions.

By utilizing multiple acid groups on the polymer sidechain and nanofiber supports, 3M was able to overcome this problem and demonstrate that its PFIA membranes can survive these dry-wet cycles and have high proton conductivity and low area-specific resistance (ASR) at 120 degrees Celsius (C) and 25% RH, similar ASR to Nafion at 80 C and 100% RH. The PFIA membranes were subjected to RH cycling tests and survived more than 20,000 RH cycles (Figure 1, left). In addition, these membranes exceeded the chemical durability target, surviving for more than 650 hours at open circuit voltage (target is 500 hours), as shown in the right plot in Figure 1. While membrane performance and durability have been demonstrated, MEA performance and durability under high-temperature conditions must still be demonstrated. The cost must also be independently evaluated.

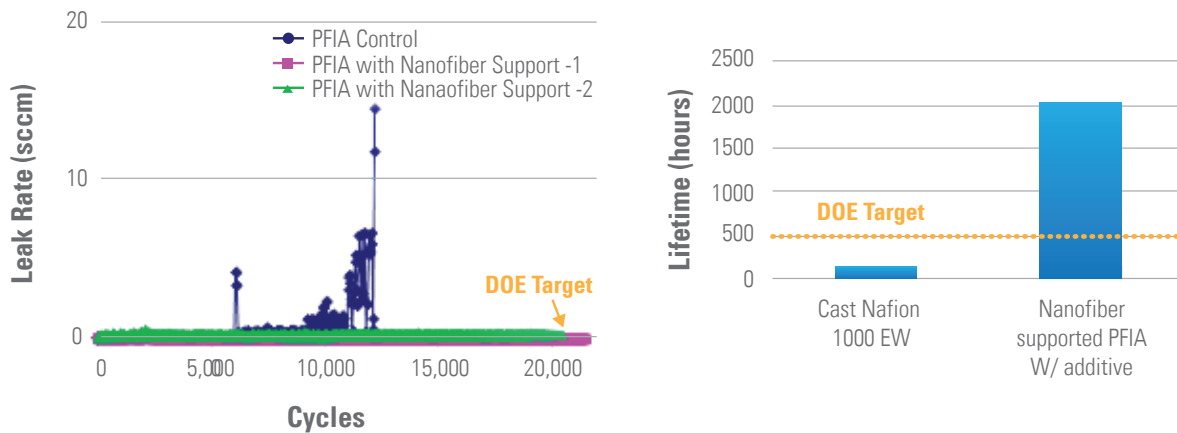


Figure 1. Supported 3M PFIA membrane exceeds mechanical durability (% RH cycle test, target 20,000 cycles) and chemical stability (OCV test - target 500 hours) targets

Multi-Metallic Nanoparticles with Tailored Composition Reduce Cost, Improve Durability of Fuel Cell Catalyst

Alloying Pt with low-cost, abundant base metals shows improved durability over Pt and reduced costs by approximately 80%.

Argonne National Laboratory

A major contributor to the cost of fuel cells for the automotive application is the platinum group metal (PGM) cathode catalyst. One way to lower this cost is to improve the performance of the catalyst while also replacing platinum with less expensive metals. Argonne National Laboratory (ANL) has improved the activity of platinum by combining Pt with low-cost and abundant base metals, such as nickel, cobalt, and iron.

ANL synthesized and tested catalyst nanoparticles of many combinations of platinum, nickel, cobalt, and iron. The highest activity catalyst was a novel combination of platinum, cobalt, and nickel, which achieved an activity approximately five times that of the standard platinum catalyst and approximately 35% higher than the binary platinum-nickel catalyst highlighted last year (Figure 1). This improvement could reduce fuel cell catalyst cost by approximately 80%.

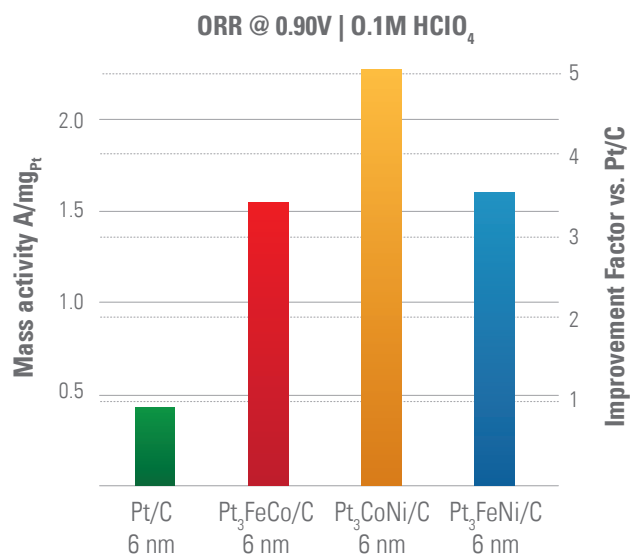


Figure 1. Platinum-cobalt-nickel alloy catalyst (Pt₃FeCo/C) shows higher oxygen reduction activity per weight of platinum than baseline platinum catalyst (Pt/C)

Another route toward improving catalyst performance is through the enhancement of catalyst durability by nanostructuring—coating several overlayers of the platinum alloys on gold particle cores. For example, a platinum-iron alloy on a gold core had an initial activity 3 times that of platinum; however, after 60,000 potential cycles, had an activity 10 times that of platinum (Figure 2).

Further improvements in activity and stability are expected by applying additional post-fabrication treatments (acid treatment and heat treatment) to these multi-metallic catalysts. Previous work suggests an additional doubling of catalyst activity can be achieved using such processes, leading to another \$100 in vehicle savings. Future work will investigate combining the multi-metallic and core shell approaches to achieve additional improvement.

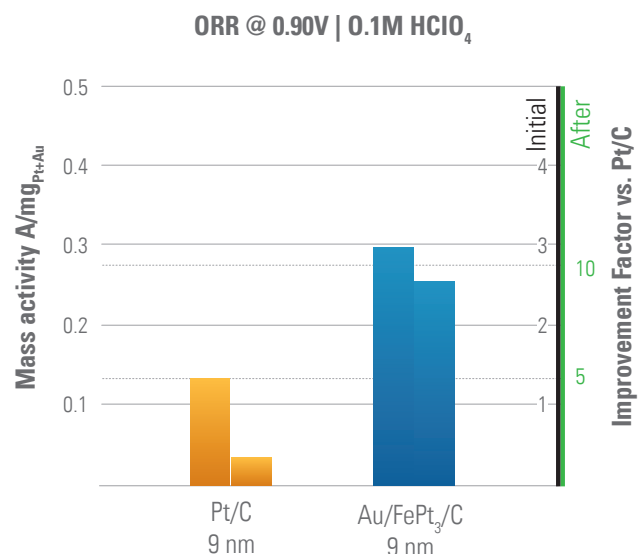


Figure 2. Platinum-iron alloy on a gold core shows 3 times the activity of platinum initially and 10 times the activity after 60,000 potential cycles

Novel Techniques for Measurement of Key Fuel Cell Transport Parameters

New tools developed for measuring water and proton transport in fuel cell membranes provide critical data to accurately model fuel cell performance.

Giner Electrochemical Systems

One of the major challenges for developing commercially viable fuel cell power systems is the ability for the fuel cell systems to handle the water that is generated within the fuel cell during operation. Certain parts of the fuel cell, such as the membrane, need to remain hydrated in order to conduct protons. Other parts, such as the gas diffusion layer, cannot function effectively when filled with liquid water, preventing the flow of gases to the electrodes. In order to develop models to predict where the water will go during fuel cell operation, it is imperative to have accurate parameters for water transport in the individual components and at the interfaces between components as a function of operating conditions.

Giner Electrochemical Systems has developed several novel techniques for measuring water transport, as well as gas and proton transport within fuel cell components. One particularly valuable technique

measures the water transport in the thin (<25 μm) membrane (see Figure 1). Giner's technique eliminates any boundary layer effects by controlling the device so that only water vapor, and no other gases, is present. Measurements taken using this new technique have shown conclusively that there is no interfacial transport resistance between the membrane and the vapor phase. This finding casts a new light on claims by several other researchers that an interfacial resistance is needed for Giner's fuel cell models.

Giner has also developed a method for simultaneous measurement of membrane proton conduction and water uptake as a function of temperature and relative humidity. Future work includes developing a cell model that can incorporate the parameters measured using these techniques to accurately predict water transport and fuel cell performance throughout the entire fuel cell.

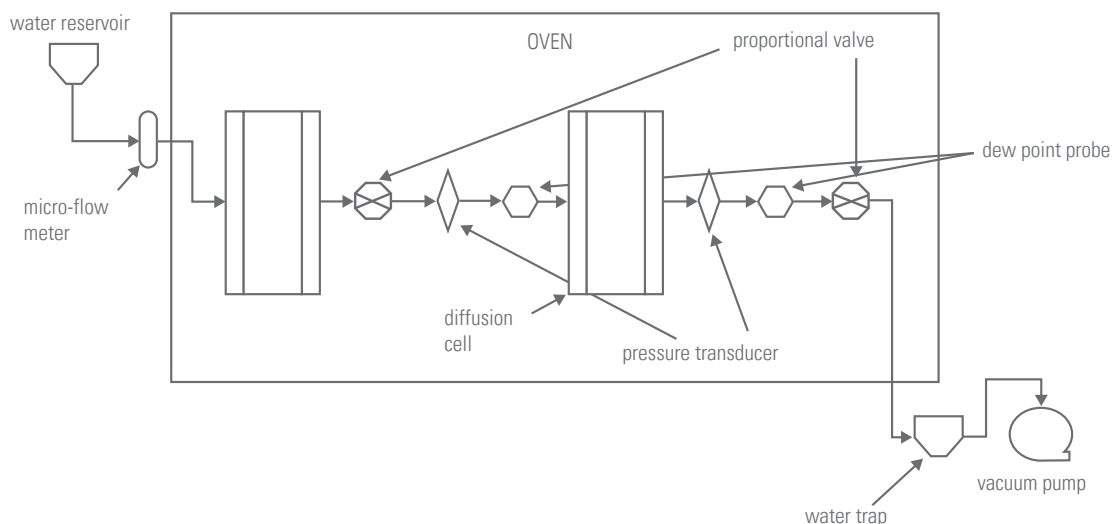


Figure 1. Schematic of novel apparatus developed at Giner to measure water transport across a thin membrane without interference from boundary layer effects

Two-Dimensional Dynamic Model Developed for Fuel Cell Freeze Start Operation

LBNL developed a freeze start model that can accurately predict the kinetics of ice formation in porous gas diffusion media that could limit low-temperature operation.

Lawrence Berkeley National Laboratory

Although successful startup of fuel cell vehicles under freeze conditions has been demonstrated by numerous automakers, the ability to maintain freeze startup in the context of advanced materials is still critical to meeting U.S. DRIVE fuel cell targets. Fuel cell vehicles require higher performing catalysts to decrease the loading of precious metals. However, as the amount of precious metals decreases, the likelihood of flooding the catalyst increases. For this reason, research projects focused on gaining a fundamental understanding of water transport mechanisms in fuel cells are necessary.

The project at Lawrence Berkeley National Laboratory (LBNL) focuses on transport phenomena associated with freeze conditions. In particular, LBNL begins by studying how water is distributed among the membrane, catalyst layers, gas diffusion layers, and flow channels upon vehicle shutdown, and then how this water distributes as stack temperature reduces to freeze conditions. The resulting humidification state affects how the vehicle starts at freezing temperatures, which relates to the ultimate objective of the LBNL project: to develop the models necessary to help stack manufacturers predict freeze start robustness.

One key aspect of predicting fuel cell performance under freeze conditions is the ability to model phase changes, such as the freezing of liquid water into ice. Some water will be frozen in the channels and porous media when the vehicle starts. Water that is produced by the fuel cell reactions can also freeze. LBNL has developed a model that regards the freezing of water to occur in two sequential mechanisms: induction and growth. Induction was modeled with classic nucleation theory, while growth was associated with the heat loss due to freezing. The resulting model was

capable of accurately predicting the fractions of water that turned to ice in porous media during isothermal experiments using differential scanning calorimetry (DSC). As shown in Figure 1, the model matched DSC data throughout the range of subzero temperatures that are of interest in fuel cell vehicle development. Having accounted for phase changes between liquid water and ice, LBNL is in an excellent position to deliver the freeze start prediction model expected by the completion of the project.

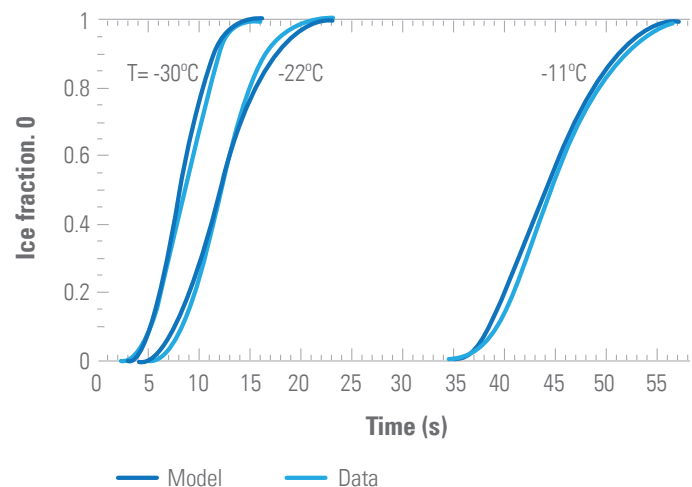


Figure 1. The model to predict ice formation in a porous gas diffusion layer was able to accurately match data from a calorimetry experiment

Novel Techniques Provide Insight into Fuel Cell Component Degradation

ORNL developed novel microscopy techniques to track nano-scale morphology changes in fuel cell membranes and point to ways to make platinum catalysts more stable.

Oak Ridge National Laboratory

A key element of tackling the issue of fuel cell component degradation is the ability to closely examine morphology and composition of both fresh and aged samples, as well as correlate the characteristics of components aged by real-world operation in the field with components aged ex-situ by accelerated stress testing.

Oak Ridge National Laboratory (ORNL) applies conventional and novel techniques to reveal microstructural and compositional characteristics. The information is used by component developers to adjust compositions and processing parameters to achieve the desired components.

ORNL used electron energy loss spectroscopy (EELS) in a transmission electron microscope/ scanning transmission electron microscope (TEM/STEM) to characterize the nature of recast ionomer within electrode structures, and to understand the nanometer-scale phase separated morphology observed in

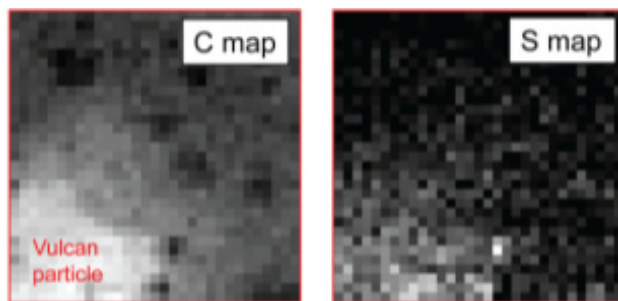


Figure 1. EELS spectrum imaging data from 61 wt% ionomer sample

Nafion® electrolyte in fuel cell electrodes. Figure 1 shows that sulfur was consistently associated with the Vulcan (carbon) black, where the Pt is dispersed in fuel cell electrodes. This discovery sheds light on how the Nafion adsorbs onto the catalyst surface and suggests that the sulfonic acid sites of the Nafion may limit access to the Pt surface.

ORNL also used Z-contrast STEM to begin elucidating Pt nucleation and growth on carbon and graphitic surfaces by identifying preferred Pt deposition sites on carbon. Figure 2 reveals that all platinum atoms deposit at edge sites and not on sites associated with the smooth surfaces. This information helps guide identification of more stable sites for Pt deposition to enhance catalyst stability and, thus, increase fuel cell life.

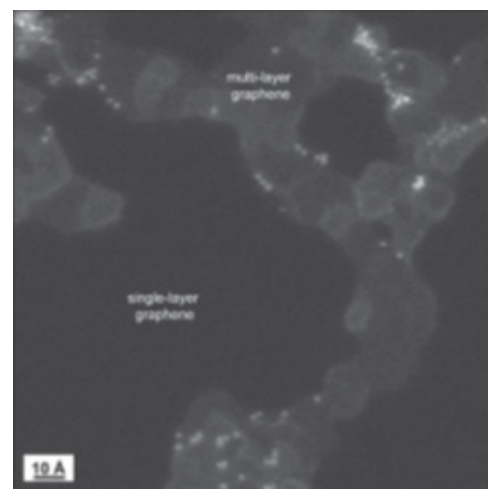


Figure 2. Z-contrast STEM image showing the different layers of graphene and individual platinum adatoms (bright spots) deposited on surface

High Spatial Resolution of Neutron Imaging for Water Management Analysis in Fuel Cells

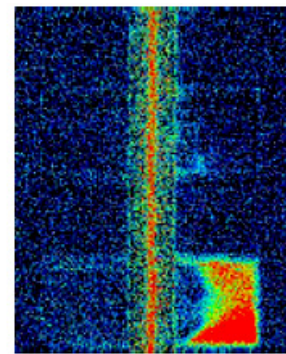
NIST developed a neutron imaging method with high spatial resolution that enables identification of conditions that lead to electrode flooding and membrane dry out.

National Institute of Standards and Technology

Water management in proton exchange membrane fuel cells (PEMFC) is a major technical challenge. It is necessary to manage the water in the fuel cell to avoid excess water within the flow channels, so the reactant gas can reach the electrocatalyst, yet without drying out the electrolyte membrane, which needs water to promote proton conductivity. In addition, proper water management is important for reliability, durability, and freeze start-up capability.

The National Institute of Standards and Technology (NIST) has been using advanced neutron imaging techniques to determine precisely where the water is during fuel cell operation. Neutron imaging is a non-destructive measurement technique for detecting condensed water. This past year, NIST successfully developed a new neutron detection method utilizing a micro channel plate. This method achieved neutron detection with the highest spatial resolution and the largest field of view relative to other technologies. This technology is able to achieve 10 μm level spatial resolution over a 35 by 35 mm field of view. While other types of imaging technologies are able to achieve this resolution, they cannot achieve such a large field of view. This high resolution allows NIST to characterize water transport across the membrane electrode assembly (MEA). Figure 1 shows an example of an MEA cross section during operation. Red portions indicate higher concentration of condensed water. This improved technique has already been applied to several ongoing water management studies. For example, Los Alamos National Laboratory leverages this technique to detect the water profile of the gas diffusion layers of the cell various materials and operating conditions. Through this collaboration, they found that the water profile changes during corrosion of the carbon in the electrocatalyst.

NIST is continually enhancing its neutron imaging capabilities to accommodate the needs of industry and academia, including further improvement of spatial resolution (up to 1 μm) applied to larger field of view.



MCP

Spatial Resolution: 13 μm
Field of View: 3.5 cm x 3.5 cm
Frame Rate: 10s - 20 min

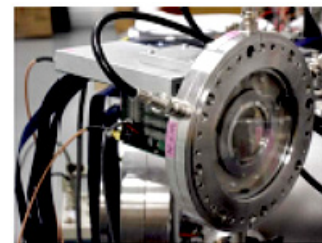


Figure 1. Example of MEA Cross Section Neutron Image with MCP High Spatial Resolution (above), MCP Detector at NIST (below)

Materials



Development of the Ablation Casting Process for High-Volume Production

Novel, new casting process can produce large volumes of high-strength cast aluminum components that will allow mass reduction in vehicles.

U. S. Automotive Materials Partnership

Cast components are widely used in the manufacture of vehicles. One cost-effective approach to reduce the mass of vehicles is to reduce the weight of those castings by increasing the strength of castings. This can be accomplished by improving the casting process or through the use of new alloys.

The ablation casting process is a novel, new casting process that has demonstrated the ability to produce aluminum castings with superior properties compared to conventional casting processes. The physics of the process allow for parts to be produced with the properties of forgings, but with complex shapes that only castings can provide.

The process, shown in Figure 1, is essentially a sand casting process that utilizes a water soluble media binder that allows the mold to be washed away by water sprays. This produces very high-temperature gradients and short solidification times, which are highly desirable. These thermal characteristics also allow the process to cast high-strength alloys that are difficult or impossible to cast by conventional processes.

The purpose of this project was twofold. One objective was to determine if this process is capable of high-volume production. The other objective was to identify process steps unique to this process and to determine their associated costs (or savings) compared to conventional casting processes. This information was used to create a cost model, so that this process can be compared to existing production processes.

The project determined that there are no technical barriers to the implementation of this process for high-volume production. In fact, since this process uses inorganic molding media binders and reuses the molding media, it is also very environmentally friendly.

The cost model developed in this project will allow potential automotive suppliers to make informed decisions, based on their own constraints and requirements, about adopting this process for their manufacturing needs.

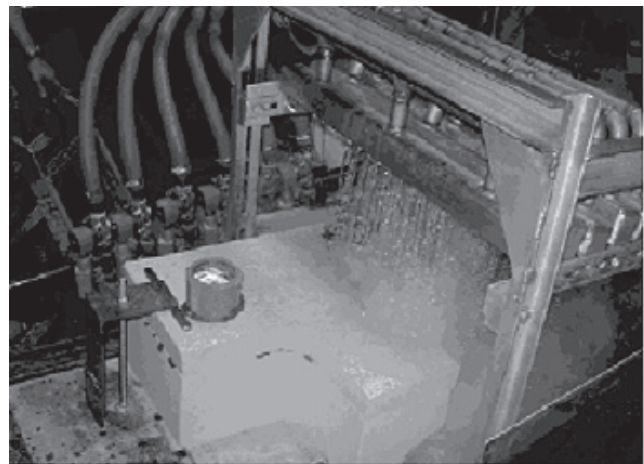


Figure 1. Photograph of the ablation casting process. The mold is being translated beneath the water shower. The water shower washes away the mold media and impinges directly on the part. This creates high cooling rates in the casting, improving its mechanical properties.

Friction Stir Spot Welding of Advanced High-Strength Steels II

Developing robust, high-speed, low-cost methods for joining advanced high-strength steels.

Oak Ridge National Laboratory and Pacific Northwest National Laboratory

An initial project on friction stir spot welding (FSSW) of advanced high-strength steels (AHSS) confirmed that FSSW of AHSS could be accomplished with currently available tool materials, and that the process could make spot welds with high tensile lap-shear strengths (LSS). This follow-on project is designed to demonstrate that FSSW is an acceptable, cost-effective alternative for AHSS, which is difficult to resistance spot weld (RSW), and that FSSW will support lightweighting objectives through down-gauging of sheet thicknesses by enabling dissimilar steel bonding.

Numerous spot welds were made on the combinations of steel shown in Table 1 using Si₃N₄ stir tools. Process parameters included tool rotation speeds of either 800 rpm or 1,600 rpm; plunging of 1, 2, or 3 time segments; and total welding times of either 4 s or 8 s. For each combination, it was possible to make spot welds where LSS exceeded the minimum American Welding Society values for RSW of the weaker of the two types of steel. For two of the combinations, HSBS-TRIP780 and DP780GA-HSBS, a total of 50 additional welded coupons were made for each set and supplied to the University of Michigan for fatigue testing and analysis under a subcontract.

A concerted effort was also undertaken with Ceradyne to examine issues related to durability and cost of Si₃N₄ tooling. Figure 1 shows the estimated conditions under which FSSW tooling would reach cost parity with that used for RSW. For instance, FSSW tools costing around \$10 each would need to last for at least 5,000 spot welds to approach the same cost as RSW tooling. According to cost estimates from Ceradyne, FSSW tooling costs will be sensitive to volume and amenable to scalable economics, which approach conditions of cost neutrality with RSW.

The project includes a committee of consultants from Chrysler, Ford, General Motors, Kawasaki (robot manufacturer), MegaStir (producer of PCBN friction stir tooling), and Ceradyne Inc. (producer of Si₃N₄ tooling).

AHSS Alloys	Plunge Steps	Avg. LSS, kN	AWS Min, kN
TRIP590 to DP780	2	11.0	7.98
DP780 to TRIP590	2	10.9	7.98
DP980 to TRIP780	1	12.6	10.32
DP980 to TRIP780	1	11.4	10.32
DP780GA to HSBS	1	12.2	10.32
DP780GA to HSBS	2	11.2	10.32

Figure 1. Initial results for FSSW of dissimilar AHSS alloys (800 RPM)

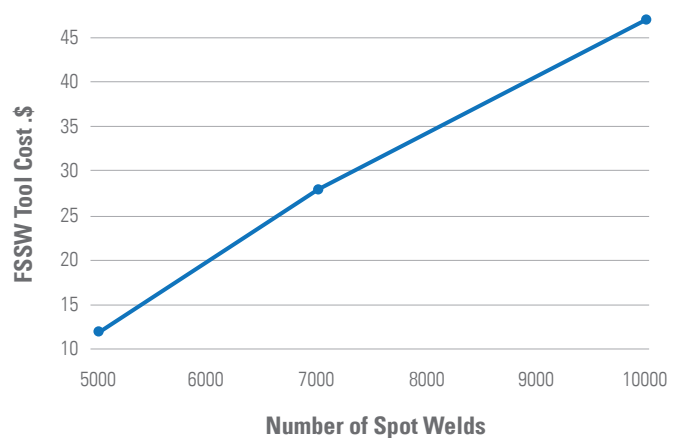


Figure 2. Comparative estimate of FSSW tool cost and life that will produce approximate cost neutrality with RSW

Lower-Cost Carbon Fiber from Textile-Based Precursors

Reducing the cost of automotive-grade carbon fiber by using high-volume polyacrylonitrile textile fiber as a carbon fiber precursor.

Oak Ridge National Laboratory

Currently, carbon fibers with the properties needed for automotive applications sell for \$8–\$15 per pound. About 50% of that cost is attributable to the cost of the precursor used to make the carbon fiber. A collaborative international program by Oak Ridge National Laboratory (ORNL) and FISIFE S.A. (an acrylic fiber company in Portugal) is working to render textile-based polyacrylonitrile (PAN) suitable for conversion into carbon fiber. Textile fiber sells for half the cost of conventional carbon fiber precursors and would result in a savings of more than \$2 per pound in the finished carbon fiber manufacturing costs.

Recently, the two organizations have defined several textile formulations that yield suitable carbon fibers. They are modifying materials that can be oxidized near conventional oxidation temperature. In addition, they have developed a way to modify the chemistry of the starting materials by adding a small amount of a third component to the polymer chemistry. They also have defined a chemical pretreatment protocol for further altering the fiber chemistry.

Different levels and conditions of the pretreatment also were evaluated. Key to incorporating these changes has been the ability to perform the chemical modification in current production facilities and at current production speeds and temperatures. Mechanical properties now well exceed the program requirement, as shown in Figure 1.

Oxidative stabilization is the low-speed bottleneck in the carbon fiber conversion process. The oxidative stabilization of the modified textile precursors requires only about 70 minutes compared to a time of 80–120 minutes for conventional carbon fiber precursors. As a result, modified textile precursors may be carbonized at much higher speeds and significantly lower production costs.

FISIFE is a commercial fiber production facility and intends to offer this new fiber as a lower-cost precursor to current and future carbon fiber manufacturers. ORNL has other parallel efforts to develop new production technologies that will enable manufacturers to develop high-volume, commercial carbon fiber plants that use textile-based PAN precursors, along with other advanced manufacturing methods.



Figure 1. Development of Textile Fiber Strength as a Function of Time



Figure 2. Carbon Fiber Precursor from Textile-Based PAN

Enhanced Formability of Aluminum at Room Temperature Through Pulse-Pressure Forming

Pulse-pressure forming of aluminum has the potential to replace steel by high-strength aluminum alloys in the manufacture of automotive structural components, including outer panels, decklids, hoods, and doors.

Pacific Northwest National Laboratory

Pacific Northwest National Laboratory (PNNL) has demonstrated that the formability of annealed AA5182 aluminum (Al) alloy sheet can be enhanced 2.5 to 6 times at room temperature—through pulse-pressure forming (PPF) techniques—to levels typically expected during the forming of Al at elevated temperatures. The implication of this result is that automotive parts can potentially be formed at room temperature using lightweight Al sheet with equal ease as conventional mild steel sheet. This research will help the U.S. auto industry overcome the cost barrier associated with the traditional elevated temperature forming of Al and enable cost-effective weight reduction in automobiles through replacement of heavier mild steel with lightweight Al.

While the phenomenon of increased metal formability at high-strain-rates has been generally known, the automotive industry has not been able to take advantage of it due to the lack of detailed quantitative information about the deformation process. This has prevented a clear understanding of the phenomenon and hindered the development of validated numerical models. To address these technological gaps, PNNL has developed a unique experimental capability that can measure deformation history (i.e., displacement, velocity, strain, strain-rate, and strain-path as a function of time) on the sheet metal surface when they are formed—e.g., into dome shapes (Figure 1)—by PPF techniques such as electro-hydraulic forming (EHF). This experimental capability has enabled researchers to quantify the deformation conditions that are necessary for achieving formability enhancements in Al alloys at room temperature. For example, in EHF tests lasting approximately 0.5 ms, a peak strain-rate of about 3,900/s and a plane-strain strain-path at the apex of the dome were found to enhance formability of

Al by approximately 2.5 times relative to its formability at quasi-static strain-rates. Even greater formability enhancement (about 6 times) was observed where the peak strain-rate was only about 1,700/s, but the sheet was impacted and formed inside a conical die.

The project included industry partners from Ford, General Motors, and Chrysler. Efforts are now underway to develop validated numerical models to describe the formability of Al at high-strain-rates and extend the work to high-strength Al alloys as well.

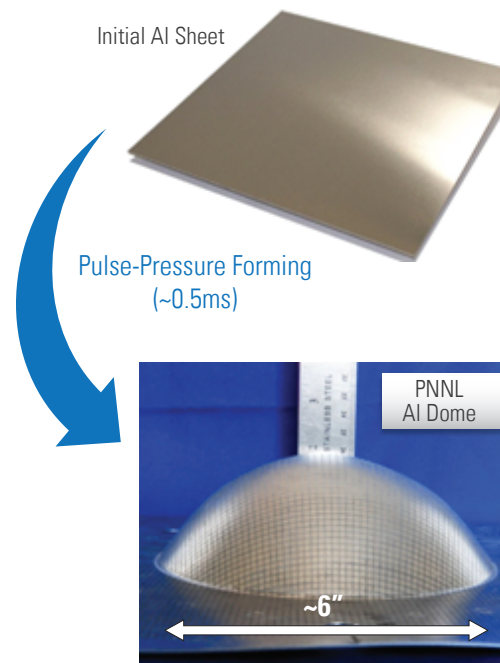


Figure 1. An Al dome formed out of a AA5182 Al alloy sheet (1 mm thick) using the EHF technique. The peak velocity, normal to the dome apex, is typically ~100 ms or greater.

Ultrafine Grain Magnesium Foil and Sheet by Large Strain Extrusion Machining

Developing a reduced cost method for manufacturing Mg sheet product from wrought feedstock material.

Pacific Northwest National Laboratory and Purdue University

Pacific Northwest National Laboratory (PNNL) and Purdue University are collaborating on a solution to overcome the cost barrier of implementing sheet magnesium (Mg) alloys in automotive applications. Large Strain Extrusion Machining (LSEM), under development by the Purdue University group, is a hybrid cutting-extrusion process in which sheet metals can be produced in a single stage deformation process. The motivation for this work is that the current methods for producing Mg wrought sheet products require extensive thermo-mechanical processing steps, which result in high material cost and energy consumption. Alternate continuous casting technology has limited ability to process the range of Mg alloys and results in less-than-optimum sheet microstructures. The objective of this project is to demonstrate the ability to make sheet thickness Mg strip directly from wrought and cast Mg feedstock materials using the LSEM process.

A rotary LSEM configuration, as implemented on a lathe, is shown schematically in Figure 1. In the LSEM process, a constraining edge is used in addition to a cutting edge to impose large shear strains while controlling the product thickness. The strains induced in the metal by the LSEM process results in reduced grain size, which is desirable for sheet formability. Phase 1 experimental results showed that LSEM can be tailored to produce 25 mm-wide sections of sheet material from wrought feedstock, and at the limit of the current experimental tooling, can reach the nominal 2 mm-thickness goal.

Phase 2 work extended the range of deformation and temperature conditions to map the resulting grain size as a function of processing conditions. In addition, Phase 2 demonstrated that the LSEM process could also be applied to cast feedstock materials and generate microstructures typical of the wrought

product. Figure 2 shows an example of the strip produced from the casting and compares the LSEM to conventional sheet processing methods on three key cost factors: number of processing steps, material loss, and energy usage.

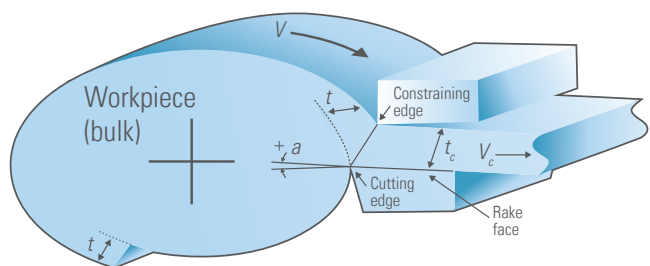


Figure 1. In the LSEM process, a cutting tool is used to “peel” Mg strip from a round ingot similar to wood paneling. The strain induced in the metal creates desirable fine grain structure

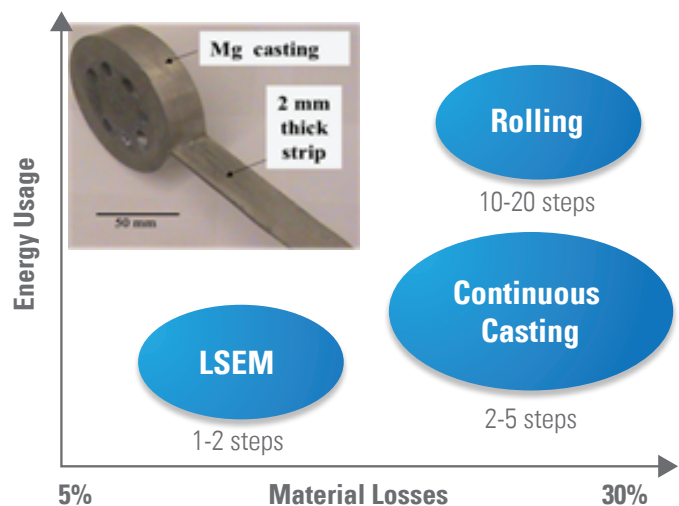


Figure 2. LSEM is a more direct method compared to conventional sheet processing with potential to reduce material losses and energy usage

Direct Compounding of Structural Engineering Composite

New processing and materials technologies that enable low-cost processing of high-performance polyamide 66 engineering polymers have been developed and demonstrated.

U.S. Automotive Materials Partnership

Direct compounding of thermoplastic composites has become well established within the automotive supply base. Reported key advantages include reduced raw materials cost and improved part properties. However, to date, the process has been limited primarily to the development of polypropylene-based composites. This prompted a new study to investigate the feasibility of extending the technology to process high modulus polyamide 66 engineering thermoplastics.

The project statement of work was divided into four distinct work packages. Initially, developments focused on the derivation of new polymer formulations that were suited to direct compounding. Early trials were performed to determine mechanical performance relative to conventional materials processed by compression and injection molding. Once the base formulations were validated, the second phase concentrated on establishing the impact of material additives and dosing levels on performance of molded parts before and after durability testing. This provided an optimized solution and an understanding of the processing window for new polymer formulations.

The third phase of the project was devoted to understanding the impact of processing on the dispersion of fiber reinforcement and final properties of molded panels. Trials were performed using a Dieffenbacher twin screw direct compounder, which enabled both process setup and extruder screw design to be changed as part of the processing study. The outcome of this trial was an assessment of the effect of machine parameters on fiber attrition and fiber length in the molded part. Hence, optimized machine parameters could reduce fiber breakage while promoting distribution and filament dispersion.

The final phase of the project was a full-scale processing trial using a front-end grill opening reinforcement automotive component (Figure 1) to demonstrate capability to produce complex three-dimensional parts. A pilot production facility, featuring a 3600 MT press and 70 mm direct compounding extruder, was used to process a series of parts at rates representative of high volume production. More than 200 parts were produced under a broad range of processing conditions to validate flow characteristics of new polyamide materials formulations.

Throughout each phase of the program, new direct compounded formulations were shown to match or exceed the performance of pre-compounded material systems, while also offering the economic advantages of a low-cost processing approach.

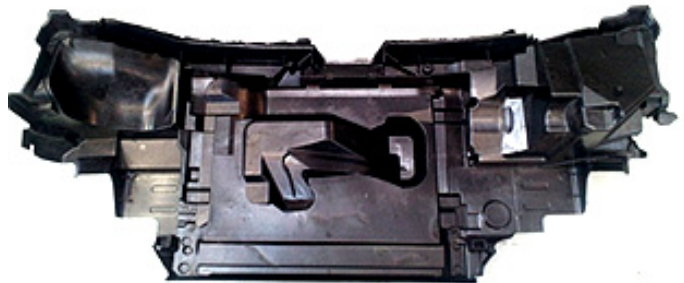


Figure 1. Front end grill opening reinforcement demonstrator component

Lightweight Sealed Steel Fuel Tanks for Advanced Hybrid Electric Vehicles

Demonstrating significant mass savings for advanced hybrid electric vehicle fuel tanks through optimized design and use of advanced high-strength steels.

U. S. Automotive Materials Partnership

While running in the electric mode, advanced hybrid electric vehicles (AHEV) and extended range electric vehicles (EREV) carbon canisters, used for fuel evaporative emissions control, cannot be purged. Consequently, in current designs, the fuel tanks are sealed, which raises the internal pressure of the tank. Current plastic tank designs cannot meet the high internal operating pressures, so thick-walled (1.4 to 2.0 mm) steel tanks are used, which result in high mass. Therefore, the purpose of this nine-month project was to enable and demonstrate the manufacturing feasibility of low-mass, sealed steel fuel tanks suitable for use in AHEV/EREV while achieving equivalent performance and cost.

Steel tanks from two current AHEV models were acquired and used as initial benchmarks. The tanks were re-engineered, without significant shape change, to allow use of thinner AHSS carbon steels or stainless steels.

Computer-aided engineering studies show that thinner AHSS carbon (TRIP) steel or stainless steels coupled with structural enhancing techniques, such as stiffening ribs, structural baffles, and weld-bonded reinforcements, can be used to significantly reduce the mass of current-generation sealed steel fuel tanks. In this study of two benchmark tanks, mass reductions of 20.7% to 40.7% were obtained, depending on the steels selected and structural options used.



Figure 1. Photograph of one of the baseline sealed steel fuel tanks. Gross fuel tank mass 65 lbs/29.3 kg and 16 gallon capacity.

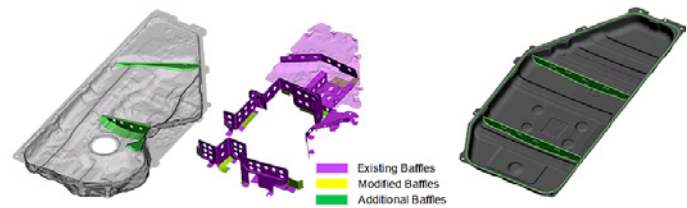


Figure 2. Optimized fuel tank design and use of AHSS and Stainless Steel.

Material Type	Steel Grade	Initial Tank Mass (kg)	Reduced Tank Mass (kg)	Mass Saving (%)	Cost Changes High/Low Vol. %	Shell Thickness	
						Upper	Lower
AHSS	TRIP 450/800	29.3	19.4 (-9.9)	33.8	+2.1 / +5.6	1.1	1.2
	Stainless Steel 301LN - 1/4 Hard		17.4 (-11.9)	40.7	+37.7 / +35.0	0.9	1.1

Figure 3. Summary of mass and cost impacts of steel alternatives.

Reliability Tools for Resonance Inspection

Resonance inspection is a low-cost, high-volume, non-destructive test method that enables the use of lightweight materials in safety-critical automotive components by ensuring the quality of those components.

U.S. Automotive Materials Partnership

Resonance inspection (RI) has entered the world of computational automotive design. This project developed some of the software tools necessary to enable the RI of computer models of lightweight safety-critical automotive components. The utilization of lightweight materials in safety-critical automotive components is contingent upon verifying the quality of their design, materials, and workmanship via rigorous testing. Typically, these safety-critical parts are inspected with specialized, time-consuming, non-destructive testing (NDT). RI can replace these tests with a single inspection that can be completed in two seconds for less than 10% of the cost of NDT. Industry acceptance of RI has been slow due to the empirical nature of the method. Traditional RI requires several hundred samples of acceptable and rejectable components to develop a sorting module that can accommodate the natural variations that occur in the manufacturing process while maintaining the ability to discriminate and reject flawed parts. This project developed a physics-based sorting module to replace the current empirical methodology (see Figure 1). Significant progress has been made toward testing a virtual part with RI and developing an acceptance criteria and sorting module that can be used on the shop floor to inspect parts as soon as manufacturing begins.

The Reliability Tools for Resonance Inspection of Light Metal Castings Project has completed an experimental program of casting tensile bars, which were inspected with multiple NDT methods and RI. The resonance shifts noted in the RI were correlated to different flaw types and material strength. This cor-

relation data was used to develop several software tools that, when used together, can generate an RI sorting module based only on computer simulations. The team has written an American Society for Testing and Materials style standard to ensure reliability and reproducibility in the use of RI.

Future work has been identified, which includes the expansion and refinement of the computer-based flaw library and development of software tools to predict the probability-of-detection of resonance inspection to performance-critical casting flaws.

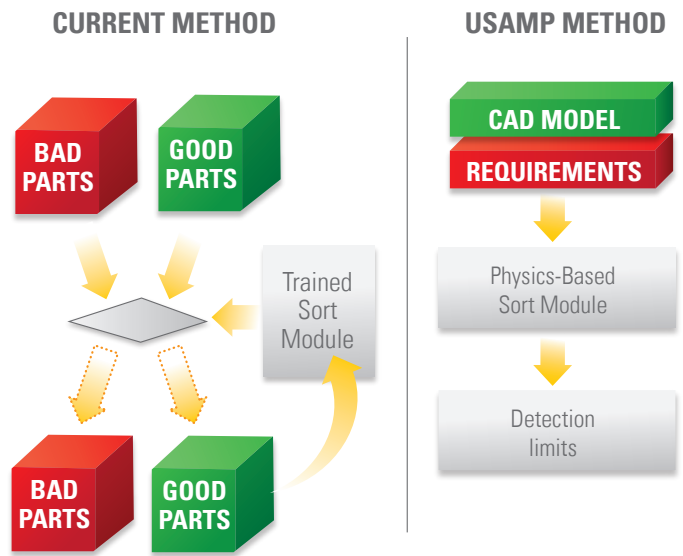


Figure 1. The current empirical method is illustrated on the left and the physics-based method of RI developed in this project on the right

Vehicle Systems Analysis



Thermal Research to Improve Electric Vehicles

Integrated thermal management research focuses on reducing vehicle cost while delivering greater range, battery life, safety, reliability, and comfort.

National Renewable Energy Laboratory

The goal of the National Renewable Energy Laboratory's (NREL's) integrated thermal management research is to reduce the cost and increase the efficiency of electric drive vehicle (EDV) cooling systems. Achieving these goals will result in increased driving range between charges; longer battery life; and improved safety, reliability, and comfort.

Vehicles with internal combustion engines use radiators and oil coolers to remove heat from the engine and transmission. With EDVs, more complicated systems are required in order to meet the additional thermal demands of advanced power electronics (APE) and energy storage (ES) systems.

Researchers at NREL's Center for Transportation Technologies and Systems are evaluating the potential benefits of combining the APE and ES cooling loops with the engine cooling and passenger compartment cooling systems. Reducing the number of cooling systems and related components will have several benefits, including lower maintenance costs and better fuel economy due to lighter weight and reduced aerodynamic drag. NREL's development of thermal systems designed specifically for EDVs builds on research already funded by the U.S. Department of Energy (DOE) in the areas of battery life, vehicle cost/performance, and electric motor thermal analysis.

NREL's researchers used software and vehicle component data to create thermal models of APE and ES cooling loops, the passenger compartment, and air conditioning systems. These models calculate component temperatures and power requirements under varying conditions. A vehicle cost/performance model calculates component heat generation and range. A battery life model calculates battery degradation and capacity.

A baseline model of a full EDV thermal management system was created in the first phase of NREL's research. The results of the simulations for three ambient air temperatures are shown in Figure 1.

In future research phases, NREL will link the vehicle performance, battery life, and thermal models to evaluate strategies for combining EDV cooling systems and loops. The most promising concepts will be tested in the lab and on the road.

Analysis will determine potential benefits, along with the cost reductions and performance improvements needed to reach DOE's goal of increasing U.S. consumer adoption of EDVs.

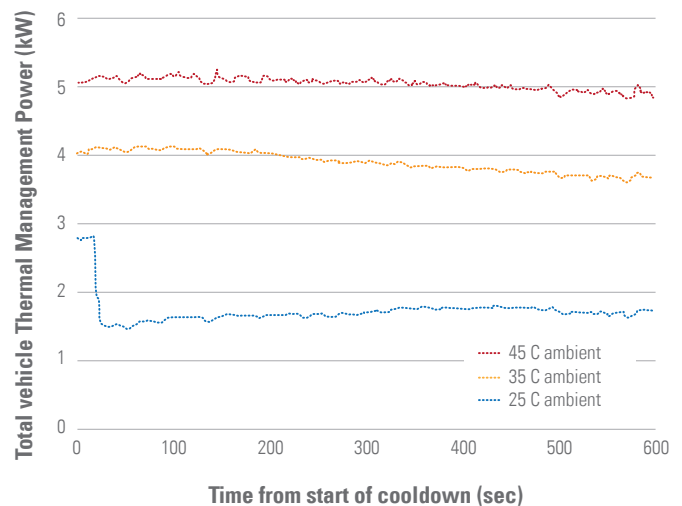


Figure 1. Total thermal management power required at three ambient air temperatures in a 10-minute simulation (including A/C compressor, APE fluid pump, and ES fluid pump)

Idle Stop Vehicle Fuel Consumption Benefits Based on a Comprehensive Dynamometer Study

Engine idle stop technology is a low-cost option to reduce fuel consumption; however, its benefits strongly depend on the driving situation. For city-type driving, small cars may see fuel consumption improvements of up to 15%.

Argonne National Laboratory, Idaho National Laboratory, and ECotality North America

This controlled dynamometer study involved testing on the following three different idle stop vehicles:

- Smart ForTwo Micro Hybrid Drive, 1.0 liter (L) gasoline, belt alternator/starter
- Mazda 3 iStop, 2.0 L direct injection gasoline, 'combustion-assisted' start, crank starter + extra 12-volt battery
- Golf, 2.0 L turbocharged direct injection diesel, advanced crank starter.

Figure 1 shows Fuel Consumption (FC) test results, as well as vehicle improvements on the U.S. and European city test cycles. On the U.S. cycle, an average improvement of only 4% is achieved among the different vehicles, compared to an average improvement of 10% on the European city test. This variance is explained by the amount of time the vehicles spent stopped during the tests. For the U.S. cycle, the vehicles were stopped for fewer than 18% of the time, compared to more than 30% of the time for the European cycle. These cycle-

specific benefits may contribute to the larger availability of idle stop vehicles in the European market compared to the U.S. market.

The correlation of FC benefit to the vehicle stop time is illustrated in Figure 2, which summarizes test results from a number of test cycles. The higher the vehicle stop time, the larger the FC benefit. The smallest vehicle exhibits the largest FC improvement due to the lower average power required to drive the vehicle compared to the engine idle fuel flow. The diesel vehicle demonstrated the lowest FC improvement due to its comparatively low engine idle fuel flow, almost half of its gasoline counterpart.

The emissions impact is not as clear. The Smart produces some modest emissions spikes at each engine start. The Mazda 3's emissions are unchanged, most likely due to the sophisticated 'combustion assisted start.' The Golf lowered its emissions by reducing the engine operating time. Emission controls for cold start operation may limit the achievable benefits of the technology.

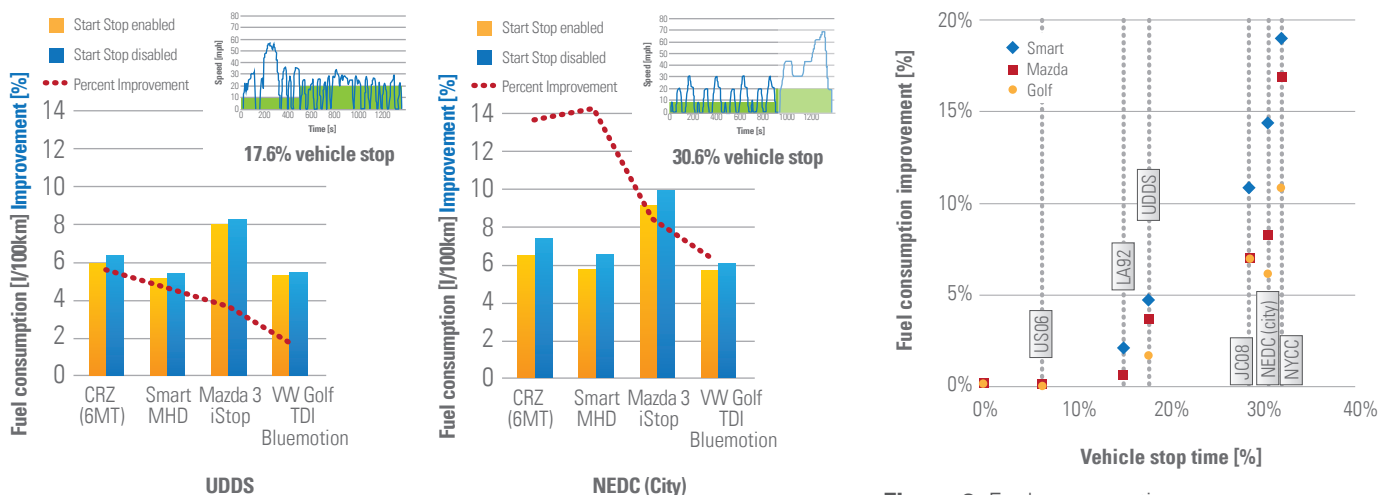


Figure 1. Comparison of fuel consumption improvements for idle stop vehicles between U.S. and European certification cycles (hot start test results)

Figure 2. Fuel consumption improvements as a function of vehicle stop time for different drive cycles (all hot start test results)

Electric Drive Vehicle Advanced Battery and Component Testbed

A testbed to provide on-road testing capabilities of advanced energy storage systems designed for grid-connected vehicles in real-world driving and charging conditions.

Idaho National Laboratory, Oak Ridge National Laboratory, and ECOTality North America

As part of the testing and data collection support provided to the U.S. Department of Energy (DOE), the Vehicle Systems Analysis Tech Team, and DOE's Advanced Vehicle Testing Activity (AVTA), Idaho National Laboratory tests grid-connected vehicles in on-road fleets, on test tracks, and in laboratory settings to determine the real-world petroleum reduction potential of various grid-connected vehicle technologies. This testing identifies the significant fuel reduction benefits enabled by the utilization of advanced onboard energy storage systems (ESS). With increased ESS performance and utilization, vehicle miles may shift from petroleum-based fuel to electricity. In order to identify the benefits of ESS technology advancement and areas of future improvements, laboratory and on-road testing of new ESS solutions is required. To conduct on-road testing of advanced ESS, a testbed is constructed for the purpose of testing a variety of ESS' designed for grid-connected vehicles. This testbed operates the subject ESS during on-road driving and charging—over a wide range of operating and ambient conditions—to quantify the capabilities, limitations, and performance fade over the life of the ESS.

To permit on-road testing of a wide range of ESS' of varying size and mass, the Electric Drive Vehicle and Advanced Batter (EDAB) testbed is constructed on a mid-size pickup truck chassis. This testbed is integrated into a series plug-in hybrid electric vehicle (PHEV) designed to enable vehicle operation consistent with battery electric vehicles, extended range electric vehicles, and PHEVs. Sophisticated software algorithms are developed and integrated into the testbed to control the powertrain operation, such that the ESS experiences the intended duty cycle. This is vital for proper ESS operation because the testbed is larger and heavier than the target vehicle for which it is emulating. On-road testing is conducted

over a variety of ambient temperature and driving route types, ranging from 'stop-and-go' city driving to constant-speed highway driving. Additionally, testing is conducted for various charging patterns generated from those of real-world fleet drivers in the AVTA PHEV data collection. The charging patterns range from frequent charging events (multiple times per day) to as seldom as once per week. Charging behavior impacts the level of energy in the ESS during testing, influencing the performance and capacity fade of the subject ESS. Testing with the EDAB testbed serves to quantify these impacts.

EDAB accomplishments at the end of Fiscal Year 2011 include

- Completed test plan, including on-road testing and ESS laboratory reference performance testing
- Completed ESS beginning-of-life baseline reference testing
- Installed first subject ESS (70 Ah Lithium ion ESS designed for an all-electric vehicle)



Figure 1. Testbed demonstrating on-road capability with development Nickel Metal Hydride ESS (not intended for on-road testing program)

Grid Interaction



National Permit Template Can Help Make Homes Electric Vehicle-Ready

New tools can streamline the process for making consumer's homes ready for plug-in electric vehicles.

National Renewable Energy Laboratory and Grid Interaction Tech Team

The National Renewable Energy Laboratory (NREL), with significant input from the Grid Interaction Tech Team, developed a model template to streamline the process for permitting and inspecting home-charging stations for plug-in hybrid electric and electric vehicles (PHEVs/EVs). The team also provided input to the U.S. Department of Energy's Clean Cities Initiative on the development of related information tools for the actual installation process.

The tools, which were announced by DOE as part of its Clean Cities Initiative, are available online, making them easily accessible to consumers, installers, governments, and businesses.

The first tool is a six-page permitting template that can be easily adapted by local governments to help standardize permitting and inspection procedures for plug-in electric vehicles between different regions. The second tool is a 30-minute video titled, "Electric Vehicle Supply Equipment (EVSE) Residential Home Charging Installation," and is intended for electrical contractors and inspectors. It covers all aspects of setting up a home charger. Both tools will help accelerate the approval process for home charging stations.

The Grid Interaction Tech Team helped to identify and address roadblocks that would prevent successful commercialization of all types of plug-in electric vehicles. The GITT also identified ways to streamline the EVSE installation and permit process as the number one priority to support the adoption of PHEVs and EVs – if PHEVs and EVs are to gain mass acceptance by consumers, it is mission-critical to reduce the amount of time vehicle buyers have to wait to have vehicle chargers installed at their homes.

The team, working with the National Renewable Energy Laboratory (NREL) and EVSE installers, mapped out a model permit streamlining strategy that included creating a national EVSE permit template that provides consistent language and format for use by community electrical inspectors and EVSE installers (the electrical contractors).

Additionally, GITT members helped the Energy Efficiency and Renewable Energy (EERE) Clean Cities team develop content requirements for training materials to support the permit process, and train electrical contractors and inspectors who will be on the front line of making their communities EV-ready.

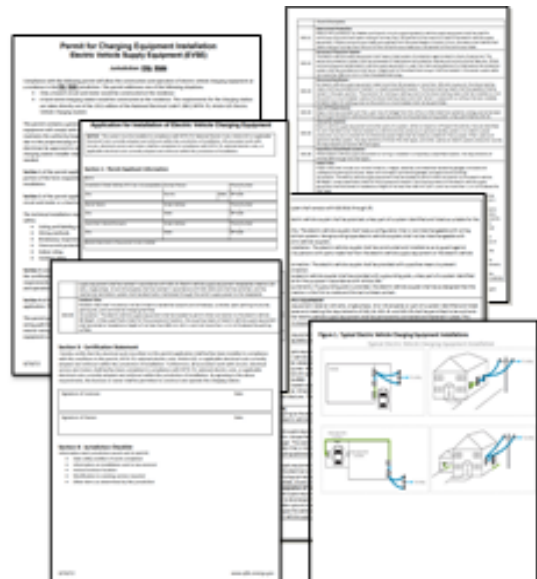


Figure 1. National Permit Template for installing equipment at residential locations for charging plug-in electric vehicles. Available at the Clean Cities Web site

http://www.afdc.energy.gov/afdc/vehicles/electric_deployment.html#permit

Auto-REM Module Developed for Effective Vehicle-Grid Communication

Automotive-oriented module for vehicle-grid communication.

Argonne National Laboratory

National laboratories support the development of communication standards by providing expertise and independent test data to Society of Automotive Engineers committees as they debate the merits of candidate technologies and methods. Argonne National Laboratory is currently evaluating two options for vehicle-grid communication—G3 and Homeplug GreenPhy (HPGP)—despite the lack of production components.



Figure 1. Auto-REM Module

To generate data as soon as possible, ANL commissioned development of an automotive-oriented G3 communication module (Auto-REM). The Auto-REM module was based on the Texas Instruments pre-production Octave universal baseband chip set and the G3 power line communication (PLC) method. Thirty copies of the module were produced and shared openly with vehicle industry representatives. The test data from the modules was the first power line communication (physical layer) over pilot wire validation results supplied to the standards committees.

The Freescale Kinetis K60 processor tower system has been used as the host for benchmark testing to compare cross-talk effects, maximum throughput, and worst-case latency. Figure 2 shows three physical layer solutions connected to the same serial port on the tower:

1. Auto-REM T.I. Octave G3 Narrow Band Orthogonal Frequency Division Multiplexing (N-OFDM) to Controller Area Network (CAN) module (center, below Kinetis tower)
2. Maxim MAX2992 module for evaluating similar criteria as Auto-REM (left)
3. Qualcomm-Atheros wide band HPGP solution.

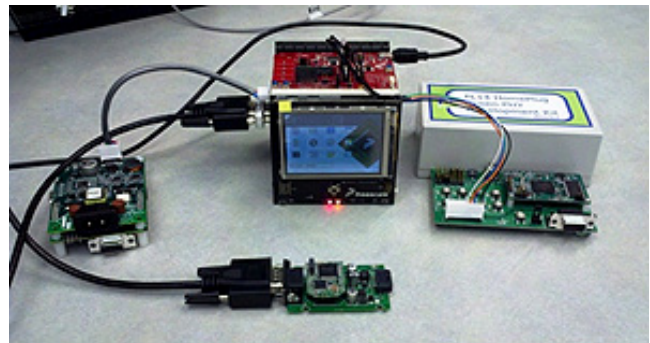


Figure 2. Communication Module Testing

Electric Vehicle Measurement Device Developed for End Use Metering

Low-cost 'smart' module combines revenue-grade power meter and wired/wireless communication to enable separate measurement of electric vehicle charging energy and electric vehicle supply equipment-to-grid communication.

Argonne National Laboratory

Argonne National Laboratory has combined compact metrology and communication technologies to demonstrate a low-cost option for accurate measurement of electric vehicle (EV) recharge energy consumption and communication with the grid.

The End Use Measurement Device (EUMD) has the capabilities of a smart meter (i.e., revenue-grade power measurement and communication) in a compact package that is less intrusive and much lower cost than a standard meter. Three versions/generations were developed this year to assess the relative merits of different current sensors and communication technologies. The utility of this device is that it can function as a sub-meter to separately measure EV recharge energy and transmit data to the service provider to support smart grid management (i.e., balancing electricity supply and demand and sequencing vehicle charging to avoid local transformer overloads).

Key characteristics of the EUMD include low cost (projected to be \$10–\$20 materials cost in volume, depending on the sensor type), compact (roughly the size of a business card), accurate (capable of meeting American National Standards Institute C12 standards), and compliant with standard communication protocols over an Institute of Electrical and Electronics Engineers 802.15.4 Zigbee physical layer to a standard gateway device. This device also communicates directly with an advanced metering infrastructure meter.

The design has been adapted for various installation locations in the vehicle-grid connectivity path (i.e., the vehicle, electric vehicle supply equipment (EVSE), power distribution panel, secondary panel, plug receptacle, and the distribution transformer) (as a smart monitor to enable local grid optimization).

The configuration shown in Figure 1 was designed to fit in a standard, low-cost 60A fused disconnect that can be located downstream of the main premises meter. This could add sub-metering functionality without a circuit panel upgrade (or replacement) and could be applied to multi-family dwellings with shared parking areas and a single utility service connection.

The design has also been configured as a low-cost transformer monitoring system with meshed network communication to enable EV charge scheduling within the service area of a neighborhood transformer.

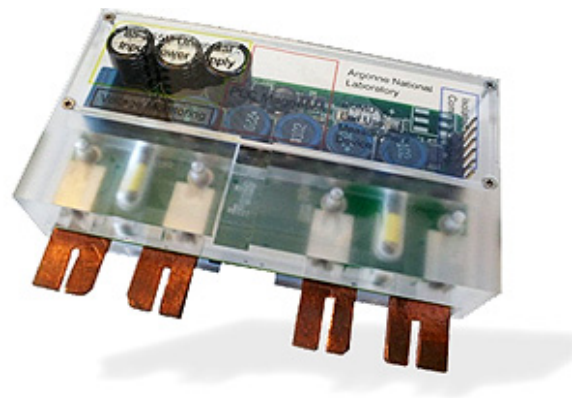


Figure 1. EUMD with Flux Gate Magnetometer Current Sensor

Vehicle-Grid Interoperability (SAE J2931) Demo

Energy measurement and communication; vehicle-electric vehicle supply equipment-network-smart meter-grid.

Argonne National Laboratory

Interoperability implies (ideally) that any plug-in vehicle can be charged using any electric vehicle supply equipment (EVSE), and that the method of communication to the service provider is standard to enable billing (despite roaming) or more sophisticated interactions, such as two-way communication and load management.

A prerequisite for interoperability is standard messaging and protocols between the apparent elements of the system (the vehicle, EVSE, and service provider), as well as intermediate data handlers (home or commercial networks) and operating systems beyond the service providers (grid operators and utilities). Standards are still under development, but vehicle manufacturers and suppliers need to soon make

decisions for their next generation of plug-in vehicles. Therefore, a variety of technologies and methodologies are being explored to identify plausible near- and mid-term options.

Argonne National Laboratory assembled such a system of plausible components—connecting the vehicle to the EVSE, home area network, smart meter, and a smart distribution transformer monitor—and demonstrated energy measurement and communication between all of the elements. Figure 1 shows tabletop ‘fixture,’ constructed primarily of familiar residential/commercial components, housing various configurations of the EUMD in series with a home area network and smart meter.



Figure 1. Vehicle-grid Interoperability Demonstration

Codes and Standards



Science-Based, Data-Driven International Standard for Fuel Quality Published

This guidance document uses science to protect fuel cell performance while reducing impact on fuel cost.

Los Alamos National Laboratory

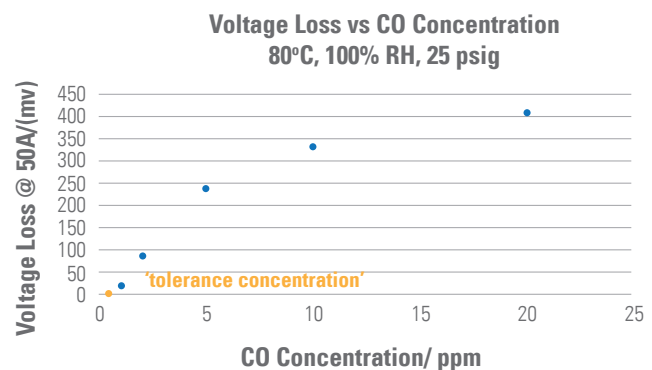
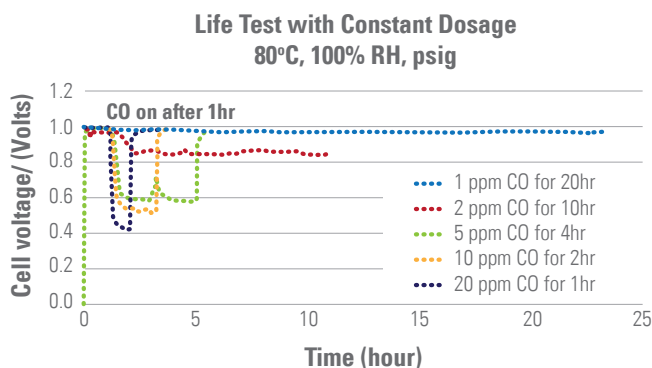
Los Alamos National Laboratory scientists played a key role in implementing a collaborative, science-based approach to develop a final draft international standard for hydrogen fuel quality for polymer electrolyte membrane (PEM) fuel cells in road vehicles that was submitted to the International Organization for Standardization (ISO) for promulgation and adoption. They determined the maximum carbon monoxide (CO) concentration that an operating fuel cell could tolerate without employing mitigating strategies and measured the impact of mixtures containing impurities at the proposed ISO levels, including ammonia (NH₃), hydrogen sulfide, CO, and hydrocarbons. The maximum CO concentration was determined by single-cell fuel cell tests performed on membrane electrode assemblies that meet U.S. Department of Energy (DOE) 2015 fuel cell target loading (total Pt loading of 0.2 mg/cm²; anode loading was 0.05 mg/cm²).

The DOE team also included the University of Hawaii/HNEI (CO and toluene), University of Connecticut (hydrocarbons and halocarbons), University of South Carolina (sulfur compounds and NH₃), and Savannah River National Laboratory/Clemson University (sulfur compounds and NH₃). The National Renewable Energy Laboratory collected and organized the test data, Argonne National Laboratory performed modeling, and the American Society for Testing

and Materials International is developing and validating standardized methods to sample and analyze the presence of contaminants at the levels prescribed in the draft standard. This collaborative effort, organized and coordinated by DOE, was critical to the success of the science-based approach to developing an international hydrogen fuel quality standard.

Modeling and analysis show that the cost of producing hydrogen compliant with the specification may not be significant. However, the costs of analyzing and verifying compliance with the specification are still under study. The ISO standard¹ will help ensure that the effects of possible contaminants on PEM fuel cell performance and durability in early commercial road vehicles are acceptable. The draft standard was developed through a consensus process with automobile and fuel cell manufacturers, hydrogen suppliers, national laboratories, universities, as well as other research institutions in North America, Europe, and Asia. The research and testing efforts focused on the critical contaminants (NH₃, CO, sulfur compounds, and their mixtures) that are the technical and economic drivers for hydrogen fuel quality in PEM fuel cells for road vehicles.

¹ The ISO specification has been harmonized to the extent possible with SAE-2719 - *Hydrogen Fuel Quality Guideline for Fuel Cell Vehicles*, June 2011.



Experiments were run to determine CO tolerance by using constant CO dosage in an operating fuel cell. The 'voltage loss vs. CO concentration' graph (right) was obtained by subtracting the voltages before the CO was introduced and immediately after it was turned off from the graph on the left. And, by extrapolating the voltage loss to 0 mV, the 'tolerance concentration' was determined. Results indicate the 'Common MEA' (Anode: 0.1 mg Pt/cm² and Cathode: 0.4 mg Pt/cm²) could tolerate approximately 0.5 ppm of CO for at least 40 hrs. This is 5 times the CO concentration listed on the fuel specification.

Hydrogen Storage



Selection of Ammonia Borane Hydrogen Storage System Concept

To focus resources, fluid-phase designs were selected through experimental validation, modeling, and cost analysis from multiple ammonia borane system concepts.

Pacific Northwest National Laboratory and Los Alamos National Laboratory

As part of the Hydrogen Storage Engineering Center of Excellence (HSECoE), researchers from Pacific Northwest National Laboratory and Los Alamos National Laboratory performed comprehensive engineering analyses and performance assessments of solid- and fluid-phase chemical hydride material systems designs against key U.S. Department of Energy system targets. They evaluated and modeled multiple system configurations based on an ammonia borane (AB) hydrogen storage material. These designs included both solid and liquid materials, as well as various concepts on how hydrogen is released onboard. Based on modeling analyses and component validation tests, the HSECoE decided to focus future efforts on fluid systems (i.e., chemical hydride slurries or AB in ionic liquids). Discontinuing solid-based system research enables the HSECoE to focus its resources on the most promising architectures.

The selection of a chemical hydride as a viable solution for onboard hydrogen storage hinges on the identification of an efficient hydrogen-release reactor. It is critical that the reactor design account for reactant and product phases (i.e., solid, liquid, and gas); reaction

thermodynamics (i.e., exothermic, endothermic, or autothermal); catalyst activity and selectivity; reactor geometry, volume, and mass; and reactant/product transport. The team acquired fundamental empirical data for solid and liquid AB formulations in order to construct accurate system models for each design. These models were used to evaluate the relative performance of each reactor concept.

In addition to the reactor design, practical methods for refueling chemical hydride media were considered, as fresh fuel must be filled, and spent fuel removed from the vehicle (as opposed to hydrogen gas refilling for other storage classes). Liquid-phase hydrogen storage media outperformed solid-phase storage media. As a result of these experiments, the decision was made to discontinue work on solid-phase chemical hydrogen storage materials and focus efforts on liquid-phase chemical hydrogen storage materials, which possess more desirable materials transport properties (i.e., refueling, kinetics, etc.), as seen in Figures 1 and 2.

	Powder	Pellets
	kg/min (% target)	kg/min (% target)
Open-Ended (22')	14-15 (>100%)	14-15 (>100%)
Fill (14' hose)	2.5 (~27%)	5.4-6.9 (60-75%)
Drain (14' hose)	4.5 (~49%)	4.8-9.2 (50-100%)

Figure 1. Refueling Feasibility Test Results for Solid AB Surrogates

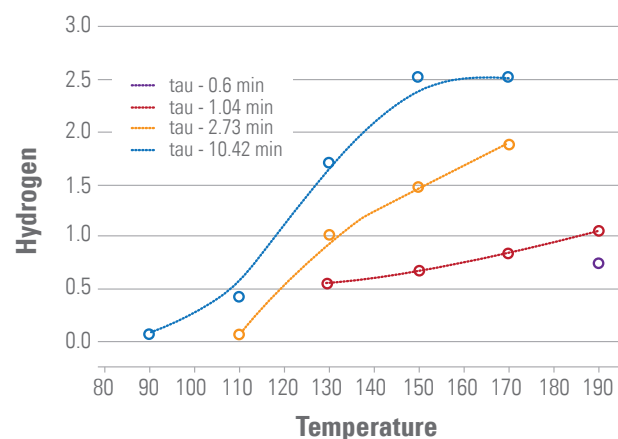


Figure 2. Kinetic results of fluid-phase AB obtained from validation test bed for on-board hydrogen production

Reduced Size Improves Performance of Hydrogen Storage Materials

Experiments confirm that both thermodynamics and kinetics of metal hydrides are altered substantially when particle size is reduced below 2–4 nanometers, enhancing storage properties of the materials studied.

Sandia National Laboratories, University of Missouri-St. Louis, and Massachusetts Institute of Technology

Experiments confirmed the strong size-dependent effects on the reaction pathways and kinetics predicted by first principles calculations. Nano-sized metal hydrides confined in carbon templates demonstrate that hydrides, which are otherwise either too stable or possess slow kinetics, can be made more viable for hydrogen storage applications.

Quantum Monte Carlo computations and other theoretical methods had previously suggested that nano-meter-sized particles of hydride materials would have different performance than bulk phase materials. Significant predictions from these calculations include the following: (1) the creation of Mg-Al-H nanoclusters will shift MgH_2 desorption into a more favorable thermodynamic regime, and (2) the decomposition of 1–4 nanometer (nm) NaAlH_4 nanoclusters will occur in a single step versus the two-step process observed

with bulk materials. Confirming these predictions, Figure 1 illustrates how nanometer-sized particles of sodium alanate decompose through the single-step pathway. The reduction to a single-step process would effectively increase the net reversible storage capacity by approximately 50%.

These experiments on nanophase NaAlH_4 , confined within hexagonal columnar carbons with approximately 2–3 nm pore sizes, also showed the decomposition temperature decreased compared to bulk.

Figure 2 shows that similar nano-confinement of LiBH_4 alters both solid-solid and solid-melt transitions, as well as lowering decomposition temperatures when compared with bulk behavior. Enhanced diffusion and kinetics are the proposed explanation, as no change in desorption energy was found when compared to bulk LiBH_4 .

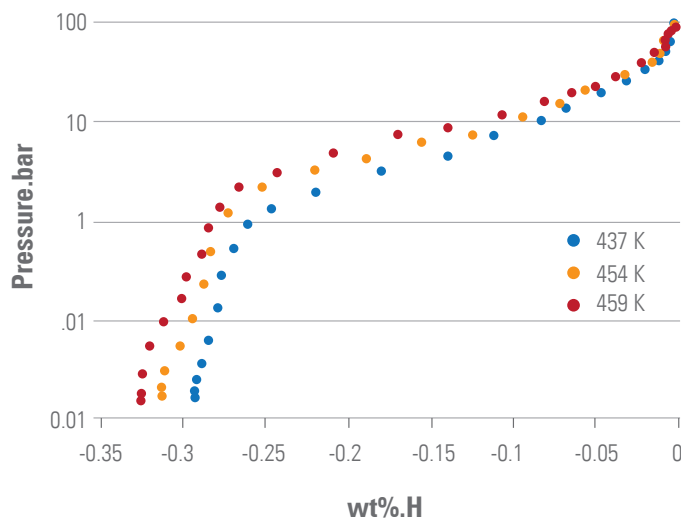


Figure 1. Pressure composition isotherm showing a single-step desorption of nanophase sodium alanate in contrast to a two-step desorption, as would be seen with bulk samples

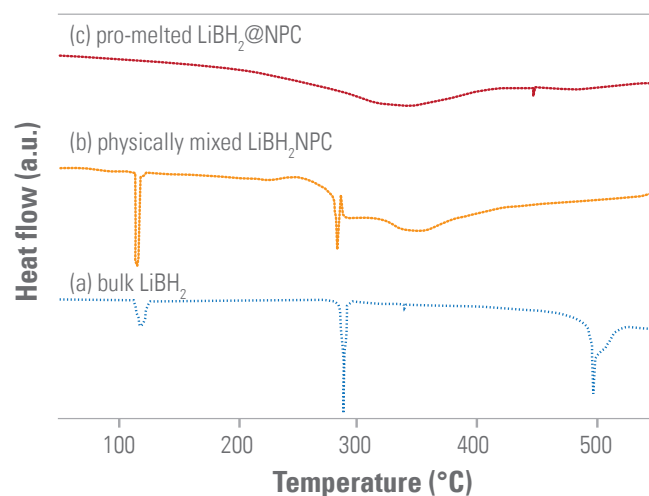


Figure 2. Differential scanning calorimetry measurements on LiBH_4 infiltrated into 2-nm templates of nanoporous carbon reveal major changes from properties of the bulk hydride

Alane: Improved Hydrogen Release and Regeneration

This high-capacity material now can be regenerated offboard, potentially simplifying hydrogen vehicle refueling.

Brookhaven National Laboratory and Savannah River National Laboratory

Brookhaven National Laboratory (BNL) and Savannah River National Laboratory (SRNL) have made progress by storing hydrogen in chemical form. This work has demonstrated fast, controllable hydrogen release from high-density slurries of alane (BNL), as well as increased rates of regeneration of alane through an electrochemical process with an unconventional solvent (SRNL). Alane (AlH_3) is a solid material that has very high hydrogen density by volume (149g H_2 /liter), holds 10% hydrogen by weight, and releases its hydrogen at a convenient temperature. A slurried form is best for use in vehicles because it can be pumped onboard and offboard, and can be regenerated offboard under optimal conditions.

Researchers at BNL have created a slurry that contains 60% by mass alane crystallites. This makes the 25–50 microns crystallites pumpable, and the slurry still releases 6% hydrogen relative to the total slurry weight. Hydrogen release was rapid at temperatures near 100 degrees Celsius. BNL researchers controlled

the hydrogen release by adjusting the temperature. As shown in Figure 1, the hydrogen could be turned on and off by simply increasing or decreasing the temperature of the slurry. These important steps indicate alane has promise for onboard hydrogen storage applications.

The electrochemical method developed at SRNL regenerates alane from the spent fuel at normal pressures with only a non-aqueous electrolyte, hydrogen, and electricity. Several key advances in this process are the use of LiAlH_4 solution as the electrolyte, the addition of LiCl as an electrochemical additive to accelerate alane formation, and use of dimethyl ether (DME) as the solvent. The addition of LiCl increased the cell current by 80%, which increased the cell's electrical efficiency and nearly doubled the rate of alane production. Additionally, the overall process efficiency was dramatically improved by reducing the required energy to separate the alane from the electrolyte and solvent by using DME, which is a gas at ambient temperature and pressure.

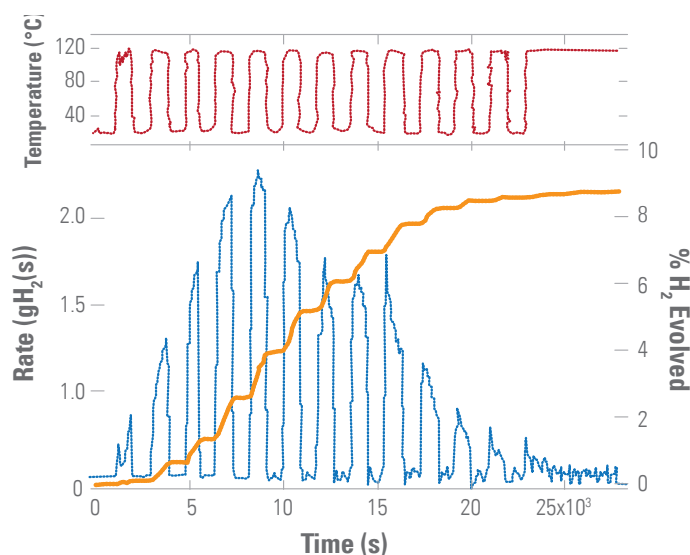


Figure 1. Demonstration of the on/off control of hydrogen release from alane through temperature control

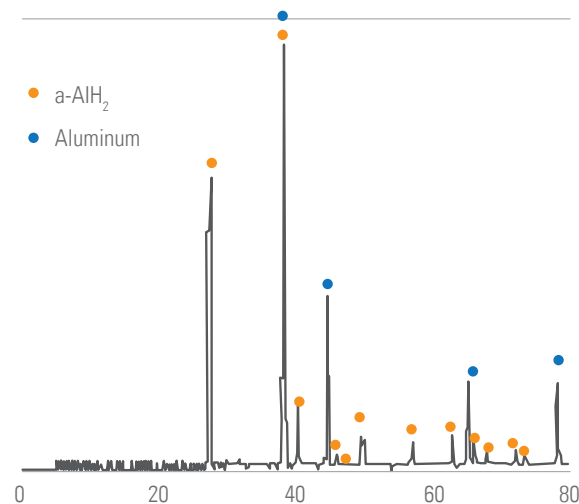


Figure 2. X-ray diffraction pattern showing pure alpha-alane produced in an electrochemical cell

Development of Integrated System Model for the Evaluation of Hydrogen Storage Technologies

Several material-based hydrogen storage system designs were assessed and prioritized in a consistent modeling framework.

Ford Motor Company, General Motors, Los Alamos National Laboratory, National Renewable Energy Laboratory, Pacific Northwest National Laboratory, Savannah River National Laboratory, and United Technologies Research Center

The Hydrogen Storage Engineering Center of Excellence (HSECoE) has developed a complete integrated hydrogen storage model that can simulate performance of a wide range of hydrogen storage systems under various vehicle driving conditions. The team evaluated high-temperature metal hydrides (e.g., NaAlH₄), low-temperature adsorbent materials (e.g., AX-21), and chemical hydrides (e.g., ammonia borane). To evaluate these systems on a consistent and equivalent basis, the team developed a common verification model framework in the commercial platform Simulink®. As shown in Figure 1, the framework consists of a vehicle-level modeling block, a fuel cell system modeling block, and interchangeable hydrogen storage system modeling blocks.

The framework provides an excellent structure for simulating the hydrogen storage system interactions with the fuel cell system and the vehicle. The ultimate benefit of the framework is a common approach to evaluating each storage system in comparison to U.S. Department of Energy (DOE) hydrogen system targets. The model can assess trade-offs between storage systems on a common basis, ensuring differences reflect storage system attributes rather than differences in the simulation approach or assumptions. Finally, the framework offers the advantage of considering vehicle synergies, such as utilization of waste heat from the fuel cell or allowance of energy utilization from the vehicle with the hybrid battery system.

By design, the framework has an interchangeable library of hydrogen storage system models that have been developed by individual or multiple partners within the HSECoE. The user can select the desired storage system as part of the parameter inputs, along with other settings including the drive cycle. In conjunction with DOE and the Hydrogen Storage Tech Team, HSECoE has established a set of standardized drive cycles based on U.S. Environmental Protection Agency fuel economy tests to assess the storage system under a variety of driving conditions, including start-stop city, high-speed highway, aggressive, cold temperature, hot temperature, and extended dormancy. At the end of the simulation, the framework determines whether the storage system provided the required range and met the dynamic transient responses required to satisfy the drive cycles and DOE targets.

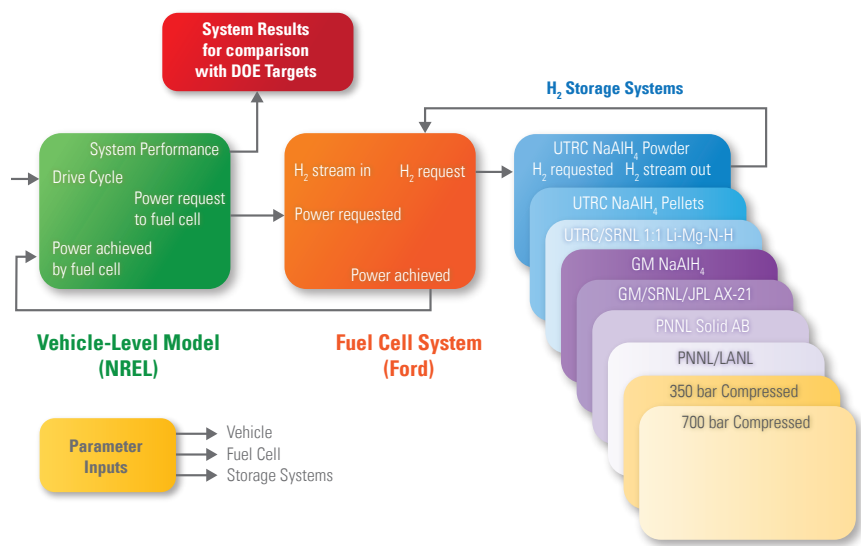


Figure 1. Illustration of the Hydrogen Storage Engineering Center of Excellence – Verification Model Framework

Fuel Pathway Integration



Hydrogen Threshold Cost Apportionment

DOE recently apportioned the hydrogen threshold cost between the hydrogen production and delivery subsystems, setting a target of \$2/kg H₂ for each subsystem.

U.S. Department of Energy

In 2010, the U.S. Department of Energy (DOE) established a hydrogen threshold cost range of \$2–\$4 per gasoline gallon equivalent (gge) (delivered, untaxed, 2007\$) (see Figure 1). Replacing the previous value of \$2–\$3, the hydrogen threshold cost is a “top-down” analysis of the cost at which hydrogen would be competitive with gasoline in the light-duty vehicle market. The previous cost target range was set in 2005, so the projected cost of the hydrogen fuel cell electric vehicle (FCEV) was equivalent to the competing vehicle (hybrid electric vehicles (HEVs) were the competing vehicle for the lower end of the range; internal combustion engine powered vehicles were the competing vehicle for the upper end of the range).

The projected gasoline price (\$1.30/gallon, untaxed) and the projected incremental ownership cost of the FCEV have significantly changed since then, thus requiring the cost target to be updated. The threshold cost is used to guide DOE’s hydrogen and fuel cell research and development activities and is updated periodically. It is pathway-independent with respect to hydrogen production and delivery technology options; however, in order to set top-down targets for production and delivery technologies, the threshold cost has recently been apportioned to \$2/kilogram (kg) hydrogen (H₂) for the central production subsystem and \$2/kg H₂ for the delivery subsystem. The Fuel Pathway Integration Tech Team, in addition to other stakeholders and the Hydrogen and Fuel Cell Technical Advisory Committee, reviewed DOE’s analysis process, methodology, assumptions, and data, providing industry perspective.

Because all production and delivery pathways must ultimately compete with the lowest-cost pathway, the lowest-cost production technology—central steam reforming—was used to set the hydrogen production target. The 2020 projected levelized production cost for central steam reforming units was calculated us-

ing the Annual Energy Outlook 2009 reference case cost projections for industrial natural gas prices. The resulting levelized production cost of \$1.88/kg H₂ was rounded to set a central production target of \$2/kg H₂. The delivery target was set to the difference between the high end of the threshold cost range (defined as \$4/kg H₂) and the production target (\$2/kg H₂). Thus, it was set to \$2/kg H₂. Those targets were used in setting equipment cost and performance targets for central production technologies and associated delivery technologies.

Distributed production pathways must also meet the high end of the threshold cost range (\$4/kg H₂). The cost apportionment of those pathways will be performed in 2012.

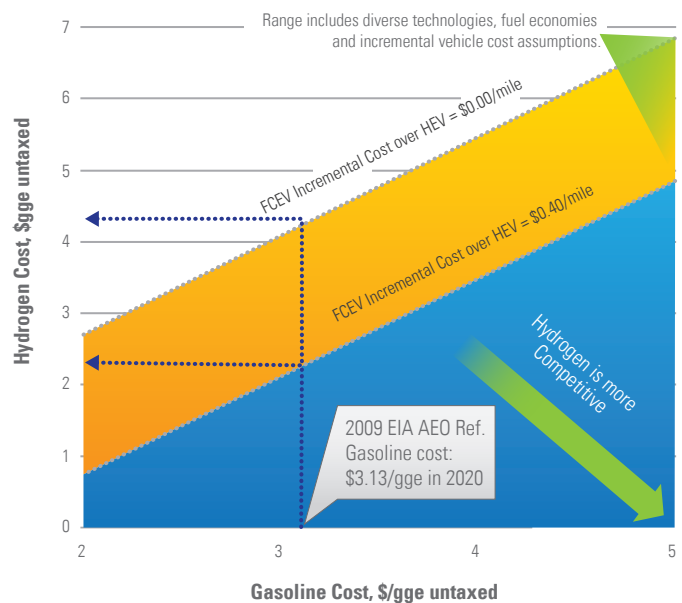


Figure 1. Hydrogen threshold cost analysis showing the competitive cost of hydrogen compared to gasoline HEV is ~\$2.00-\$4.00/gge

Infrastructure Costs for Biomass-Based Hydrogen Production

Biomass availability limits siting options for biomass plants, but hydrogen pipeline construction is the most significant driver of delivered hydrogen cost.

National Renewable Energy Laboratory

The National Renewable Energy Laboratory (NREL) analyzed biomass delivery and hydrogen transport infrastructure requirements and costs for central biomass-based hydrogen production. NREL accounted for various factors, including the effect of land availability on hydrogen transportation costs and the proximity of biomass resources to potential plant locations. The Fuel Pathway Integration Tech Team reviewed NREL's analysis process, methodology, assumptions, and data, providing industry perspective.

Woody biomass (forest residues, mill residues, and urban wood waste) hydrogen plants were characterized based on the Hydrogen Analysis (H2A) current central biomass case study.¹ The plant output was assumed to be the H2A case design capacity: 155,000 kilograms (kg) per day hydrogen output, requiring 727,472 dry metric tons (MT) per year of biomass feedstock.

The limit of economical truck transport of biomass to hydrogen plants was assumed to be 100 miles. Plants were located where they could be supplied with sufficient biomass within a 100-mile radius. The costs of trucking biomass to plants (average of 60 miles) on existing roads and piping hydrogen from plants to demand centers were then calculated. The cost of piping hydrogen to demand centers included terrain, land-availability, and right-of-way factors. In Figure 1, white represents areas where a sufficient quantity of

biomass to support a hydrogen production plant cannot be obtained within 100 miles; black dots represent hydrogen demand centers; and colors represent the calculated infrastructure costs associated with the hydrogen plants.

While biomass availability limited plant locations in this analysis, hydrogen pipeline construction was the most important cost factor. For example, for forest residues, biomass transportation cost added \$0.10–\$0.30/kg hydrogen, whereas pipeline cost added \$0.20–\$1.30/kg.

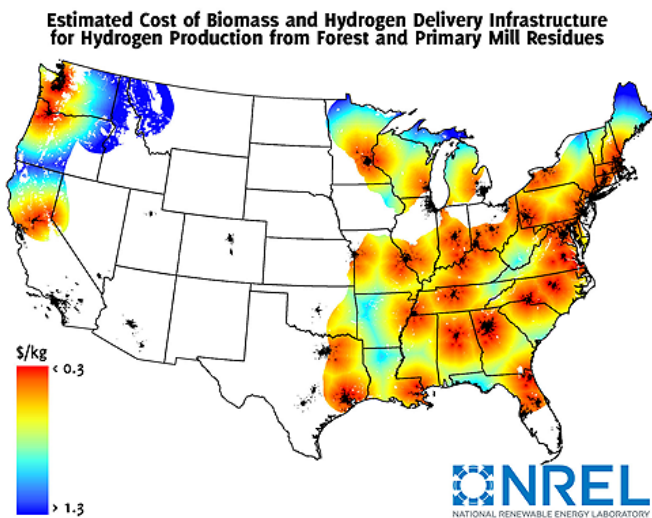


Figure 1. Biomass hydrogen plant infrastructure costs (trucked forest residue and piped hydrogen)

¹ http://www.hydrogen.energy.gov/h2a_prod_studies.html

Hydrogen Fuel Station Cost Analysis for Early Transition

Using stakeholder input and analysis, potential hydrogen fuel station cost reductions from economies of scale, “learning-by-doing,” and station component pre-competitive R&D were investigated.

Fuel Pathway Integration Tech Team

In Fiscal Year 2011, the Fuel Pathway Integration Tech Team (FPITT) investigated the cost of constructing a hydrogen fueling station of unspecified type and potential cost-reduction opportunities. This was accomplished through a multi-stakeholder workshop and a screening analysis to identify cost reductions that can be gained from economies of scale, “learning-by-doing” station installations, and station component pre-competitive research and development (R&D) conducted by the U.S. Department of Energy (DOE).

The multi-stakeholder workshop was conducted in February 2011 by the National Renewable Energy Laboratory. Stakeholders included companies from the energy, industrial gas, automotive, component, and construction sectors, along with the national laboratories. The goal of the workshop was to investigate the key drivers influencing the cost of first-of-a-kind installed hydrogen fueling stations. Workshop participants indicated that economies of scale from installing multiple stations of the same capacity could reduce the station cost by 30%–50%, and additional station cost reduction could be achieved by implementing improvements based on lessons learned through repetitive station installations. The workshop also identified the level of compression and storage necessary at the station as opportunities for pre-competitive R&D to reduce the delivered hydrogen cost.

Workshop results were combined with analysis conducted using the existing Hydrogen Analysis (H2A) portfolio of production and delivery models to develop cost-reduction profiles for hydrogen fueling station installations, ranging from first-of-a-kind stations to “nth” station installations. A general cost-reduction

profile (or cost “waterfall” chart) for a hydrogen fueling station with delivered hydrogen is exhibited in Figure 1, which highlights the degree of potential station cost reduction. This analysis can be used by the Production and Delivery Tech Teams and DOE to focus their efforts and activities to reduce station and station component costs. To complete the analysis, FPITT drafted a scope of work to quantify the station cost-reduction opportunities for each component of the station to include compression, storage, and dispensing.

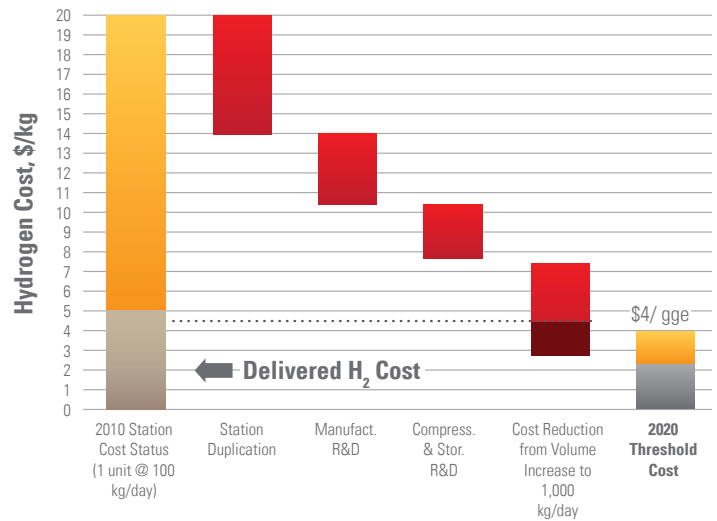


Figure 1. Cost-reduction opportunities to achieve \$4/gge hydrogen cost

Hydrogen Delivery



Electrochemical Hydrogen Compressor Development

Electrochemical hydrogen compressor achieves 40% increase in hydrogen flux at 7,000 psi of compression.

FuelCell Energy, Inc.

In 2011, researchers at FuelCell Energy, Inc. demonstrated a bench-scale, two-stage electrochemical hydrogen compressor (EHC) that is capable of 7,000 pounds per square inch (psi) compression—equivalent to a compression ratio of 300:1—at a hydrogen flux 40% greater than that previously achieved in their first-generation design. In addition, test units have been successfully operated for 3,000 hours; a 5 times increase in durability relative to the first-generation technology. The work significantly advances the state-of-the-art for hydrogen compression and is on target to meet the U.S. Department of Energy's near-term hydrogen refueling compressor targets for hydrogen compression ratio, durability, and operating efficiency.

Current hydrogen compressor technology will not adequately meet projected infrastructure demands; onboard storage of hydrogen on light-duty vehicles will require compression pressures up to 12,000 psi at the refueling station. Existing mechanical compressors are inefficient and susceptible to rapid component wear, requiring substantial maintenance. As a result, high-pressure compressors are the single most expensive component at hydrogen refueling stations and represent a key economic barrier to establishing the infrastructure needed for the widespread deployment of hydrogen as a transportation fuel.

EHC is a solid-state hydrogen compressor that has no moving parts and promises a 50% reduction in capital and operation and maintenance costs. It employs a modified polymer electrolyte membrane fuel cell architecture. When supplied with low-pressure hydrogen and an electrical current, the device ionizes the hydrogen, transports the resulting protons across the electrolyte membranes within a stack set of cells, and recombines these with rerouted electrons to reform hydrogen inside of a closed chamber. As

long as hydrogen and current are delivered to the EHC, hydrogen will continue to be transported and accumulated at higher pressure inside the chamber. In addition to its use at hydrogen refueling stations, EHC can be used to compress hydrogen for industrial and commercial applications, such as metals heat treatment and fine chemicals and electronics production. Compressed hydrogen can also be used in stationary polymer electrolyte membrane fuel cell systems to produce peak power for smart grid applications or for secure back-up power systems. Currently, FuelCell Energy, Inc. is modifying the EHC to demonstrate 10,000 psi compression at an additional 40% increase in hydrogen flow.

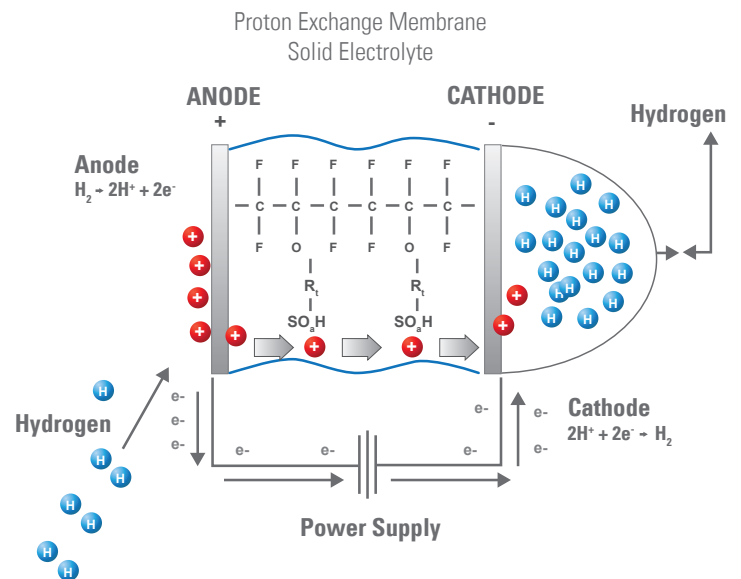


Figure 1. Schematic of the primary cell component in an electrochemical hydrogen compressor.

Hydrogen Production



Reforming of Bio-Oil for Production of Hydrogen

NREL demonstrates greater than 30% increase in yield and efficiency for hydrogen production from biomass through process optimization.

National Renewable Energy Laboratory

Through optimization of process conditions, the National Renewable Energy Laboratory (NREL) demonstrated increases in yield (36%) and efficiency (32%) for hydrogen production from biomass via catalytic autothermal steam reforming of pyrolysis oil at laboratory scale. For this process concept, an ultrasonic nozzle is used to atomize a 90% bio-oil/10% methanol mixture. The volatilized bio-oils are then broken down by catalytic partial oxidation and converted to hydrogen by autothermal reforming. This process potentially could be applied for both centralized and distributed production of hydrogen.

Biomass has the potential to become an important renewable resource for the production of hydrogen. Assuming bio-oil can be transported at a much lower cost than biomass, the location of the plants for pyrolysis and reforming can be decoupled and optimized with respect to the availability of the feedstock and the infrastructure for hydrogen distribution and use.

This research is focused on developing a compact, low-capital-cost reforming system to enable the achievement of the cost and energy efficiency targets set by the U.S. Department of Energy (DOE) for distributed reforming of renewable liquids. In Fiscal Year 2011, NREL replaced its catalyst with a better-performance, commercial Pt/Al₂O₃ catalyst and decreased the amount of oxygen used for the process, resulting in less hydrogen oxidized to H₂O during reforming. These changes resulted in an increased yield from 7.4 grams (g) hydrogen (H₂) to 10.1 g H₂ per 100 g bio-oil (i.e., from 7.4% to 10 wt% H₂) with 90% bio-oil to gas conversion during short-term, bench-scale tests of catalytic steam reforming at approximately 850 degrees Celsius, an increased process efficiency from 47% to 62%, and an approximate 10% decrease in the projected cost of delivered hydrogen.

Recently, NREL completed construction and shake down of a laboratory-scale integrated system for producing 100 L/h (STP) of pure hydrogen from bio-oil. Longer-term tests of the system (at least 100 cumulative hours of catalyst operation) will be performed in FY 2012 and are expected to demonstrate the potential technical and economic feasibility of the process. Optimizing the operation of the integrated system will lead to improvements in the yields, energy efficiency, and cost of hydrogen to close the gap with DOE targets.

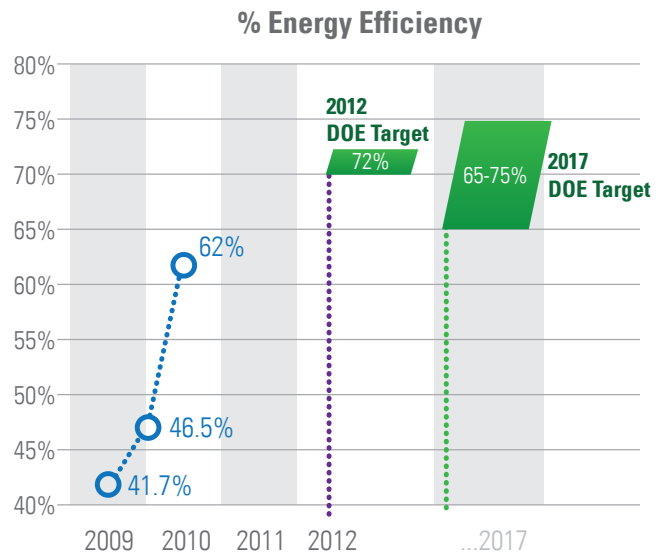


Figure 1. Estimated process efficiency is nearing DOE performance targets

Significant Cost Reductions in Capital Costs of Electrolyzer Stacks

A 15% decrease in projected capital costs of electrolyzer stacks has been realized in one year since 2010, representing an 80% decrease since 2001.

Giner Electrochemical Systems and Proton Onsite

In 2011, Giner Electrochemical Systems and Proton Onsite reported projected high-volume capital costs of proton exchange membrane (PEM) electrolyzer stacks less than \$400 per kilowatt (kW), already surpassing the U.S. Department of Energy (DOE) 2012 capital cost targets. This represents a 15% reduction from the 2010 projected costs and an 80% reduction since 2001, as illustrated in Figure 1. This reduction in electrolyzer capital cost, which has been achieved through technical improvements in stack components and optimization in stack design, represents an important step toward meeting the DOE hydrogen production cost threshold.

The significant capital cost reductions have been achieved on the component level through successful reduction in catalyst loading and reduced-cost membrane structures. Figure 2 (a) represents the new catalyst application techniques developed at Proton Onsite, which have resulted in a 55% reduction in precious metal catalysts loading on the anode and a greater than 90% reduction on cathode compared

with the company's previous technologies. Further reductions in the projected stack capital cost were realized through the optimization of stack designs with reduced part count for ease of manufacturing. For example, the part count in the "DOE Stack," developed by Giner Electrochemical Systems, shown in Figure 2 (b), has been successfully reduced from 16 to 10 since 2010.

Future research and development is expected to achieve projected capital costs of \$125/kW, which would enable electrolyzer-based hydrogen production to be cost-competitive in regional settings with inexpensive electricity feedstocks.

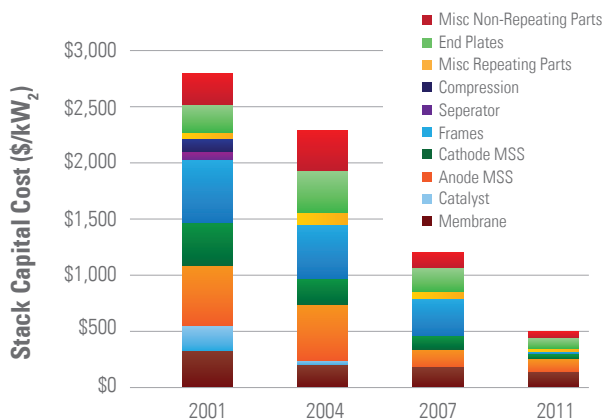


Figure 1. Electrolyzer stack capital cost projections reported by Giner Electrochemical Systems for its "DOE Stack" have been reduced to less than \$400/kW in 2011 (shown in the bar chart with capital cost contributing factors). This represents an 80% reduction since 2001, and a one year reduction of 15%.

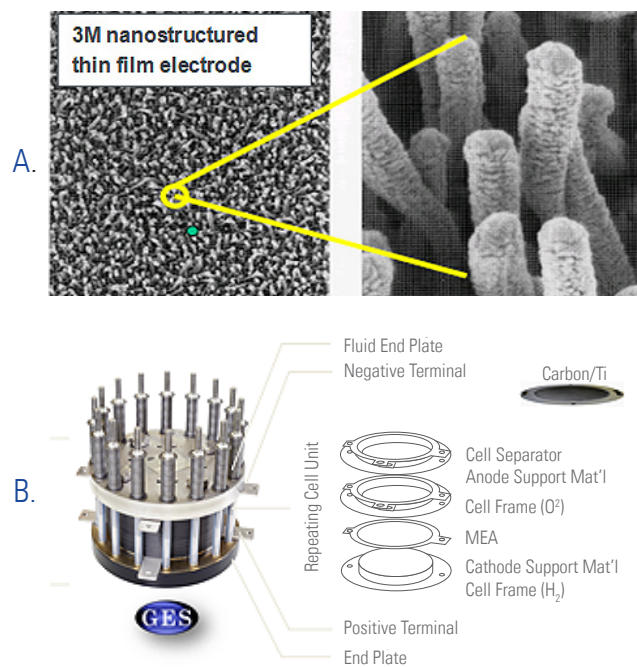


Figure 2. (a) Reductions in precious metal catalyst loading have been achieved by Proton Onsite through novel application of catalyst particles onto nanostructured thin film electrodes; (b) Reductions in stack part count have been achieved by Giner Electrochemical Systems in its "DOE Stack."

